# FORMATION EVALUATION USING WIRELINE LOG DATA OF BAKHRABAD GAS FIELD

**Mohammad Islam Miah**

**DEPARTMENT OF PETROLEUM & MINERAL RESOURCES ENGINEERING**

**BANGLADESH UNIVERSITY OF ENGINEERING AND TECHNOLOGY**

**DHAKA, BANGLADESH**

**NOVEMBER, 2014**

# FORMATION EVALUATION USING WIRELINE LOG DATA OF BAKHRABAD GAS FIELD

A project

Submitted to the Department of Petroleum and Mineral Resources Engineering

In partial fulfillment of the requirements for the

Degree of Master of Engineering in Petroleum Engineering

By

**Mohammad Islam Miah**

**DEPARTMENT OF PETROLEUM & MINERAL RESOURCES ENGINEERING**

**BANGLADESH UNIVERSITY OF ENGINEERING AND TECHNOLOGY**

**DHAKA, BANGLADESH**

**NOVEMBER, 2014**

## CANDIDATE'S DECLARATION

It is hereby declared that this project or any part of it has been submitted elsewhere for the award of any degree or diploma

Signature of the Candidate

……

(Mohammad Islam Miah)

## RECOMMENDATION OF THE BOARD OF EXAMINERS

The undersigned certify that they have read and recommended to the Department of Petroleum & Mineral Resources Engineering, for acceptance, a project entitled "**FORMATION EVALUATION USING WIRELINE LOG DATA OF BAKHRABAD GAS FIELD**" submitted by **MOHAMMAD ISLAM MIAH** in partial fulfillment of the requirements for the degree of Master of Engineering in Petroleum Engineering.

Chairman
(Supervisor):

……
Dr. Mohammad Tamim
Professor
Dept. of Petroleum & Mineral Resources Engineering
Bangladesh University of Engineering and Technology

Member:

……..
Afifa Tabassum Tinni
Assistant Professor
Dept. of Petroleum & Mineral Resources Engineering
Bangladesh University of Engineering and Technology

Member:

……
Farhana Akter
Lecturer
Dept. of Petroleum & Mineral Resources Engineering
Bangladesh University of Engineering and Technology

Date: 29 November, 2014

*This Research Is Dedicated To*

*My beloved Mother and Father*

# ACKNOWLEDGEMENT

At first, I am very much grateful to the most powerful, the gracious almighty Allah for giving me knowledge, energy and patience for completing the research work successfully.

I would like to express my deepest indebtedness and gratitude to my thesis supervisor Dr. Mohammad Tamim, Professor, Department of Petroleum & Mineral Resources Engineering (PMRE), Bangladesh University of Engineering and Technology (BUET), for his continuous guidance, valuable suggestions, constructive comments and endless encouragement throughout the research work and the preparation of this thesis paper.

I acknowledge my heartfelt gratitude to Md. Abdus Sultan (General Manager-In charge, Reservoir and Data Management Division, Petrobangla) for his valuable suggestions to interpret the log data and formation evaluation.

It is my pleasure to express my gratitude to all teachers of PMRE department, BUET to complete this thesis.

I would like to express my enormous gratitude to Sheik Muktadir and Engr. Ashraf, Bangladesh Gas Fields Company Limited (BGFCL) for their loyal support in conducting different task associated with the thesis.

In addition, thanks are due to those who helped me directly and indirectly during the different stages of this thesis work.

Finally, I record with deep appreciation the patience, understanding and encouragement shown by my wife and parents throughout the period of my study.

# ABSTRACT

Formation evaluation can be performed in several stages such as during drilling, after logging as detailed log interpretation, and core analysis in the laboratory, etc. This study shows the formation evaluation using wireline log data of Bakhrabad Gas Field (BK#9). Lithology has been identified from Spectral and Natural Gamma Ray logs where hydrocarbon bearing zones are detected by resistivity and lithology logs including cross checking of porosity logs. The shale volume is estimated from Gamma Ray and True resistivity methods, respectively. Porosity has been estimated from single log methods as well as from Neutron-Density combination formula. Formation water resistivity is estimated from Inverse Archie's, $R_{wa}$ analysis. The Archie's, Indonesia and Simandoux models have been used for water saturation estimation. According to log data analysis, there are six sands present in this well where small mud cake is present within gas bearing sand zones depth interval. Lithology is laminated shale. The average gamma ray value and resistivity ranges are 96-111 API and 13-23 ohm-m of reservoir sands. The shale volume is about 11 and 18 percent from Natural Gamma Ray and True resistivity methods of thick sand with 18 meter reservoir thickness. Average formation water resistivity for virgin zone is 0.10 ohm meter. These gas bearing reservoir sands porosity and permeability quality is good. The average water saturation is 14-40 percent using aforementioned models, which is close to estimation by Interkomp Kanata Management Limited, 1991 and RPS Energy, 2009. This water saturation is more reliable for estimating reserve estimation and future reservoir analysis of this formation.

# TABLE OF CONTENTS

# CHAPTER THREE

## LITERATURE REVIEW 15



# CHAPTER FOUR

## RESULTS AND DISCUSSIONS 32



# CHAPTER FIVE

## CONCLUSIONS AND RECOMMENDATIONS 44

# LIST OF TABLES

# LIST OF FIGURES

# NOMENCLATURE

| | |
|---|---|
| a | Tortousity exponent |
| CEC | Cation Exchange Capacity |
| $G_g$ | Geothermal gradient |
| h | Reservoir thickness |
| $I_{sh}$ | Shale Index |
| K | Potassium (percentage) |
| $K_L$ | Log derived permeability (mD) |
| m | Cementation exponent |
| mD | mili Darcy |
| N/A | Not Available |
| n | Saturation exponent |
| ppm | Parts per million |
| psi | Pound per square inch |
| $\rho_b$ | Bulk density (g/cc) |
| $R_{mf}$ | Mud filtrate resistivity (ohm-m) |
| $R_t$ | True resistivity (ohm-m) |
| $R_w$ | Formation water resistivity (ohm-m) |
| $R_{xo}$ | Flushed zone resistivity (ohm-m) |
| $S_w$ | Water saturation for un-invaded zone (fraction) |
| $S_{wb}$ | Saturation of physically bound water in total Pore Volume, PV (fraction) |
| $S_{xo}$ | Water saturation for flushed zone (fraction) |
| $S_{wt}$ | Water saturation of the total porosity (fraction) |
| Tcf | Trillion cubic feet |
| $T_f$ | Formation Temperature |

| | |
|---|---|
| Th | Thorium (ppm) |
| $T_s$ | Surface Temperature |
| U | Uranium (ppm) |
| $V_{sh}$ | Shale volume (fraction) |
| $V_{cl}$ | Clay content (fraction) |
| 2D | Two dimensional |
| $^0F$ | Degree Fahrenheit |
| % | Percentage |
| Ω-m | Ohm meter |
| α | Shale effect |
| β | Coefficient |
| $\rho_f$ | Fluid density (g/cc) |
| $\rho_{ma}$ | Matrix density (g/cc) |
| $\Phi_e$ | Effective porosity (fraction) |
| ΔT | Sonic travel time (μs/ft) |

Elaborations/Abbreviations

| | |
|---|---|
| API | American Petroleum Institute |
| BGFCL | Bangladesh Gas Fields Company Ltd. |
| BHTV | Borehole Tele-viewer |
| BK | Bakhrabad |
| BVW | Bulk Volume Water (fraction) |
| DD | Driller Depth |
| DELT | Sonic interval transit time (μs/ft) |
| FMS | Formation Micro-Scanner |
| GIIP | Gas Initiaaly In Place |

| | |
|---|---|
| GR | Gamma Ray log |
| GRM | Gamma Ray Method for shale volume estimation |
| HCU | Hydrocarbon Unit |
| IKM | Intercomp Management Ltd. |
| KB | Kelly Bushing |
| MHI | Moveable Hydrocarbon Index (fraction) |
| MMSCFD | Million standard cubic feet per day |
| NPHI | Neutron porosity (percentage) |
| NMR | Nuclear Magnetic Resonance Imaging log |
| OBM | Oil Based Mud |
| PHID | Density porosity (fraction) |
| PSOC | Pakistan Shell Oil Company |
| PMRE | Petroleum & Mineral Resources Engineering |
| RDMD | Reservoir and Data Management Division |
| TD | Total Depth |
| TOC | Total Organic Content |
| TVD | True Vertical Depth |
| WBM | Water Based Mud |
| WHP | Well Head Pressure (psi) |

# CHAPTER ONE
# INTRODUCTION

## 1.1 Introduction

Formation evaluation is the practice of determining both the physical and chemical properties of rocks and the fluids they contain. The objectives of formation evaluation are to evaluate the presence or absence of commercial quantities of hydrocarbons in formations penetrated by the wellbore, to determine the static and dynamic characteristics of productive reservoirs, detect small quantities of hydrocarbon which nevertheless may be very significant from an exploration standpoint, and to provide a comparison of an interval in one well to the correlative interval in another well. It can be performed in several stages such as during drilling by mud logging, logging while drilling, during logging (quick look log interpretation) and after logging (detailed log interpretation), by core analysis in the laboratory, etc. Wireline logs are one of the many different sources of data used in formation evaluation. Due to accurate depth determination and near proximity of receiver to formation, wireline logs (both conventional and special logs which include Formation Micro-Scanner (FMS), Borehole Tele-viewer (BHTV), Deep-meter logging, Nuclear Magnetic Resonance (NMR) Imaging logs, etc.) play an important role in formation evaluation (HLS Asia Limited, 2008). From log data analysis, estimated petrophysical properties give the significant information about formation, and help to make the decision of whether to set pipe and perforate or consider abandonment still hangs. These properties are shale volume, porosity, permeability, formation resistivity and water saturation. Calculated values of water saturation only provide the analyst with information about fluids are present in the formation of interest. In many cases, water saturation is not a reflection of the relative proportions of fluids that may be produced. Therefore, when making the decision to set

pipe or abandon, all available information should be taken into account. Water saturation should be the basis for that important decision, but other factors also enter into the decision making process such as irreducible water saturation, bulk volume water and moveable hydrocarbons, etc. The petrophysical properties such as porosity, sand thickness and hydrocarbon saturation is important for estimating of hydrocarbon reserve and reservoir performance analysis. Also the gas recovery efficiencies depend on number of factors including porosity and permeability of the reservoir, fluid properties, reservoir drive mechanism, abandonment pressure etc. The estimation of hydrocarbon reserves using petrophysical and production data, is a fundamental aspect of reservoir engineering and is conducted throughout the life of a reservoir. The validation of new data can be achieved from subsurface geological log and production data that can be found by several development wells drilled within a field. In July 2013, Bakhrabad gas field drilled a development well named as BK#9. Using wireline log data, formation evaluation and petrophysical analysis gives reservoir data that can be used for future reserve estimation and reservoir analysis.

## 1.2 Objectives of the Study

The main objective of the present study is formation evaluation of BK#9 that is to ascertain the followed parts:

i) Lithology identification and detection of hydrocarbon bearing zone
ii) Estimation of shale volume and reservoir thickness
iii) Assessment of effective porosity
iv) Determination of water saturation and
v) Estimation of log derived permeability
vi) Comparison of petrophysical properties of this reservoir with different studies

## 1.3 Methodology

In manual interpretation of the available wireline log data and formation evaluation, some standard rules and practices used in the current study which mentioned as below:

### 1.3.1 Lithology identification and hydrocarbon bearing zone detection

Lithology has been identified from spectral and natural gamma ray (GR) log response. Hydrocarbon bearing zone is detected by resistivity log and porosity log comparing with GR log response (Darling, T., 2005; HLS Asia Ltd., 2007).

### 1.3.2 Estimation of shale volume and reservoir thickness

Shale volume ($V_{sh}$) has been calculated individually from Spectral and Natural Gamma Ray log, and True resistivity methods, respectively (Schlumberger, 1998; Hamada, 1996; Asquith, G. and Krygowski, D., 2004). Sand thickness has been calculated from Gamma Ray comparing with Resistivity and Porosity logs.

### 1.3.3 Assessment of porosity

Porosity has been calculated from Neutron log, Density log and Sonic log individually. Then Neutron-Density combined formula has been applied with clay corrected (HLS Asia Limited, 2008) and the arithmetic average porosity is estimated for further interpretation.

### 1.3.4 Geothermal gradient and formation temperature

These have been calculated from Arps'formula (HLS Asia Limited, 2008).

### 1.3.5 Formation water resistivity

Formation water resistivity ($R_w$) has been calculated from Inverse Archie's method ($R_{wa}$ analysis). Then estimated $R_w$ is corrected for formation depth which is used for estimating water saturation (HLS Asia Limited, 2008; Miah, M. I. and Howlader, M. F., 2012).

### 1.3.6 Determination of water saturation

Water saturation has been estimated from Archie's formula (Archie, 1942), Indonesia model (Hamada, 1996) and Simandoux model (1963) individually and the values are compared with each other.

### 1.3.7 Moveable hydrocarbon index and bulk volume water

Moveable hydrocarbon index (MHI) is the ratio of $S_w$ (water saturation of un-invaded zone) and $S_{xo}$ (Water saturation of flushed zone). Hydrocarbon Bulk Volume Water (BVW) has been estimated from Archie's formula, Indonesia and Simandoux model by taking the product of porosity and water saturation of un-invaded zones. Then sand grain sizes have been estimated from BVW ranges (Asquith, G. and Krygowski, D., 2004).

### 1.2.8 Log derived permeability

It has been calculated using Wyllie & Rose equation (Crain, 1986).

The summarized methodology of formation evaluation has been shown in the flow chart in Figure 1.1 (Asquith, G. and Krygowski D., 2004; Hamada, 1996).

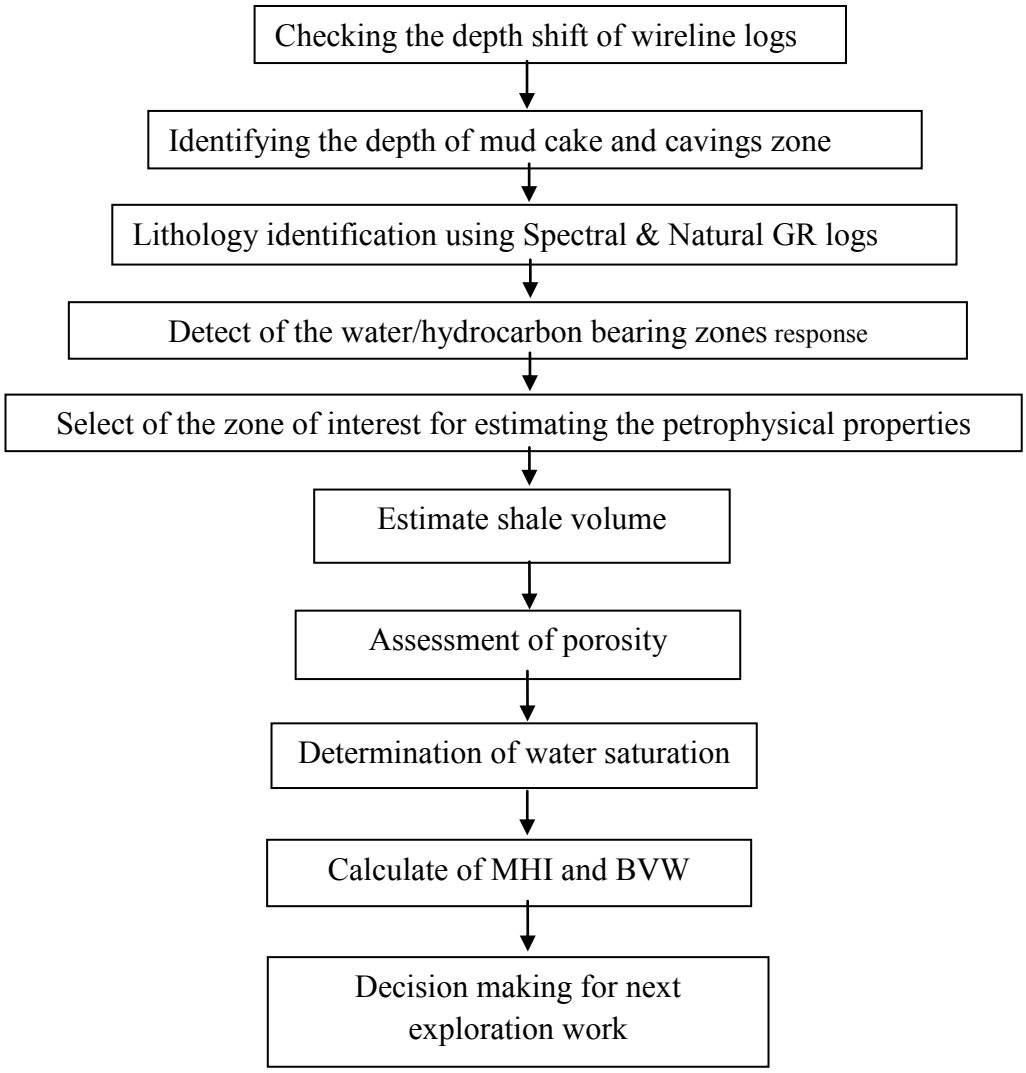


Figure 1.1 Flow chart for log interpretation and formation evaluation

# CHAPTER TWO

## OVERVIEW OF THE BAKHRABAD GAS FIELD

The Bakhrabad gas field is one of the onshore gas fields in Bangladesh for which RPS Energy has conducted series of reservoir studies for Petrobangla (RPS Energy, 2009a). This field is located in the Bengal (Surma) Basin, which is a Miocene gas producing province in the North Eastern part of Bangladesh located south of Narshingdi town about 50 km southeast of Dhaka. The structural map of the thick reservoir sand of this field is shown in Figure 2.1.

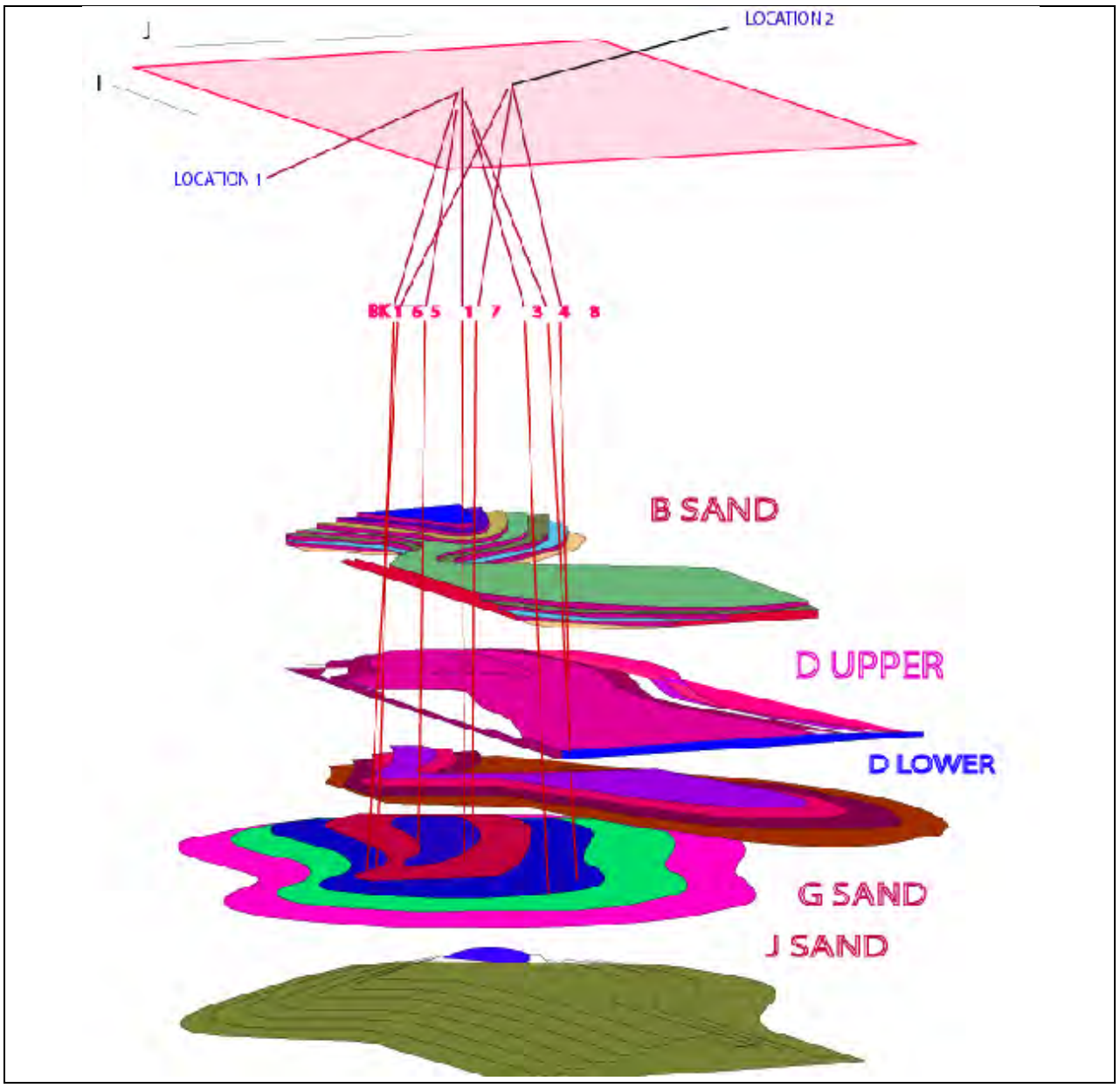


Figure 2.1 Subsurface reservoir structural map of the Bakhrabad gas field (After BGFCL, 2008).

## 2.1 Structure

The greater Bakhrabad (BK) structure was delineated by Shell who divided the structure into three separate culminations. They are Bakhrabad Main ('A' closure), Marichakandi ('B' closure) and Narshingdi Field which is corresponding to the 'C' closure, immediately to the north of the 'B' closure. The structure was first mapped by Shell in 1966 with a single fold seismic grid. The structure lies 47 km SE of Kamta and 50 km SSW of the Titas gas field. The structural trend main axis lie NNW-SSE, curving slightly NNE toward the northern end. The structure lies on the southern fringes of the Surma Basin which is located at the western margin of the north-south trending Chittagong-Tripura folded belt. The structural dip at the Bakhrabad closure is quite steep (Figure 2.2), estimated to be about 15 degrees and indicates stronger compression and uplift than its northern counterparts (RPS Energy, 2009a).

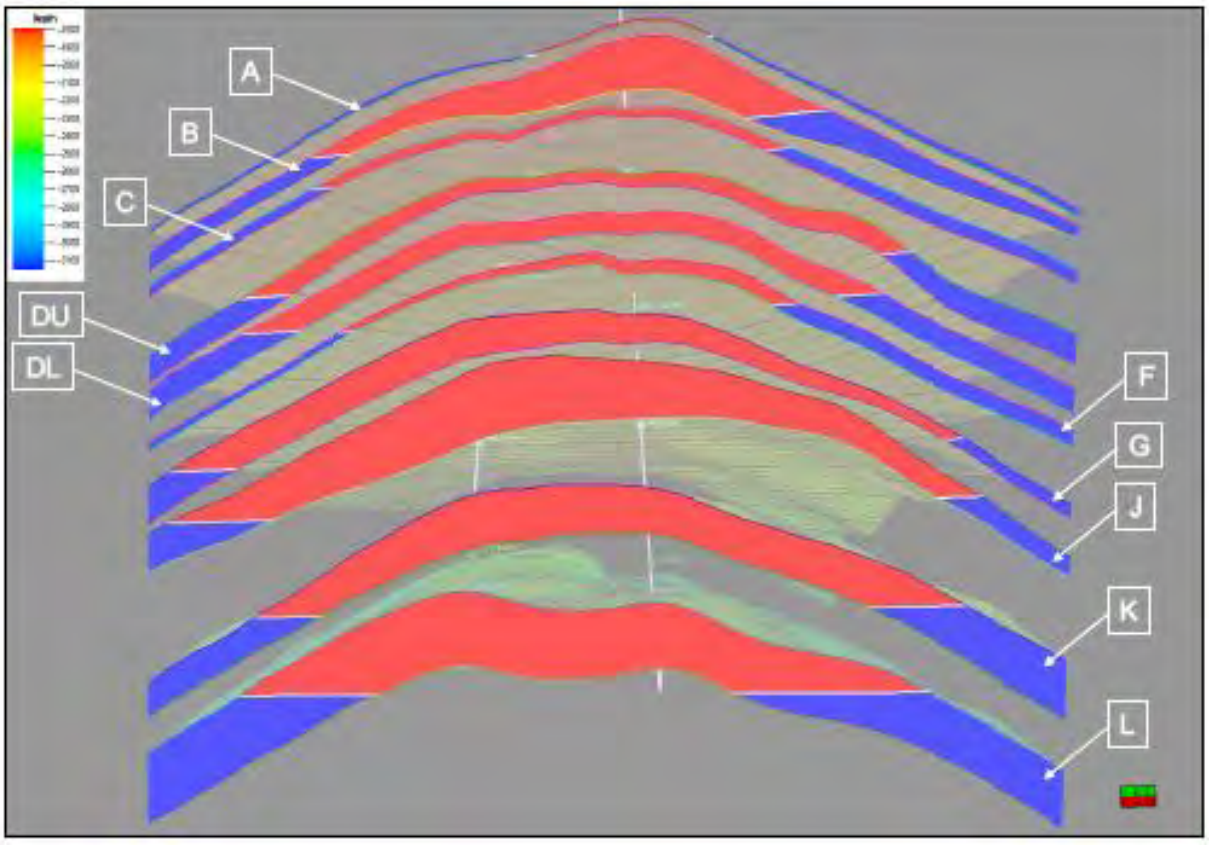


Figure 2.2 Structural cross-section through this field anticline (RPS Energy, 2009a)

The depth structure map of G sand is shown in Figure 2.3. A few minor faults were observed from the 2D seismic data at the Bakhrabad structure and vicinity. This is probably due to the low resolution of the variable quality 2D seismic data and probably

more faults can be expected to be seen in a higher resolution 3D seismic dataset (RPS Energy, 2009a).

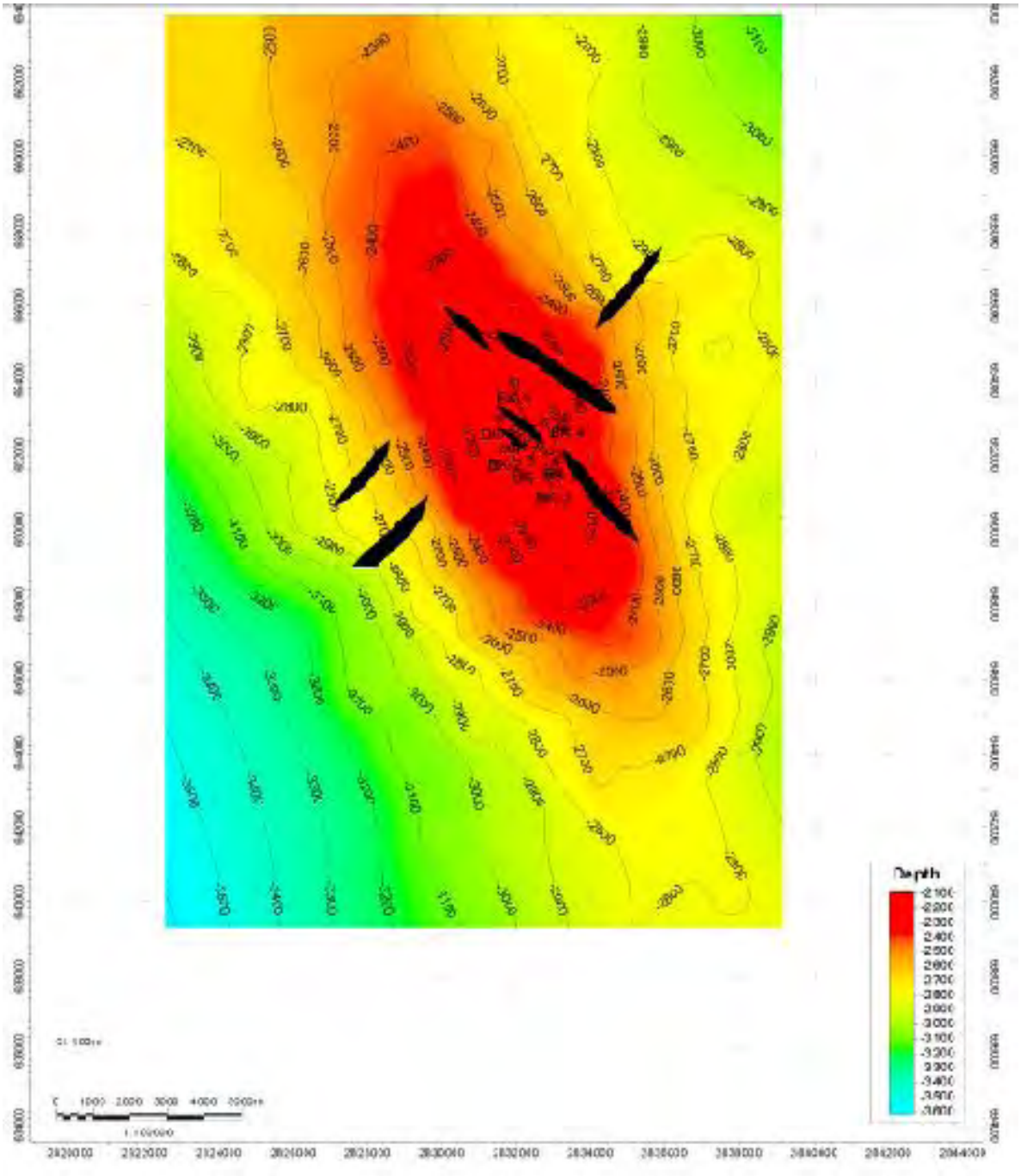


Figure 2.3 Depth structure map of G sand (RPS Energy, 2009c)

## 2.2 Stratigraphy

Stratigraphically, the Bakhrabad area is part of Surma Basin located in the southern part of the basin. The Bakhrabad field is in a N-S trending anticline trap with the gas bearing zones in the Lower Miocene sands. As with most fields in this trend, the depositional environment is stated to vary from proximal-distal fluvio-marine to delta plain type deposits resulting in barrier bar, delta fringe and channel sand complexes. The accumulations are in multiple stacked sands with individual fluid contacts and with inconsistent continuity of individual lenses. This lenticular nature is a more likely reservoir barrier limit in the area than the less-well defined fault interpretation proposed by Interkomp Kanata Management Ltd. (IKM), 1990. As the results of drilling activities, the following sedimentary cycles are confirmed:

Sequence I: from the surface to the upper marine shale, about 500 m thick.

Sequence II: from the upper marine shale to the top of "A" Gas Sand, about 1200 m thick.

Sequence III: from top of "A" Gas Sand to the base of "L" Gas Sand, about 650 m thick.

Sequence III is subdivided into "A", "B", "C", "D Upper", "D Lower", "F", "G", "J", "K", "L" Sands and the main reservoirs are in "B", "D Upper", "D Lower", "G", and "J". The sediments making up the reservoirs are composed of sandstone and shale, and considered to have deposited in the delta or delta front environment (RPS Energy, 2009a).

## 2.3 Petroleum System

Regionally, Bakhrabad area is a part of the Hatia Petroleum System that is located in the south of the Tangail-Tripura High. The hydrocarbon system is characterized by Plio-Pleistocene traps in sandstone reservoirs of upper Miocene to Pliocene age. Gas with little or no condensate is produced. The hydrocarbon source is probably from Miocene Bhuban shales, which have generated primarily natural gas with minimal condensate (RPS Energy, 2009a).

### 2.3.1 Trap

A large elongated anticline structure with trending NNW-SSE is the trap type for the Bakhrabad Gas Field. This compressional structuring took place from Miocene to Recent age (RPS Energy, 2009a).

### 2.3.2 Source rock

It has been mentioned that all the Bakhrabad wells penetrated the Bhuban shale. The Miocene Bhuban Shale is widely developed over the Bengal Basin, including the Eastern Fold belt, and is probably the youngest source rock unit capable of generating gas. The formation, deposited under a wide range of environmental regimes, from shallow marine deltaic to fluvio-deltaic, has been characterized by different proportions of alternating shales, silts and sands, with an overall increase of shale content southwards. The sequence is poor to lean in terms of source rock potential, with total organic content (TOC) values averaging from 0.2 to 0.7 % (RPS Energy, 2009a).

### 2.3.3 Vertical seal

The Upper Marine Shale (late Miocene-early Pliocene) is clearly recognized from seismic and is supposed to be a regional vertical seal in the Bakhrabad area. Intraformational seals are also recognized both from well and seismic sections (RPS Energy, 2009a).

### 2.3.4 Timing and migration

Bakhrabad is part of Hatia area, the rapid sedimentation rates during the Miocene pushed the Oligocene and earlier source rocks through the oil and gas windows well before the formation of the structural traps in the Pliocene to Recent. The most likely gas source is in the shaly sections of the middle to lower Miocene. The migration pathway is probably a combination of vertical migration from earlier Miocene through flanking faults and lateral migration form upper Miocene in basinal, "kitchen" areas (RPS Energy, 2009a).

## 2.4 History of Field Development and Production

This field was the last gas discovery in the Bengal folded belt by Shell in 1968. The discovery well was targeted to 12,000 ft Kelly Bushing (KB) but as over pressures were encountered at 9070 ft KB, the well was terminated at 9310 ft KB, the deepest and the only vertical well of this field during this time. The J sands proved to be the best pay sands in the area of present development drilling, that production tested 54 MMSCFD between 7035 and 7360 ft KB. The other two tests in the discovery well were unsuccessful. The test in the deepest L sands in the interval between 8150 and 8206 ft KB did not flow, obviously because it is tight, being clay plugged and finer grained. The shallowest test between 624 and 6255 ft KB produced 1200 bbls of water. No connate salinity data from the water reported. In fact, this sand was not a part of the B sand, being separated from its base at 7040 ft KB, by a 175 ft thickness of shale and virtually water-wet sands. The well was suspended as a potential producer (IKM, 1990a).

### 2.4.1 First stage of development drilling

It involved drilling four deviated wells BK-2, BK-3, BK-4 and BK-5 in 1981-1982 from the same pad as BK-1. Four comprehensive tests of the thick sands were undertaken in BK-2 through 1/64 inch choke with different flow rate with respective sand depth. The well BK-2 was completed in D-L sands where BK-3 was completed the G sands, that production tested 40.22 MMSCFD between 8720 and 8910 ft Driller depth (DD). BK-4 and BK-5 were completed in the D-U (7110-7200 ft DD) and B that production tested 40 and 29 MMSCFD, respectively (IKM, 1990a; Choudhury, Z., 1999; Choudhury, Z. and Gomes, E., 2000).

### 2.4.2 Second stage of development drilling

It was successfully achieved by the drilling and completion of the three gas wells, BK-6, BK-7 and BK-8 under the auspices of ADM in 1989. BK-6 was drilled from a separate pad and the J sand production tested 35.72 MMSCFD. BK-7 and 8 were drilled from a separate pad, 1500 ft to the ENE of pad no. 1 (Figure 2.4). The J sand of BK-8 production tested 43.0 MMSCFD (IKM, 1991a; Choudhury, Z., 1999).

### 2.4.3 The latest round of development drilling

The last development well was drilled by BAPEX in July, 2013.

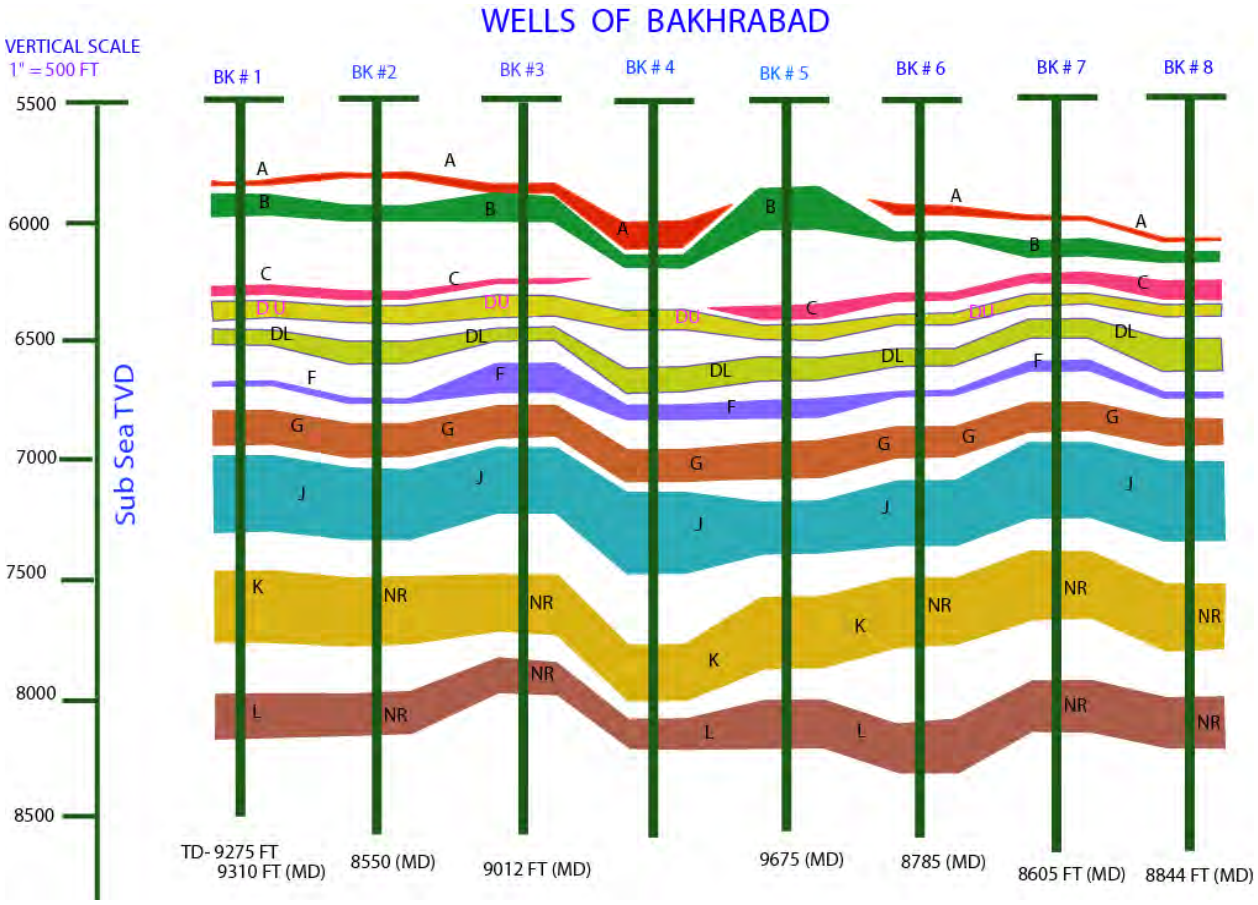


Figure 2.4 Depth of eight drilled wells of Bakhrabad gas field (BGFCL, 2008).

### 2.4.4 Gas reserves

Several studies of reserve estimation have been done at different stages of this field. Reserve estimations of the Bakhrabad gas field were initially done by Shell Oil in late sixties and also by DeGolyer and McNaughton in 1975. These studies suggested that Gas Initially In Place (GIIP) in the field is in the range of 2.78 to 2.90 Tcf. Proved gas in place was calculated as 1.578 Tcf by Natural Gas Reserves and Deliverability Study, Bangladesh by JALECO (1980). However reappraisal of the gas reserve of the field by IKM in 1992 estimated the GIIP at 1.432. In 1999, Choudhury, Z. estimated of total gas in place value of this field as 1.122 and 1.127 Tcf by flowing well method and conventional material balance, respectively. Petrobangla published a re-estimated GIIP of 1.70 Tcf for the gas field based on the evaluation by RPS Energy, 2009.

### 2.4.5 Production data

Gas production from this field started in 1984. By 1989 there were eight wells and a steady increase of production. At the end of 1992, gas production rate reached its peak with average of 195MMSCFD. Some historical production test results and production status till December, 2012 of this field are shown in Table 2.1 and Table 2.2.

Table 2.1 Sand free production test results (Choudhury, Z., 1999)

| Well | Perf. (MD), feet | Choke size, Inc. | WHP, psia | Gas production rate, MMSCFD | Condensate production rate, bbls/day | Water rate, bbls per MMSCF | Sand production rate, Gram/day |
|---|---|---|---|---|---|---|---|
| BK 1 (J) | 7035-7360 | 47 | 1040 | 14 | 0.6 | 1.6 | 6.3 |
| BK 2 (DL) | 7290-7360 | 74 | 920 | 16 | 0.0 | 0.9 | 13.7 |
| BK 3 (G) | 8720-8910 | 45 | 1265 | 15.7 | 0.3 | 0.2 | 9.6 |
| BK 4 (G) | 7694-7838 | 36 | 790 | 6 | 0.1 | 57 | Trace |
| BK 5 (DL) | 7592-7704 | 32 | 870 | 5.5 | 0.0 | 69.2 | 264 |
| BK 6 (J) | 8194-8450 | 96 | 825 | 16 | 1.8 | 17.5 | Trace |
| BK 7 (J) | 8143-8450 | 50 | 1080 | 16 | 0.9 | 0.3 | 14.4 |
| BK 8 (J) | 8209-8559 | 56 | 960 | 14.8 | 1.8 | 9.8 | 57.0 |

However, two of the wells had to be shut down because of excessive pressure drop and water production in 1994. This was accompanied by sanding problem (production of loose sand with the gas flow). Production continued to decrease as more wells were shut down. The gas production rate decreased to 50 MMSCFD by 1999 and to 35 MMSCFD

by January, 2000. In September 2012, the gas field was producing 31 MMSCFD. Some experts opine that the sanding problem and pressure drop in this field resulted due to excessive production rate at some points in time. Till December 2011, cumulative production of gas from this field stood at 0.736 Tcf (Imam, B., 2013).

Table 2.2 Production and pressure history of Bakhrabad gas field (Petrobangla, 2012)

| BK well name | Well completion date | Initial flow rate (MMSCFD) & FWHP (psi) | Gas rate (MMSCFD) & FWHP (psi) | Cumulative gas production, Bcf till December, 2012 | Present Status |
|---|---|---|---|---|---|
| 1 | 09.06.1969 | 14.150 & 2780 (Aug., 85) | 5.303 & 418 | 140.203 (J) | Producing |
| 2 | 13.10.1981 | 6.301 & 2500 | 2.533 & 561 | 83.922 (DL & G) | Producing |
| 3 | 16.04.1982 | 13.276 & 2600 (Nov., 86) | 7.532 & 549 | 151.177 (G) | Producing |
| 4 | 06.06.1982 | 19.823 & 2420 (Nov., 86) | 1.934 & 819 (June, 98) | 56.850 (DU & G) | Suspended |
| 5 | 21.08.1982 | 8.476 & 2120 (Nov., 84) | 0.067 & 966 (B sand-June, 97) | 51.983 (B & DL) | Suspended |
| 6 | 05.02.1989 | 5.531 & 2400 (Jan., 90) | 2.257 & 808 (Aug., 98) | 50.949 (J) | Suspended |
| 7 | 15.06.1989 | 14.470 & 2300 (Dec., 89) | 4.729 & 430 | 105.288 (J) | Producing |
| 8 | 06.09.1989 | 8.117 & 2300 (Jan., 90) | 11.484 & 566 | 107.888 (J) | Producing |

# CHAPTER THREE

# LITERATURE REVIEW

Several studies have been conducted for different purposes at different development stages of this gas field. The presence of a potential gas bearing structure at Bakhrabad was first recognized from the results of the gravity survey made by Pakistan Petroleum Company in 1953 (Welldrill, 1989). Pakistan Shell Oil Company (PSOC) took over the relinquished lease and conducted at extensive single fold seismic program during 1960-1966. Bakhrabad seismic mapping was prepared by Hydrocarbon Habitat Study (HHS) in 1986. Before May 2013, there were eight wells penetrated within this structure. The first well, BK-1 was spudded by Shell in September 1968 with a target depth of 3657 m. The deviated wells as BK-2 to BK-5 were drilled during the first phase of development in 1981-1982. The deviated wells of BK-6 to BK-8 were drilled later during the next round of development drilling in 1989. In 1990, IKM studied about "Gas Field Appraisal Project-Geological, Geophysical, Petrophysical and Reservoir Engineering report of the BK Gas Field" for BK-1 to BK-8. A report on production problem of Bakhrabad Gas Field by Huq et al. (1993), made an elaborate coverage on the production history of the field. In this report it was pointed out that in Bakhrabad, produced gas and liquid from all the wells were separated centrally and through a common header, the separated liquid flows further downstream for separation of water and condensate. Reservoir Engineering report based on 1992 and 1993 Pressure Surveys of BK field was compiled by Reservoir Study Unit of Petrobangla, 1993. Several reservoir engineering studies on BK field have been done based on IKM findings (Choudhury, Z., 1999; RPS Energy, 2009d). In October 2009, RPS Energy and Petrobangla studied "Petrophysical Analysis of BK Gas Field" for BK 1 to BK 8. The formation evaluation of BK#9 has not been done yet. So this new data can be used for future reservoir analysis.

## 3.1 Theory of Well Logs and Formation Evaluation

### 3.1.1 Lithology logs

The first goal of formation evaluation is to attempt to identify the lithology down hole and its depth of occurrence. The spontaneous potential (SP) curve and the natural gamma ray (GR) log are recordings of naturally occurring physical phenomena in in-situ rocks. The SP curve records the electrical potential (voltage) produced by the interaction of

formation connate water, conductive drilling fluid and certain ion-selective rocks (shale). The GR log measures the strength of the natural radioactivity present in the formation. Nearly all rocks exhibit some natural radioactivity and the amount depends on the concentration of potassium, thorium, and uranium. Both the SP curve and GR log are generally recorded in left track of the log. They are usually recorded in conjunction with some other log such as the resistivity or porosity log. Indeed, nearly every log now includes a recording of GR log. The Spectral Gamma Ray tool works on the same principal as the gamma ray, although it separates the gamma ray counts into three energy windows to determine the relative contributions arising from Potassium (K), Uranium (U) and Thorium (Th) in the formation. The presence of clay minerals or shale (Table 3.1) in a reservoir may either be good or bad in terms of reservoir quality. Small amounts of clay minerals (high cation exchange capacity, CEC result in higher conductivity and lower resistivity) within the pore space of a reservoir may, because of the increased surface adhesion and capillary pressures associated with such small particle sizes, trap interstitial water. The result can be virtually water-free hydrocarbon production from reservoirs of relatively high calculated water saturation. On the other hand, the presence of a large amount of clay may result in the porosity (PHI) and permeability of the reservoir being reduced to the point where the reservoir becomes non-productive. All lithologies are includes limestone and dolomite which may potentially contain some amount of clay minerals. More commonly, however, clay minerals are found associated with sandstone reservoirs. Because of this, log analysts typically make reference to the "shaly sand problem" (HLS Asia Ltd., 2008).

Table 3.1 Petrophysical properties of common clay minerals (HLS Asia, 2008)

| Clay type | CEC | Bulk density, g/cc | PHI | Minor Constituents | Spectral GR components | | |
|---|---|---|---|---|---|---|---|
| | | | | | K (%) | U (ppm) | Th (ppm) |
| Mont-morillonite | 0.8-1.5 | 2.45 | 0.24 | Ca, Mg, Fe | 0.16 | 2-5 | 14-24 |
| Illite | 0.1-0.4 | 2.65 | 0.24 | K, Mg, Fe, Ti | 4.50 | 1.5 | <2 |
| Kaolinite | 0.03-0.06 | 2.65 | 0.36 | ……. | 0.42 | 1.5-3 | 6-19 |

Shale can be classified as the following three types. Laminated shale refers to thin layers of clay minerals--from a fraction of an inch to several inches in thickness--that are interbedded with thin intervals of sandstone. Structural clay refers to detrital clay minerals that exist as individual grains, clasts, or particles along with the framework grains of a reservoir. This type of clay typically has little impact upon reservoir quality because it does not restrict or block pore throats. Dispersed clay refers to very fine grained particles that exist within the pore space space of a reservoir and actually replace fluid volume. These types of clays, because of their disseminated fibrous and plate-like morphologies, may be very damaging to reservoir quality. The presence of clay minerals in a reservoir may seriously affect some log responses, particularly resistivity and porosity. The end result is an erroneously high value of water saturation, and in some cases a productive reservoir may appear to be wet. Field engineers and log analysts should be able to recognize the effects of clay minerals and be able to correct for their presence to yield more accurate values of water saturation. This emphasizes the need for "shaly sand analysis". Shale Index ($I_{sh}$) is calculated from GR logs as the following equations:

Shale Content ($I_{sh}$) or Shale Volume,

$$Y_{Vsh} = \frac{X_{log} - X_{min}}{X_{max} - X_{min}}$$

where Y= GR/K/Th

$X_{log}$ = GR/K/Th response in the formation of zone interest,

$X_{min}$ = GR/K/Th response in clean shale free formation and

$X_{max}$ = GR/K/Th response in clean shale zone over the entire log.

Using Gamma Ray Method (GRM), $I_{sh}$ as a linear expression of Shale volume, $V_{sh}$ is most suitable for laminated shales. In this case, the resulting ratio reflects the percentage of clay minerals contained in the reservoir. Again, when this ratio exceeds 15%, then it should be assumed that the formation is indeed a shaly sand and that the Archie equation should be abandoned for a technique that will yield better results of water saturation ($S_w$) in the presence of clay minerals. Some analysts prefer to use Gamma Ray Index, Ish as a shale indicator in all types of shales. However, the relationship between $I_{sh}$ and Shale volume ($V_{sh}$) becomes non-liner for both structural clays and dispersed clays. There is a wide variety of non linear relationships can be between $I_{sh}$ and $V_{sh}$, but none of these is universally accepted (Schlumberger, 1998a).

Shale volume ($V_{sh}$) can be calculated from non- linear relationships are listed below (Bassiouni, Z., 1994):

For tertiary rocks, the Larionov equation is $V_{sh} = 0.083(2^{3.7I_{sh}} - 1)$

Shale volume can be calculated from true resistivity method, TRM (Hamada, 1996):

$$V_{sh} = \left[ \frac{R_{cl}}{R_t} \times \left\{ \frac{R_{tmax} - R_t}{R_{tmax} - R_{cl}} \right\}^{\frac{1}{1.5}} \right]$$

Where $R_{cl}$ = resistivity of clay or shale zone,

$R_{tmax}$ = the maximum true resistivity over the entire log and

$R_t$ = true resistivity of the zone of interest.

### 3.1.2 Porosity logs

Rock porosity can be obtained from the sonic log, the density log, or the neutron log. For all these devices, the tool response is affected by the formation porosity, fluid, and matrix. If the fluid and matrix effects are known or can be determined, the tool response can be related to porosity. Therefore, these devices are often referred to as porosity logs. All three logging techniques respond to the characteristics of the rock immediately adjacent to the borehole. Their depth of investigation is very shallow only a few inches or less and therefore generally within the flushed zone (Schlumberger, 1998a). Porosity may be defined as the measure of void space in the reservoir material which is available for the accumulation and storage of fluids. In general, naturally occurring rocks are permeated with water, oil, gas or combination of these fluids. Absolute or total porosity is defined as the ratio of pore space to the total volume of reservoir rock and is commonly expressed as a percentage. Two measurements, pore volume and bulk volume are required to obtain the percentage porosity in accordance with the equation. Porosity varies greatly both laterally and vertically within most reservoirs. The porosity measurements ordinarily used in reservoir studies is the ratio of the interconnected pore space to the total bulk volume of the rock and is termed effective porosity. The effective porosity is commonly 5 to 10 percent less than the total porosity. It may also be termed as the available pore space, since oil and gas to be recovered must pass through interconnected voids. Porosity in sandstone varies primarily with grain size distribution and grain shapes, packing arrangement, cementation and clay content. A reservoir having a porosity of less than 5 percent is generally considered noncommercial. A rough field appraisal of porosities is included in below Table 3.2.

Table 3.2 Field appraisal of porosity quality based on porosity range (Akhanda, A. R. and Islam, Q., 1994)

| Porosity range (%) | Porosity quality |
|---|---|
| 0-5 | Negligible |
| 5-10 | Poor |
| 10-15 | Fair |
| 15-20 | Good |
| 20-25 | Very good |

Neutron logs are porosity logs that measure the hydrogen concentration in a formation. In clean formations (shale free) where porosity is filled with water, oil or gas, the neutron log measures liquid filed porosity (NPHI). Neutrons are created from a chemical source in the neutron logging tool. When these neutrons collide with the nuclei of the formation the neutron loses some of its energy. With enough collisions, the neutron is absorbed by a nucleus and a gamma ray is emitted. Because the hydrogen atom is almost equal in mass to the neutron, maximum energy loss occurs when the neutron collides with a hydrogen atom. Therefore, the energy loss is dominated by the formation's hydrogen concentration. Because hydrogen in a porous formation is concentrated in the fluid-filled pores, energy loss can be related to the formation's porosity. The most commonly used neutron log is the compensated neutron log which has a neutron source and two detectors. The advantages of compensated neutron logs over sidewall neutron logs are that they are less affected by borehole irregularities. When the lithology of a formation is sandstone or dolomite, apparent limestone porosity from compensated neutron log must be corrected to the true porosity using appropriate chart or about 4 porosity unit. Whenever pores are filled with gas rather than oil or water, the reported neutron porosity is less than the actual formation porosity. This occurs because there is a lower concentration of hydrogen in gas than oil or water. This lower concentration is not accounted for by the processing software of the logging toll, and thus is interpreted as a low porosity. A decrease in neutron porosity by the presence of gas is called gas effect. Also an increase in neutron porosity by the presence of clays is called shale effect (Asquith, G. and Krygowski, D., 2004). Neutron porosity actually increases when clay minerals are added to the reservoir. This result from the fact that clay minerals are hydrated and contain structurally bound hydroxyl ions ($OH^-$) within their crystalline

structure. The neutron tool reflects this additional hydrogen as an increase in porosity even through the structurally bound water is not a part of the pore space of the reservoir. It must be remembered that neutron logs sense all of the hydrogen in the formation that includes the hydrogen in the oil, the gas, the water, and the crystalline water. This means it will sense the 48 percent water of crystallinity bound in gypsum crystals and, thus, will calculate out porosity too high. This is also true for other hydrous minerals such as opal, shale or clays in general. Because gas is not very dense, it has a low hydrogen count which yields too low of a porosity. In clay-bearing gas productive zones, the presence of crystalline water causes porosities too high and will mask the presence of the gas (HLS Asia Ltd., 2008). The clay corrected porosity of neutron log can be calculated as the following equation (Asquith, G. and Krygowski, D., 2004):

$\Phi_{N,corr} = \Phi_N - V_{sh} \times \Phi_{N,sh}$ + lithology correction

where $\Phi_{N,sh}$ is the neutron porosity of nearby shale and lithology correction is 0.04 %.

The density logging tool has a relatively shallow depth of investigation, and as a result, is held against the side of the borehole during logging to maximize its response to the formation. The tool is comprised of a medium-energy gamma ray source (cobalt, cesium 137 and others). Two gamma ray detectors provide some measure of compensation for borehole conditions as like sonic tool. When the gamma rays collide with electrons in the formation, the collisions result in a loss of energy from the gamma ray particle. The scattered gamma rays that return to the detectors in the tool are measured in two energy ranges. The number of returning gamma rays in the higher energy range, affected by Compton scattering, is proportional to the electron density of the formation. Gamma ray interactions in the lower energy range are governed by the photoelectric effect. The response from this energy range is strongly dependent on lithology and only very slightly dependent on porosity. Formation bulk density is a function of the amount of matrix and the amount of fluid in the formation (hydrocarbons, salt or fresh water mud, as well as their respective densities (Beaumont, A. E. et a., 1999; Asquith, G. and Krygowski, D., 2004). It can be expressed as the following equations (Bateman, R. M., 1985; Bassiouni, Z., 1994):

Formation bulk density (gram per cubic centimeter), $\rho_b = [\Phi \times \rho_f + (1 - \Phi)\, \rho ma]$.

So, density porosity, $\Phi_D = \frac{\rho_{ma} - \rho_b}{\rho_{ma} - \rho_f}$

Shale volume or clay corrected density porosity, $\Phi_{D,corr} = \Phi_D - V_{sh} \times \Phi_{D,sh}$

where $\Phi_{D,sh}$ is the adjacent clay zone density porosity.

$\Phi_{D,corr} = \frac{\rho_{ma} - \rho_{b,corr}}{\rho_{ma} - \rho_f}$ and $\rho_{b,corr} = \rho_b + V_{sh}(\rho_{ma} - \rho_{cl})$

where $\Phi_{D,corr}$ is the clay corrected density porosity.

Effective porosity is that porosity available to free fluids in the reservoir. The values of neutron and density porosity corrected for the presence of clays are then used in the equation below to determine the effective porosity, $\Phi_e$ of the formation of interest for gas (Asquith, G. and Krygowski, D., 2004; HLS Asia Ltd., 2008):

$$\Phi_e = \sqrt{\frac{\Phi_{N,corr}^{\ 2} + \Phi_{D,corr}^{\ 2}}{2}}$$

The sonic log is a porosity log that measures interval transit time (DELT) of a compressional sound wave traveling through the formation along the axis of the borehole. The sonic log device consists of one or more ultrasonic transmitters and tow or more receivers. Modern sonic logs are borehole compensated (BHC) devices are designed to greatly reduce the spurious effects of borehole size variations (Kobesh and Blizard, 1959) as well as errors due to tilt of the tool with respect to the borehole axis by averaging signals from different transmitter-receiver combinations over the same length borehole (Asquith, G. and Krygowski, D., 2004). Interval transit time (DELT) in microseconds per foot is the reciprocal of the velocity of a compressional sound wave in feet per second. A good correlation often exists between porosity and acoustic interval travel time ($\Delta T$). According to Wyllie time-average equation (Wyllie et al., 1958):

Total travel time = travel time in liquid fraction + travel time in matrix fraction.

$\Delta T = \Delta T_f \times \Phi + \Delta T_{ma}\ (1-\Phi)$.

So, total porosity by sonic log, $\Phi_S = \frac{\Delta T_{ma} - \Delta T_{log}}{\Delta T_{ma} - \Delta T_f}$

This equation applicable only for calculation in clean, compacted, and consolidated sandstones. Lack of compaction is usually indicated when the interval transit time of adjacent shales, $\Delta T_{sh}$, exceeds 100 µsec/ft.

The interval transit time of a formation is increased due to the presence of hydrocarbons (i.e. hydrocarbon effect). If the effect of hydrocarbons is not corrected, the sonic derived porosity will be too high.

Hilchie (1978) suggests the following empirical corrections for hydrocarbon effect:

$\Phi = \Phi_S \times 0.7$ for gas, and $\Phi = \Phi_S \times 0.9$ for oil.

### 3.1.3 Resistivity logs

The resistivity of a formation is a key parameter in determining hydrocarbon saturation. Electricity can pass through a formation only because of the conductive water it contains. With a few rare exceptions, such as metallic sulfide and graphite, dry rock is a good electrical insulator. Moreover, perfectly dry rocks are very seldom encountered. Therefore, subsurface formations have finite, measurable resistivities because of the water in their pores or absorbed in their interstitial clay. The resistivity of a formation depends on resistivity of the formation water, amount of water present and pore structure geometry. The units of resistivity are ohm-meters squared per meter (ohm-m). Resistivity tools fall into two main categories such as laterolog and induction type. Laterolog tools use low-frequency currents (hence requiring water-based mud-WBM) to measure the potential caused by a current source over an array of detectors. Induction-type tools use primary coils to induce eddy currents in the formation and then a secondary array of coils to measure the magnetic fields caused by these currents. Since they operate at high frequencies, they can be used in oil-based mud (OBM) systems. Tools are designed to see a range of depths of investigation into the formation. The shallower readings have a better vertical resolution than the deep readings. Micro-resistivity tools are designed to measure the formation resistivity in the invaded zone close to the borehole wall. They operate using low-frequency current, so are not suitable for OBM. They are used to estimate the invaded-zone saturation and to pick up bedding features too small to be resolved by the deeper reading tools (HLS Asia Ltd., 2008; Darling, T., 2005). Invasion and resistivity profiles are diagrammatic and theoretical, cross sectional views moving away from the borehole and into a formation. They illustrate the horizontal distribution of the invaded and uninvaded zones and their corresponding relative resistivities. These corresponding resistivities and down hole measurement, and resistivity profile are illustrated, respectively in Figure 3.1 and 3.2.

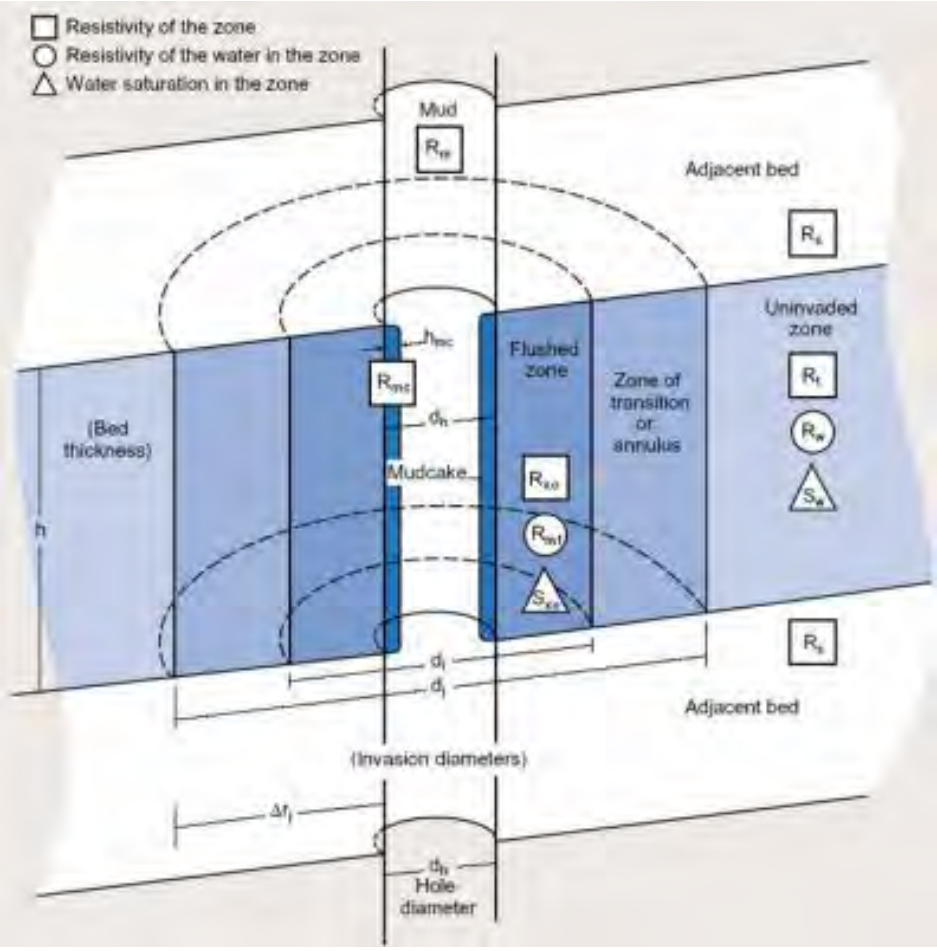


Figure 3.1 Schematic of down hole measurement environment for several zones (Schlumberger, 1998a)

Determining water and hydrocarbon saturation is one of the basic objectives of well logging. Hydrocarbon saturation is the fraction (or percentage) of the pore volume of the reservoir rock that is filled with oil or gas. It is generally assumed, unless otherwise known that the pore volume not filled with water is filled with hydrocarbons. Water saturation is defined as the ratio of the volume of water in pore space to the volume of the total pore space (Schlumberger, 1998a).

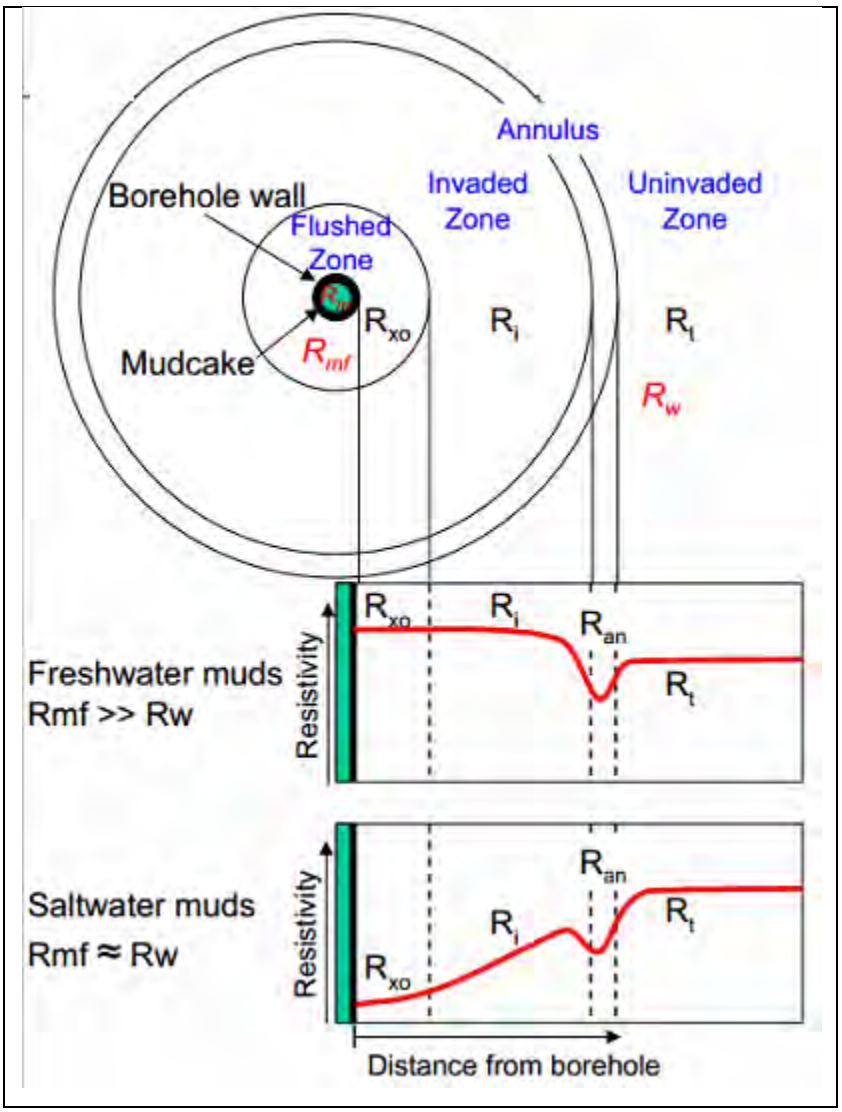


Figure 3.2 Resistivity profile for a transition-style invasion of a hydrocarbon bearing formation (Asquith, G. and Krygowski, D., 2004).

Shaly sand corrections all tend to reduce the water saturation when calculated ignoring the shale effect is ignored in the evaluation processes. Over the years, for shaly sands a large number of models relating fluid saturation to resistivity have been developed according to the geometric form of existing shales (laminated, dispersed and structural). All these models are composed of a shale term and a sand term. All models can be interpreted by clean sand model when the volume of shale is insignificant. For relatively small shale volumes, most shale models might yield quite similar results (Waxman and Smits, 1968; Poupon et al, 1970 and Schlumberger, 1987a). The comparison of the various water saturation equations in shaly sand shows that: a) The clean sand equation does not compensate for clay conductivity, the water saturation it computes is too high;

b) Simandoux or Indonesia equation (Dresser, 1982) is essentially applicable to laminated clay models, with some adaptation for non linear behavior of shale electrical properties and c) Waxman-Smits or Dual Water model (Clavier et al, 1977) is essentially designed for the case of dispersed or structural clay models and as they account for the effects occurring in the pore space, they provide lower water saturation than laminated models (Simandoux, 1963; Waxman and Smits, 1968; Fertl and Hammack, 1971; Clavier et al, 1977; Dresser, 1982, Hamada, G. M., 1996). Some equations of water saturation estimation are mentioned below:

1) The Archie's water saturation equation for clean sands (Archie, 1942):

$S_w = \sqrt[n]{\frac{F.R_w}{R_t}}$ for un-invaded zone and

$S_{xo} = \sqrt[n]{\frac{F.R_{mf}}{R_{xo}}}$ for flushed zone where

n is the saturation exponent which is obtained through lithology assumption or data manipulation and core analysis (i.e. for clean, consolidated sands, n=2),

$R_t$ is the true formation resistivity for un-invaded zone,

$R_w$ is the formation water resistivity and

Formation resistivity factor, $F= \frac{a}{\Phi^m}$ where m and n are the tortuosity factor and cementation exponent, respectively (i.e. a=1.0 and m=2.0 for carbonates, (Asquith, G., and Krygowski, D., 2004).

2) Simandoux model for shaly sand reservoir (Simandoux, 1963):

For a shaly sand partially saturated with hydrocarbons, de Witte (1957) suggested empirical equation: $\frac{1}{R_t} = \alpha \times R_t + \frac{\beta S_w^{\,2}}{R_t}$

In above equation, the values of the coefficients α and β are unique to a single sample or zone. They depend on several factors especially in clay distribution. α and β must be determined from direct measurement. Several investigators have attempted to define α and β to develop a general equation. From Simandoux's laboratory investigation (Simandoux, 1963), it has been found that α and β can be expressed

$\alpha = \frac{V_{sh}}{R_{sh}}$ and $\beta= \frac{1}{F}$ where $V_{sh}$= bulk volume fraction of the shale and $R_{sh}$= shale resistivity.

Using the aforementioned equations, the resistivity of shaly sand can be described by an equation of the form:

$$\frac{1}{R_t} = \frac{V_{sh}}{R_{sh}} \times S_w + \left(\frac{1}{F} \times \frac{1}{R_w} \times {S_w}^2\right)$$

It reduces to the Archie formula when $V_{sh} = 0$. Solving for Sw and using $F = \frac{0.81}{\Phi^2}$, Simandoux proposed the following equation for sandstone:

$$S_w = \left(\frac{0.4 R_w}{{\Phi_e}^2}\right) \times \left[\sqrt{\left\{\frac{{V_{sh}}^2}{{R_{sh}}^2} + \frac{5{\Phi_e}^2}{R_w\, R_t}\right\}} - \frac{V_{sh}}{R_{sh}}\right]$$

where $R_{sh}$ is the true resistivity of clay zone (ohm-m),

$\Phi_e$ = effective porosity that excludes the shale effect and

$V_{sh}$ = Shale volume (fraction).

The derivation and application of Simandoux water saturation model is marred by several shortcomings. These are mentioned below:

i) Simandoux made measurements on only four synthetic samples using one type of clay (montmorillonite), apparently of constant porosity.
ii) The formation factor is not included in the shale effect (α).
iii) Others researchers (Worthington, P. F., 1985) have demonstrated that the shale effect does not apply to disseminated shale condition.
iv) $V_{sh}$ is determined from total shale indicators which do not fully separate clay minerals and other shale materials. They also do not differentiate between clays with high $Q_{CEC}$ (cation exchange capacity), such as montmorillonite, and clays with low $Q_{CEC}$, such as kaolinite.
v) $R_{sh}$ is taken equal to the resistivity of adjacent shale beds. Dispersed shale is a product of diagenesis rather than the depositional process. As a result, it tends to be of different mineralogy than the associated detrital shales.
vi) The model leads to optimistic when the porosity is less than 20%.

Fertl and Hammack developed a water saturation model that inclues most of the aforementioned shortcomings. Their equation (Fertl and Hammack, 1971) can be written as $S_w = \sqrt{\frac{F\, R_w}{R_t}} - \frac{V_{sh}\, R_w}{0.4\, \Phi_e\, R_{sh}}$.

3) The Indonesia model was developed by field observation in Indonesia rather than by laboratory experimental measurement support. It remains useful because it is based on readily available standard log-analysis parameters and gives reasonably reliable results. The formula was empirically modeled with field data in water-bearing shaly sands, but the detailed functionality for hydrocarbon-bearing sands is unsupported, except by common sense and long-standing use. $S_w$ results from the formula are comparatively easy to calculate and, because it is not a quadratic equation, it gives results that are always greater than zero. Several of the other quadratic and iterative-solution models can calculate unreasonable negative $S_w$ results. The Indonesia model (Poupon, and Leveaux, 1971) and other similar models are often used when field-specific SCAL (special core analysis laboratory) rock electrical-properties data are unavailable but are also sometimes used where the SCAL exponents do not measure the full range of shale volumes. Although it was initially modeled on the basis of Indonesian data, the Indonesia model can be applied everywhere. The inputs are the effective porosity ($\Phi_e$), shale volume and resistivity ($V_{sh}$ and $R_{sh}$), formation water and deep resistivities ($R_w$ and $R_t$). The $S_w$ output is usually taken to be the water saturation of the effective porosity, but it has been recently suggested that the output is likely to estimate water saturation of the total porosity, $S_{wt}$ (Woodhouse, and Warner, 2005). Local experience in the Gulf of Suez for Wells 1 and 2 showed that the geometric form of the existing shale is a laminated one. Consequently, the Indonesia equation was used to calculate water saturation in this shaly sand case. Indonesia equation for water saturation estimation (Poupon et al, 1970; Hamada, G. M., 1996) is defined as

For un-invaded zones, $S_w = \left(\frac{1}{R_t}\right)\left[\left\{\frac{V_{cl}{}^{(1-0.5V_{cl})}}{R_{cl}{}^{0.5}}\right\}+\left\{\frac{\Phi_e{}^{(0.5m)}}{aR_w{}^{0.5}}\right\}\right]$ and

For flushed zone saturation, $S_{xo} = \left(\frac{1}{R_{xo}}\right)\left[\left\{\frac{V_{cl}{}^{(1-0.5V_{cl})}}{R_{cl}{}^{0.5}}\right\}+\left\{\frac{\Phi_e{}^{(0.5m)}}{aR_{mf}{}^{0.5}}\right\}\right]$

4) Waxman-Smits-Thomas and Dual-Water models:

The water saturation of the total porosity ($S_{wt}$), is calculated at each reservoir data point by iterative solution of the complex multi parameter Waxman-Smits-Thomas (WST) and dual-water (DW) equations. The WST and DW models are total-porosity, $S_w$ system models. The WST model is based on laboratory measurements of resistivity, porosity, and saturation of real rocks (Waxman and Smits, 1968; Waxman and Thomas, 974). This equation is expressed as

$$\frac{1}{R_t} = \Phi_t^{m*} S_{Wt}^{n*} \{\frac{1}{R_w} + \frac{BQ_v}{S_{wt}}\}$$

where $Q_v$ is the cation-exchange capacity (CEC) per unit PV, B = specific cation conductance in (1/ohm.m)/(meq/mL), and $Q_v$ = CEC in meq/mL of total PV. The exponents m* and n* apply to the total PV. The DW model (Clavier et al., 1984) is also based on the WST data. It uses clay-bound-water conductivity instead of WST's $BQ_v$ factor and an alternative shale-volume descriptor, $S_{wb}$ (The saturation of physically bound water in the total PV). When $V_{sh}$ is zero, $S_{wb}$ is zero; and when $V_{sh}$ is 100% BV, $S_{wb}$ and $S_{wt}$ are also 100% PV.

DW model gives the following equation:

$$\frac{1}{R_t} = \Phi_t^{m_0} . S_{Wt}^{n_0} [\frac{1}{R_{wf}} + \frac{S_{wh}}{S_{wt}} \{\frac{1}{R_{wh}} - \frac{1}{R_{wf}}\}]$$

where $R_{wh}$ = resistivity of clay-bound water ($R_t\Phi_t^m$) in the shales, and $R_{wf}$ = resistivity of free formation water in the shale-free water zones. Because of the different model assumptions, Dual Water exponent $m_o$ and $n_o$ must always be smaller than the WST exponents (Clavier et al., 1984) and may be values similar to "clean" sand exponents.

### 3.1.4 Geothermal gradient and formation temperature

Geothermal gradient ($G_g$) may also be determined by taking pertinent information from the header and using the following equation (HLS Asia Ltd., 2008):

$G_g = [\{\frac{BHT - T_s}{TD}\} \times 100]$ where BHT is the Bottom Hole Temperature in degree Fahrenheit, $T_s$ is the surface (ambient) temperature in degree Fahrenheit and TD is the Total Depth. Once the geothermal gradient ($G_g$) has been established, it is possible to determine the temperature for a particular depth. This is often referred to as formation temperature ($T_f$). As with geothermal gradient, Tf may be determined through the use of charts GEN- 2a or GEN-2b (HLS Asia Ltd., 2008). It may also be calculated using the following equation:

$T_f = [T_s + (\frac{G_s}{100} \times \text{Formation depth}]$.

### 3.1.5 Formation water resistivity

Formation water (connate water) is the water, uncontaminated by drilling mud that saturates the porous formation rock. The resistivity of this formation water ($R_w$) is important interpretation parameters since it is required for the calculation of saturation (water or hydrocarbon) from basic resistivity logs by Inverse Archie's method (Miah and Howlader, 2012; HLS Asia Ltd., 2008) as below equation: .

Formation water resistivity, $R_{wa} = [\frac{R_t . \Phi_{ND}{}^m}{a}]$ for un-invaded zone and

Formation mud filtrate resistivity, $R_{mf} = [\frac{R_{xo} . \Phi_{ND}{}^m}{a}]$ for flushed zone.

A more straightforward method of correcting resistivity (ohm-m) for temperature is through the use of Arp's equation (Asquith, G. and Krygowski, D., 2004):

$R_2 = R_1 \times (\frac{T_1 + k}{T_2 + k})$

Where

$R_2$= resistivity value corrected for temperature, $T_2$

$R_1$= resistivity value at known reference temperature, $T_1$

$T_2$= temperature to which resistivity is to be corrected

k= constant value (6.66 for measured temperature in degree Fahrenheit).

### 3.1.6 Moveable hydrocarbon index

Hydrocarbon movability equation is derived from a comparison of $S_w$ and $S_{xo}$. The greater the difference between $S_w$ and $S_{xo}$, the movability is greater (Serra, O., 2007). If the value for $S_{xo}$ is much greater than the value for $S_w$ then hydrocarbons were likely moved during invasion, and the reservoir will produce. An easy way of quantifying this relationship is through the moveable hydrocarbon index, MHI ($= \frac{S_w}{S_{xo}}$). Once flushed zone water saturation is calculated, it may be compared with the value for water saturation of the un-invaded zone at the same depth to determine whether or not hydrocarbons were moved from the flushed zone during invasion. If the value for $S_{xo}$ is much greater than the value for $S_{w,}$ then hydrocarbons were likely moved during invasion, and the reservoir will produce. When MHI is equal to 1.0 or greater, then this is an indication that hydrocarbons were not moved from the flushed zone during invasion of mud filtrate (Asquith, G. and Krygowski, D., 2004; HLS Asia Ltd., 2008).

### 3.1.7 Bulk volume water

Bulk volume water (BVW) is the product of porosity and water saturation which represents the percentage of rock volume that is water. Water saturation simply represents the fraction of porosity in a reservoir that is occupied by water. In some instances, it may be beneficial to know the fraction of rock volume that is occupied by water. Bulk volume water has several important applications. Within a particular

reservoir, BVW may be calculated at several depths. Where values for BVW remain constant or very close to constant throughout a reservoir, this may be taken as an indication that the reservoir is at or near irreducible water saturation ($S_{wirr}$). Irreducible water saturation is the value of water saturation at which all water within the reservoir is either adsorbed onto grain surfaces or bound within the pore network by capillary pressure. If a reservoir is at irreducible water saturation, then the water present within that formation will be immovable and production will theoretically be water free hydrocarbons. Reservoirs that exhibit variation in values for BVW are typically not at irreducible water saturation and, therefore, at least some water production can be expected. $S_{wirr}$ is related to the grain size of a reservoir. As grain size decreases, the diameters of pore throats within the reservoir will decrease, resulting in higher capillary pressures. This condition implies a reservoir in which a substantial amount of water may be trapped and unable to move. Therefore, when a reservoir is determined to be at irreducible water saturation, values for BVW may be used to estimate the average grain size of that reservoir (Table 3.3). Realizing the potential for error, this approximation may also be used in reservoirs that are not at irreducible water saturation. The presence of clay minerals in a reservoir also has an impact on values of irreducible water saturation and bulk volume water. As the volume of clay minerals in a reservoir increases, both $S_{wirr}$ and BVW will increase because of the inclination of clay to trap interstitial formation water. If a reservoir is deemed to be at $S_{wirr}$, then a log derived estimate of permeability can be made. Constant to near-constant values of bulk volume water within a reservoir indicate that reservoir is at (or at least near) irreducible water saturation (HLS Asia Ltd., 2008).

Table 3.3 Relationship between BVW and grain size in sandstone reservoirs

(Asquith, G. and Krygowski, D., 2004)

| Lithology | Grain Size (mm) | BVW |
|---|---|---|
| Coarse | 1.0-0.5 | 0.02-0.025 |
| Medium | 0.5-0.25 | 0.025-0.035 |
| Fine | 0.25-0.125 | 0.035-0.05 |
| Very Fine | 0.125-0.062 | 0.05-0.07 |
| Silt | <0.0625 | 0.07-0.09 |

### 3.1.8 Log derived permeability

Permeability is the property of a rock that permits the passage of a fluid through the interconnected pores without damage to or displacement of the rock particles Therefore, permeability is the measure of the ability of a porous material to transmit fluids. A rock is termed permeable if an appreciable quantity of fluid can pass through it in a short time and it is termed impermeable if the rate of passage is negligible. Many rocks are impervious to movement of water, oil or gas even though they may actually be quite porous. For example, shales, chalks, clays and some highly cemented sandstones. The unit of measurement of the permeability of a rock is normally expressed in millidarcys, or units of one thousandth of a Darcy. A rock has a permeability of 1 Darcy when 1 $cm^3$ per sec of fluid of unit viscosity in centipoises will flow through a section of 1 cm in length and 1 $cm^2$ in cross section when the difference in pressure on opposite faces is 1 atmosphere. The permeabilities of average reservoir rocks generally range between 5 and 1000 millidarcys (mD). Permeability along with the porosity varies greatly both laterally and vertically in the average reservoir rock. A reservoir rock whose permeability is 5 md or less is called a tight sand or dense limestone according to its composition. The permeability of a reservoir can be measured in three ways as drill stem or production test, permeameter (laboratory test) and wireline logs (Shelly, 1987). If a reservoir is deemed to be at irreducible water saturation, then a log derived estimate of permeability ($K_L$) can be made. Wyllie and Rose method (Crain, E. R., 1986) of permeability determination as

$$K_L = \left[ \frac{(CPERM \times \Phi^{DPERM})}{(S_{wirr}{}^{EPERM})} \right]^2 \text{ in mD for dry gas}$$

Where

$\Phi$ = Porosity and

$S_{w,irr}$ is the water saturation ($S_w$) of zone assumed to be at an irreducible.

# CHAPTER FOUR

## RESULTS AND DISCUSSIONS

Bakhrabad well no. 9 (BK#9) has been selected for the current research purpose where available log data is listed in Table 4.1. The quality of all log data is good except SP log. SP log has not been used in this study. In the studied well, no depth shift has been found in the logs. No environmental corrections are applied to the aforementioned logs. The potassium (percentage), thorium and uranium (ppm) have been taken from spectral gamma ray log. The Gamma Ray API value is taken from natural Gamma Ray log.

Table 4.1 Available log data of BK#9

| Log type | Log Name |
|---|---|
| Borehole measurement log | Caliper log with Bit size |
| Lithology logs | Spectral and Natural Gamma Ray log<br>Self-Potential (SP) log |
| Porosity logs | Spectral density, Dual spaced Neutron, and Sonic Log |
| Resistivity logs | Array compensated true resistivity<br>(Shallow and Deep Resistivity logs) |

### 4.1 Lithology and Hydrocarbon Bearing Zones

Logging parameters have been taken from log header of the studied well that is shown in Table 4.2. Log reading on each available log curve has been taken with respect to depth and then analyzed. The true resistivity of virgin zone is higher than the shallow zone's resistivity in the sand zone in Figure 4.1. The caliper curve shows mud-cake in the sand zone. This mud-cake indicates that the sand zone is porous and permeable. Cross over is showing between Neutron and density logs through the hydrocarbon bearing sand zone in Figure 4.2. There are six hydrocarbon (gas) bearing sand zones found from 2042 m to 2500.5 m (True Vertical Depth-TVD) based on GR log, resistivity log and porosity logs. Among them, one is thick sand from 2120 m to 2138 meter depth.

Table 4.2 Logging parameters of BK#9

| Mud Parameters | Value |
|---|---|
| Location (m) | Lat.: $23^0$36′53.31′′ N, Long.: $90^0$52′45.26′′ E |
| Drillers depth (TVD) | 3535 m |
| Logger depth (TVD) | 2532.7 m |
| Logged Interval (Top & Bottom) | 1707.5 m and 2532.06 m |
| Casing-Diller | 9.625 in @ 1709 m |
| Kelly Bushing Elevation (m) | 7.32 |
| Bit Size (Inch) | 8.5 |
| Type of Fluid | LSND Polymer |
| Density & $P^H$ | 1.14 g/cc and 9.50 |
| $R_m$ and $R_{mf}$ (Ω-m) | 0.80 and 0.75 @$80^0$F |
| BHT & Depth | 280 $^0$F @ 2532.7 m |

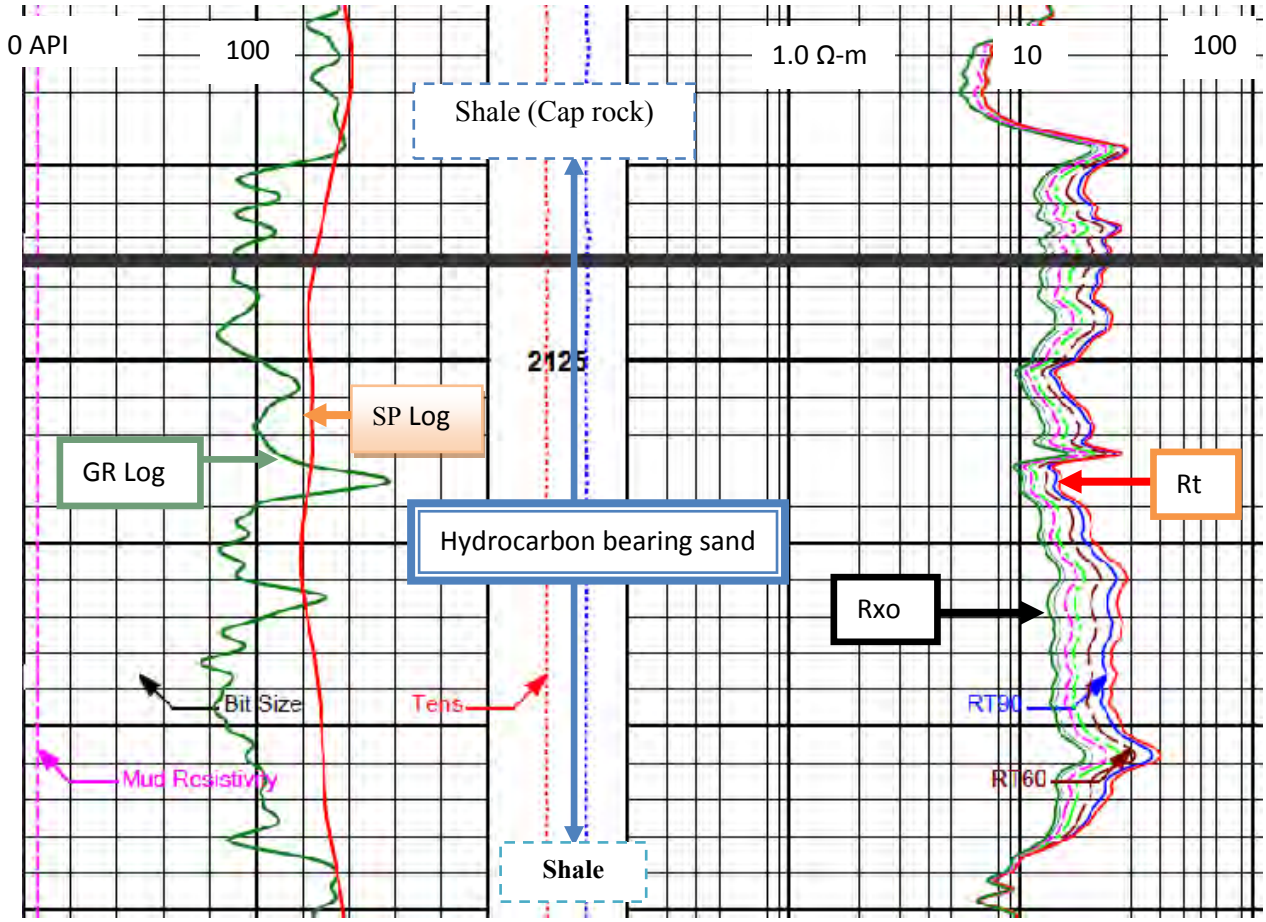


Figure 4.1 Resistivity log including lithology log of hydrocarbon bearing thick sand

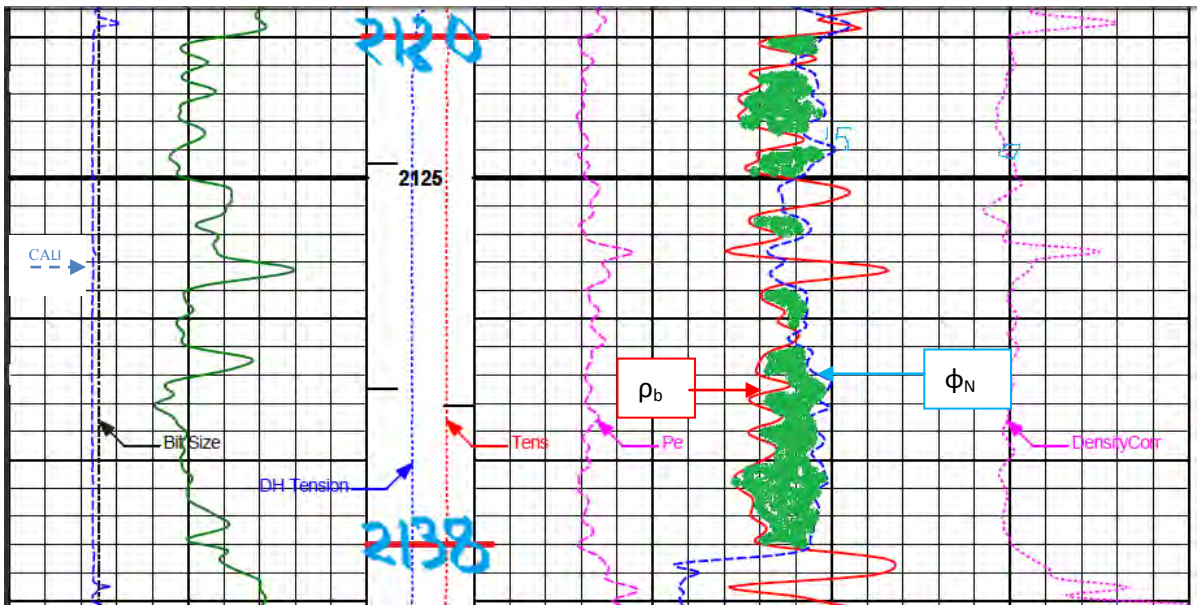


Figure 4.2 Cross-over of thick sand between spectral density and neutron porosity logs

The raw data of different well logs of hydrocarbon bearing zones of BK#9 is shown in Appendix-A1 through A5. The radioactive properties, formation resistivity with bulk density and neutron porosity of six sands are shown in Table 4.3 for BK#9. The true formation resistivity ($R_t$) and flushed zone resistivity, $R_{xo}$ (ohm-m) have been taken from deep and shallow resistivity logs of this well. The bulk density (RHOb), photoelectric absorption cross section ($P_e$) and neutron porosity (NPHI) are taken from litho-density and neutron porosity logs, respectively. According to log data analysis of drilled well, the lithology is mainly sand and shale where sand is the dominant fraction. Clay type is Kaolinite ($P_e$=3.17 from litho-density log) and Shales are laminated. The average bulk density of the six gas bearing sands are found from the litho-density log as 2.37-2.46 gm/cc. The Thorium and Uranium minerals of six sands are 10.761-13.843 ppm and 1.702-2.7 ppm, respectively. Total thickness of thick gas bearing sand reservoir is 18 m which is located at the depth of 2120 m to 2138 m. The depth of all hydrocarbon bearing zones are located in Bokabil Formation of Bengal Basin (RPS Energy, 2009a; IKM, 1990a). A graphical representation of depth versus radioactive properties minerals of thick sand is shown in Figure 4.3.

Table 4.3 Values of formation radioactive minerals, bulk density, resistivity and others

| Parameters | Thin sand-1 | Thin sand-2 | Thick sand-1 | Thin sand-3 | Thin sand-4 | Thin sand-5 |
|---|---|---|---|---|---|---|
| Top-Base (TVD), meter | 2042-2045 | 2100-2102 | 2120-2138 | 2150.5-2156.5 | 2363-2368 | 2498.5-2500.5 |
| Normal GR (API) | 96.00 | 102.00 | 99.00 | 105.00 | 103.00 | 111.00 |
| Th (ppm) | 11.407 | 12.786 | 12.340 | 13.843 | 12.833 | 10.761 |
| U (ppm) | 2.287 | 2.298 | 2.248 | 1.990 | 2.459 | 2.700 |
| K (%) | 1.506 | 1.532 | 1.702 | 1.855 | 1.657 | 1.413 |
| Rt (ohm-m) | 14.00 | 17.00 | 16.00 | 22.80 | 12.90 | 17.00 |
| RHOb (g/cc) | 2.35 | 2.35 | 2.39 | 2.42 | 2.33 | 2.46 |
| NPHI (%) | 24.50 | 19.00 | 17.33 | 16.47 | 16.50 | 12.55 |
| Pe (barns/electron) | 3.12 | 3.23 | 3.17 | 3.34 | 2.92 | 3.53 |
| DELT (µs/ft) | 96.39 | 86.33 | 92.90 | 85.26 | 70.05 | 83.68 |

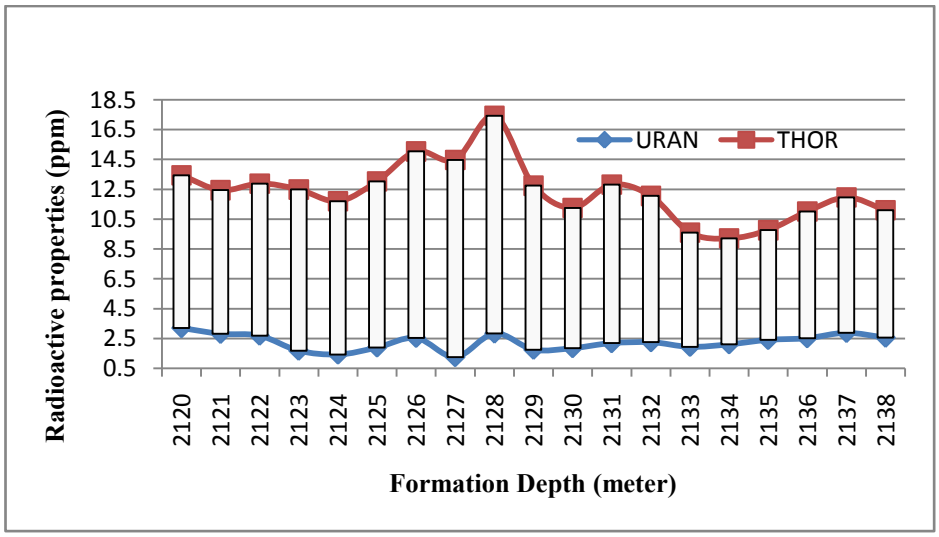


Figure 4.3 Radioactive properties with formation depth of thick sand reservoir

## 4.2 Estimation of Shale Volume and Reservoir Thickness

The maximum abundance of radioactive minerals as Thorium ($Th_{max}$) and Potassium ($K_{max}$) from spectral natural gamma ray log within the formation is 19.231 ppm and 2.818%, respectively at 2405 m (TVD). On the other hand, $K_{min}$ and $Th_{min}$ are 1.315

percent and 8.5546 ppm in 1912 m (TVD). The value of natural gamma ray as $GR_{min}$ and $GR_{max}$ are 76 and 155 API at 1912 and 2405 meter, respectively. The true resistivity ($R_t$) from resistivity log ranges from 12.9 to 22.8 ohm-m (average) of six gas bearing zones. The true resistivity of $R_{cl}$ (clean shale zone) and $R_{tmax}$ (clean sand zone) are 6.0 and 39 ohm-m, respectively. The ranges of minimum and maximum value of shale index (GR-$I_{sh}$) and shale volume of six gas bearing sands is found about 25.3 to 44.3% and 7.6 to 17.6% using GRM for uncompacted (Tertiary) rocks, respectively. Applying Potassium and Thorium concentrated minerals within formation, the shale volume of six zones has been found as ranging from 6.52-35.95% and 20.73-49.57%, respectively. On the other hand, TRM gives the shale volume ranges 14.83 to 38.98. GRM gives lower shale volume than other methods. This value has been used for further estimation of porosity and water saturation. The summarized results are shown in Table 4.4 and graphically in Figure 4.4.

Table 4.4 Estimated shale volume using spectral, natural GR and TR Methods

| Sand Type (Thickness, m) | Spectral GRM (%) | | Natural GRM (%) | TRM (%) |
|---|---|---|---|---|
| | $K\text{-}V_{sh}$ | $Th\text{-}V_{sh}$ | $GR\text{-}V_{sh}$ | $TR\text{-}V_{sh}$ |
| Thin sand-1 (3m) | 12.71 | 26.78 | 7.59 | 35.62 |
| Thin sand-2 (2m) | 14.44 | 39.68 | 11.00 | 26.93 |
| Thick sand-1 (18m) | 25.75 | 35.51 | 11.09 | 17.87 |
| Thin sand-3 (6m) | 35.95 | 49.58 | 13.08 | 29.59 |
| Thin sand-4 (5m) | 22.75 | 40.12 | 11.64 | 39.78 |
| Thin sand-5 (2m) | 6.52 | 20.73 | 17.55 | 26.53 |

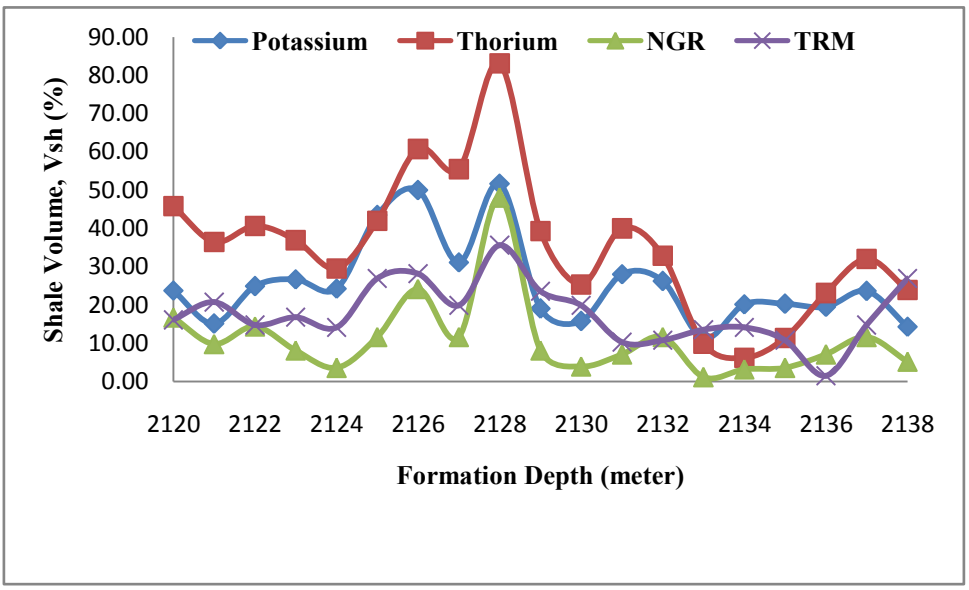


Figure 4.4 Shale volume versus formation depth of thick sand

The aforementioned result shows that the shale volume changed causes for changing the radioactive minerals (Thorium Uranium and Potassium concentration) within formation (Total GR value) with respect to depth. From GR method, estimated arithmetic average shale volume of thick sand is found about 11.09 percent which is almost close to estimated shale volume (8%) by IKM, 1991 (G sand: 2084-2140m TVD, BK#3). The gross thickness of thick sand is 18m (2120-2138m) where net thickness is 17m. The Net to Gross ratio has been estimated to be 0.94 based on spectral and natural GR log.

## 4.3 Assessment of Porosity

Porosity has been estimated from single log methods as well as from Neutron-Density combination formula. In this method, individual porosity from Neutron, Density and Sonic logs have been calculated and compared with each other. In order to interpret and analyse the log data, matrix travel time ($\Delta T_{ma}$) of 55.5µs/ft and matrix density ($\rho_{ma}$) of 2.65gm/cc (Schlumberger, 1998a) has been used for porosity assessment in sandstone reservoir. The fluid density ($\rho_f$) of 1.0 gm/cc and fluid travel time ($\Delta T_f$) of 189µsec/ft (Schlumberger, 1998a) has been used for porosity estimation. On the other hand, adjacent shale neutron porosity of 16% is used for porosity estimation. The estimated porosity results are shown in Appendix-C1 and C2. The summarized results of porosity are shown in Table 4.5 and graphically represented in Figure 4.5. Formation evaluation is

made by using cutoff shale volume (GRM-$V_{sh}$), effective porosity and water saturation of 40%, 8%, and 60%, respectively. The aforementioned cut off values is taken from the previous log interpretation report (RPS Energy, 2009c).

Table 4.5 Estimated porosity from Neutron, Density and Sonic logs

| Sand Name | Thin sand-1 | Thin sand-2 | Thick sand-1 | Thin sand-3 | Thin sand-4 | Thin sand-5 |
|---|---|---|---|---|---|---|
| NPH (%) | 24.50 | 19.00 | 17.33 | 16.47 | 16.50 | 12.55 |
| PHID (%) | 19.09 | 18.18 | 17.22 | 14.10 | 19.39 | 11.52 |
| $PHI_{N-D}$ (%) | 21.96 | 18.60 | 17.36 | 15.33 | 11.52 | 12.04 |
| $PHI_{N-De}$ (%) | 20.79 | 16.87 | 15.64 | 13.28 | 16.18 | 9.28 |
| PHIs | 30.63 | 23.09 | 28.02 | 22.29 | 10.90 | 21.11 |
| $\Phi_{sonic\ ,\ gas}$ (%) | 21.44 | 16.16 | 19.61 | 15.60 | 7.63 | 14.78 |

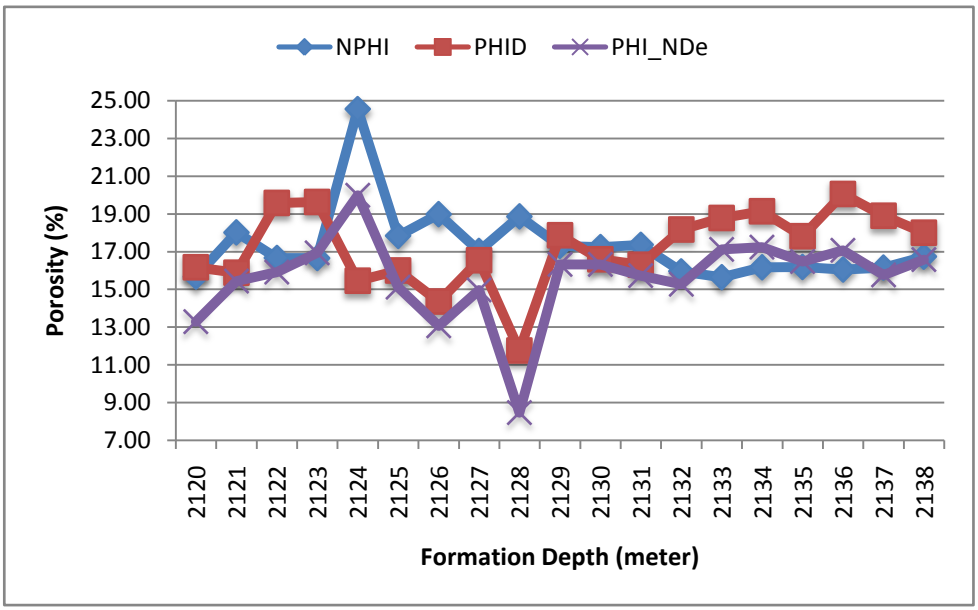


Figure 4.5 Depth versus average porosity of thick sand reservoir

The sonic log generally gives higher porosity because of gas effects. The total porosity from sonic log is 28.02% but corrected sonic porosity for gas effect is 19.61% by Hilchie formula in thick sand reservoir. Among gas sands, the arithmetic average neutron and density porosity ranges are 12.55-24.50% and 11.52-19.39% respectively, but neutron

and density combination formula gives 12.04 to 21.96 % porosity. The estimated porosity using clay corrected neutron-density combination formula is 9.28 to 20.79 % for gas bearing reservoir. This porosity quality is good for this gas pools.

## 4.4 Geothermal Gradient and Formation Temperature

The determined geothermal gradient and formation temperature of the studied well is shown in Appendix-E1. From the log data analysis, it is found that the geothermal gradient is 3.948 $^0$F per 100 meter of BK#9 with average formation temperature of thick sand depth interval of 163.71 to 164.42 $^0$F. From the analysis, it is found that this (2120-2138m TVD) well shows lower geothermal gradient compared with 5.91 $^0$F per 100m of G sand (IKM, 1990a). The geothermal gradient and formation temperature are varied with respect to depth of the formation.

## 4.5 Formation Water Resistivity

As stated earlier that formation water resistivity ($R_w$) has been calculated from Inverse Archie's method ($R_{wa}$ analysis) where tortousity factor (a) of 1.00 and cementation exponent (m) of 2.25 (IKM, 1990a) has been used. The data has been taken from several water bearing sands of the well for $R_{wa}$ analysis (Appendix-D). The minimum value of $R_w$ is 0.104 and mud-filtrate resistivity ($R_{mf}$) is 0.157 ohm-m has been found in interval from 1960 to 1969 meter (TVD). Finally considering this interval, $R_w$ and $R_{mf}$ have been calculated for others gas bearing sands and then corrected for formation temperature with respect to depth. Thus a profile of $R_w$ and $R_{mf}$ are prepared and water saturation is estimated for each thin and thick gas sands level (Appendix-E1). Salinity of thick sand interval has been estimated using Chart Gen-9 (Schlumberger, 1998b). The average formation water resistivity has been found as 0.10 ohm-m by $R_{wa}$ analysis and formation salinity is about 29000 ppm of NaCl at 164 $^0$F. The surface salinity is 32000 ppm of NaCl with respect to $R_w$ of 0.197 ohm-m at 80 $^0$F using Chart Gen-9 in Appendix-E2. The field measured resistivity is 0.38 ohm-meter at 76$^0$F with a NaCl content of 15,000 ppm and 0.2 ohm-m at 175 $^0$F by IKM, 1990a. The mud filtrate resistivity ($R_{mf}$) has also been estimated in the same way for studied well and shown in Appendix-E1.

## 4.6 Determination of Water Saturation

The tortousity (a), saturation (n) and cementation exponent (m) value of 1.00, 2.00 and 2.00 has been used for water saturation estimation for both thick and thin sands of this well, respectively (Schlumberger, 1998a). Estimated water saturation is shown in Table 4.6 for gas bearing sands, and graphical representation is also shown in Figure 4.6. The detailed results are shown in Appendix-F1, F2 and F3.

Table 4.6 Estimated water saturation from different models

| Sand type | Thickness (meter) | Archie's formula (average, %) | | Indonesia model (average, %) | | Simandoux model (average, %) |
|---|---|---|---|---|---|---|
| | | $S_{wa}$ | $S_{xoa}$ | $S_{wi}$ | $S_{xoi}$ | $S_{ws}$ |
| Thin sand-1 | 3 | 13.12 | 22.34 | 39.02 | 56.92 | 36.71 |
| Thin sand-2 | 2 | 14.47 | 25.98 | 41.64 | 64.09 | 40.77 |
| Thick sand-1 | 18 | 14.26 | 27.60 | 39.18 | 70.96 | 40.30 |
| Thin sand-3 | 6 | 18.74 | 30.15 | 51.84 | 77.83 | 53.05 |
| Thin sand-4 | 5 | 16.31 | 24.63 | 48.05 | 65.09 | 47.36 |
| Thin sand-5 | 2 | 24.08 | 37.12 | 62.31 | 99.54 | 71.21 |

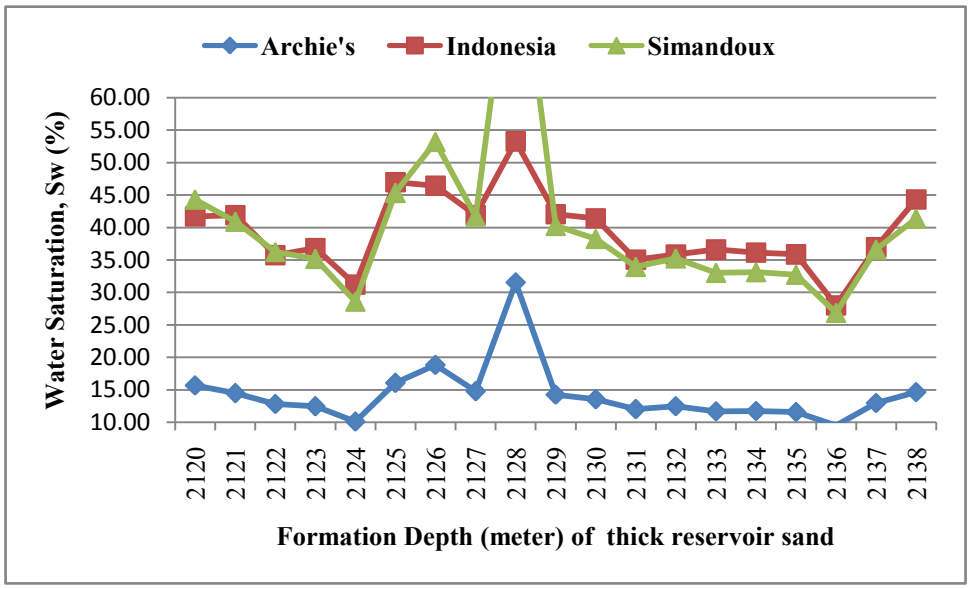


Figure 4.6 Average water saturation of thick sand of different models

From the Archie's equation, it is found that highest water saturation is about 29.3% at a depth of 2128m and the lowest value is about 9.8% at 2136m of thick sand. These highest and lowest saturation values are also confirmed by Indonesia and Simandoux model as shown in Figure 4.6. From Simandoux model, estimated water saturation is found about 89% in Figure 4.6 at 2128m depth because of shale effect. The maximum to minimum value of hydrocarbon (gas) saturation from Archie's formula, Simandoux and Indonesia models are 86.88-75.92, 63.29-28.79 and 60.98-37.69 percent, respectively. Indonesia equation and Simandoux model give more reliable saturation value than Archie's formula because this reservoir is almost shaly sand reservoir. On the other hand, Archie's formula gives better estimation of water saturation for clean sand reservoirs of any formation. This fluid saturation is most important for reserve estimation and reservoir data analysis of this well.

## 4.7 Moveable Hydrocarbon Index and Bulk Volume Water

The average moveable hydrocarbon index (MHI) of six reservoir sands ranges are 0.52 to 0.66 by Archie's formula and 0.57 to 0.74 from Indonesia equation which is an indication that hydrocarbons were moved from the flushed zone during invasion of mud filtrate. So, hydrocarbon is moveable within thick and thin sands reservoir of this formation. The BVW (Product of porosity and water saturation) has been estimated from Archie's formula, and Indonesia - Simandoux model's water saturation of gas sands which ranges from 0.021 to 0.027, 0.058 to 0.081 and 0.063-0.077, respectively. Detailed results of MHI and BVW are shown in Appendix- F1, F2 and F3. These values are indicating that the grain size of this reservoir sand is coarse to medium and very fine, respectively (After Asquith, G. and Krygowski, D., 2004).

## 4.8 Log Derived Permeability

The permeability of the reservoir sand has been calculated using Wyllie & Rose equation assuming irreducible water saturation, $S_{wirr}$ of 18%, permeability constant (CPERM) of 8581 (RPS Energy, 2010), irreducible saturation exponent (EPERM) of 2.00, and porosity constant (DPERM) of 4.40, respectively (IKM, 1990a). Using the above parameters, the average log derived permeability ranges from 7.59 to 263.90 mD by Wyllie and Rose method of six reservoir sands. Among gas bearing sands, the minimum, maximum and average values of permeability are 5.07, 85.45 and 221.99 mD,

respectively for thick sand reservoir. Detailed result of gas bearing reservoir permeability is shown in Appendix-G.

## 4.9 Comparison of Petrophysical Properties with Different Studies

The petrophysical properties of thick gas bearing reservoir (local named as G sand) of BK Field (BK#1 to BK#9) including the current studied well in a tabular form is shown in Table 4.7.

Table 4.7 A comparison of petrophysical properties of different wells (thick sand)

| Parameters/ Properties | IKM, 1991 | | | | | | | | RPS Energy, 2009 (P10 to P90) | Current Study |
|---|---|---|---|---|---|---|---|---|---|---|
| Well No. | BK# 1 | BK# 2 | BK# 3 | BK# 4 | BK# 5 | BK# 6 | BK# 7 | BK# 8 | BK# 1-8 | BK#9 |
| G or Thick sand interval, ft (TVD) | 6850 - 7030 | 6920 - 7000 | 6840 - 7020 | 6920 - 7000 | 6960 - 7103 | 6920 - 7100 | 6820 - 7000 | 6912 - 7028 | 7813 – 8826 (MD) | 6953 - 7013 |
| Net Pay, ft | 49.5 | 74.5 | 81.5 | 58.0 | 100 | 59.5 | 89.0 | 61.5 | 32.5- 144 | 63 |
| $V_{sh}$ (%) | 18.0 | 23.0 | 11.0 | 17.0 | - | 19 | 20.0 | 18.0 | 8.5-32.0 | 11.0 |
| $\Phi_e$ (%) | 19.8 | 16.8 | 21.6 | 20.0 | - | 15.7 | 16.7 | 19.0 | 13.6 -21.2 | 15.6 |
| $S_w$ (%) | 26.8 | 26.2 | 37.5 | 27.9 | - | 35.5 | 31.0 | 25.9 | 18.4 - 37.8 | 39.1 |
| $R_w$ (Ω-m) | 0.2 at $175^0$F | | | | | | | | 0.2 at $175^0$F | 0.1 at $164^0$F |
| $R_t$ (Ω-m) | 30-70 | | | | | | | | N/A | 17-38 |
| $K_L$ (mD) | 109.4 (BK#2) and 98.8 mD (BK#3) from Production Test Data | | | | | | | | 61.3 - 219.3 | 34.2 - 222.0 |
| MHI | N/A | | | | | | | | N/A | 0.57 |
| BVW | N/A | | | | | | | | N/A | 0.06 |

## 4.10 Justification and Uncertainty of the Results

The available logs are interpreted and analyzed using different methods and different approaches. Each method has some limitations in their applicability. Some uncertainties are also there in assumption and application for formation evaluation of this well. Some error may also be there in picking the correct log values. However, uncertainty on logs as well as on the analytical procedure has been described under the following headings:

- Shale volume: This may be changed due to heterogeneity of radioactive minerals within the formation.
- Porosity assessment: Single log porosity method and Neutron-Density combination formula have been used for porosity estimation. Individual porosity logs give big differences of porosity values. Cross-Plot method (gives best result other than core) could not be followed as pure water bearing zones are uncommon in the studied well. The assumed values of both fluid and matrix density, and travel time may be changed due to inhomogeneity of the lithology. Porosity from core analysis is more reliable than the aforementioned methods.
- Formation water resistivity and selection of exponents: The water bearing clean sands are uncommon in the studied well. As a result, the estimation of corrected $R_w$ may be wrong due to changing of cementation exponent (m) and actual sub-surface formation temperature. This is an important parameter for estimation of formation water saturation. These exponents (a=1, m=2 and n=2) are critical in calculating porosity, formation water resistivity and water saturation of flushed zones as well as un-invaded zones.

# CHAPTER FIVE

## CONCLUSIONS AND RECOMMENDATIONS

### 5.1 Conclusions

Based on the log interpretation and formation evaluation using available wireline log data for BK#9 well, the conclusions are as follows:

- Thick gas bearing sand (G sand) is the main reservoir of this well where lithology is mainly medium to coarse grained sand with subordinate shale of laminar type. The average Gamma Ray and resistivity ranges are 96-111 API and 13-23 ohm-m of reservoir sands where shale content is about 11 and 18 % from Natural Gamma Ray and True resistivity methods of thick sand, respectively.
- Neutron-Density combination formula gives better effective porosity value of shaly sand reservoirs which is about 9.28-20.79 % as compared to the single log method. This is good quality porosity of this formation.
- Log analysis shows that the average formation water resistivity ($R_w$) of thick gas bearing sand is 0.10 ohm-m from $R_{wa}$ analysis and formation salinity is about 29000 ppm of NaCl and surface salinity is about 32000 ppm (NaCl) with Rw of 0.197 ohm-m.
- Simandoux and Indonesian model give a pessimistic value of water saturation of virgin zone in thick sand as 40 and 39%, respectively compared with the Archie's formula (14%). The first two saturation methods are more reliable for shaly sand reservoir and they also match with earlier interpretations. Thus, average gas saturation of thick sand is found to be about 60% at depth interval 2120-2138m (TVD). Gas is also moveable within thick and thin sands reservoir of this reservoirs or formation. The estimated log derived average permeability from Wylie-Rose method has been estimated as 34-222 mD which is a good permeability for sand reservoirs. So the gas pools of this formation are potential for production gas.

## 5.2 Recommendations

Bakhrabad field is one of the onshore gas fields of Bangladesh. From the current study of the available log data of this gas field, the following recommendations may be drawn:

- In order to assess the quality of the reservoir sands of variable thickness, whether it is thick or thin, this field should be given careful attention in the light of formation evaluation with data from new drilled wells.
- To estimate the water saturation of a reservoir, the special or routine core analysis is required. The estimated reservoir thickness, porosity and hydrocarbon saturation can be used for future reserve estimation and reservoir properties analysis of this formation.
- To assess the quality of the gas reservoirs of Bangladesh accurately, special logging tools such as Nuclear Magnetic Resonance (NMR) and Formation Micro-Scanner (FMS) logs can be run with conventional wire line logs.
- All the nine wells drilled so far in this structure are mainly located to the northern part of the structure. To date, no wells has been drilled in the flank of the structure that could tell the extension and quality of the reservoir as well as its gas saturation, presence of fluid contact (GWC), and minimize the uncertainty of estimation of hydrocarbon reserve. Additional wells may be drilled in the southern end part of the structure for better picture of the lithology of this gas field.

## REFERENCES


- Akhanda, A. R., and Islam, Q., 1994, Introduction to Petroleum Geology and Drilling, Publication-cum-Information Office, Bangladesh, p. 78.
- Archie, G. E., 1942, The Electrical Resistivity Log as an Aid in Determining Some Reservoir Characteristics, Trans. of AIME Transactions, V. 146 (1), p. 54-67. http://dx.doi.org/10.2118/942054-G.
- Asquith, G., and Krygowski, D., 2004, Basic well log analysis, American Association of Petroleum Geologists, Second Edition, Tulsa, Oklahoma, p. 216.
- Bakhrabad Gas Field, 1993, Reservoir Engineering Report Based on 1992 and 1993 Pressure Surveys-Reservoir Study Unit, PIU & BAPEX, Petrobangla, Bangladesh Gas Fields Company Limited (BGFCL) Library.
- BGFCL, 2009, Main Gas Reserves of Different Gas Fields Under BGFCL, Reservoir Engineering Section, Bangladesh
- Bassiouni, Z., 1994, Theory, Measurement and Interpretation of Well Logs, First Printing, Henry L. Doherty Memorial Fund of AIME, SPE, Richardson, TX, p. 372.
- Bateman, R. M., 1985, Open Hole Log Analysis and Formation Evaluation: IHRDC Publishers, Boston MA, p. 647.
- Beaumont A. E. and Foster H. N., 1999, Hand Book of Petroleum Geology, American Association of Petroleum Geologists, Tulsa, Oklahoma, p. 45-63.
- Choudhury, Z., 1999, Reservoir Engineering Study of Bakhrabad Gas Field, M. Sc. Thesis, PMRE Dept., Bangladesh University of Engineering and Technology (BUET).
- Choudhury, Z. and Gomes, E., 2000, Material Balance Study of Gas Reservoirs by Flowing Wellhead Method: A Case Study of Bakhrabad Gas Field, SPE Asia Pacific Oil and Gas Conference and Exhibition in Brisbane, Australia, SPE 64456, October 2000, pp. 16-18.
- Clavier, C., Coates, G., and Dumanoir, J., 1984, Theoretical and Experimental Bases for the Dual-Water Model for Interpretation of Shaly Sands, SPE Journal- 24 (2), pp. 153-168, http://dx.doi.org/10.2118/6859-PA. SPE-6859-PA.
- Crain, E. R., 1986, The Log Analysis Handbook, Volume-1, Quantitative Log Analysis Methods, PennWell Publishing Company, Tulsa, Oklahoma, USA, p. 328.
- De Witte, A. j., 1957, Saturation and Porosity From Electric Logs in Shaly Sands, Oil & Gas Journal, March 1957, pp. 89-93.
- Dresser Atlass, 1982, Well Logging and Interpretation Techniques, Dresser Ind. Inc.

- Darling, T., (2005), Well Logging and Formation Evaluation, Gulf Professional Publishing, p.326.
- Fertl, W.H. and Hammack, C.W., 1971, A Comparative Look at Water Saturation in Shaly Pay Sand, in 12th Annual Logging Symposium Transaction: Society of Professional Logging Analysts.
- Hamada, G. M., 1996, An integrated Approach to determine shale volume and hydrocarbon potential in shaly sand, 1996 SCA Conference Ppaer Number 9641. pp. 1-16.
- Hilchie, D. S., 1982, Applied Open Hole Log Interpretation for Geologist and Engineers: Douglas W. Hilchie Inc., Golden Colorado.
- HLS Asia Limited, 2008, Basic Log Interpretation, p. 106.
- Kobesh, F. P. and Blizard, R. B., 1959, Geometric Factors in Sonic Logging: Geophysics, v.24, pp. 64-76.
- Poupon,A., Clavier, C, Dumanoir,J., Gaymard,R. and Misk, A., 1970, Log Analyses of Sand-Shale Sequences-A Systematic Approach, Journal of Petroleum Technology, July 1970, p. 867-881.
- Poupon, A. and Leveaux, J., 1971, Evaluation of Water Saturations in Shaly Formations, The Log Analyst-12 (4).
- Interkomp Kanata Management (IKM), 1991a, Geological, Geophysical and Petrophysical Report of Bakhrabad Gas Field, Petrobangla, Bangladesh, p. 88.
- IKM, 1991b, Reservoir Engineering Report of Bakhrabad Gas Field, Petrobangla Bangladesh, p. 92.
- Imam, B., 2013, Energy Resources of Bangladesh, Second Edition, University Grants Commission Publication No. 151, Bangladesh, 2013, p. 324.
- Miah, M. Islam and Howlader, M. F., 2012, Prediction of Formation Water Resistivity from $R_{wa}$ Analysis of Titas Gas Field Using Wireline Log Data, Journal of Petroleum and Gas Exploration Research (JPGER), Vol. 2(4), p. 57-60.
- RPS Energy, 2009a, Bakhrabad Geological Study, Petrobangla, Dhaka, Bangladesh, p. 50.
- RPS Energy, 2009b, Bakhrabad Geophysics Report, Petrobangla, Dhaka, Bangladesh, p. 81.
- RPS Energy, 2009c, Bakhrabad Petrophysical Report, Petrobangla, Dhaka, Bangladesh, p. 109.
- RPS Energy, 2009d, Bakhrabad Petroleum Engineering Report, Dhaka, Bangladesh, p. 61.
- Schlumberger, 1998a, Log Interpretation Principles/Applications, 7$^{th}$ printing, Houston, p. 235.

- Schlumberger, 1998b, Log Interpretation Charts, Schlumberger Well Services, Houston, p. 65.
- Shelly, R.C., 1998, Elements of Petroleum Geology, Academic Press. London, p. 470.
- Serra, O., 2007, Well Logging and Reservoir Evaluation, ISBN: 978-2-7108-0881-7, p. 250.
- Simandoux, P., 1963, Measures dielectrique en milieu poreus, application a measure de saturation en eau, etude des massifs argileaux, Revue de I' ins. Francais du Petrole, (Supplementary Issue, 1963), p. 193-215.
- Waxman, M. H., and Smits, L. J. M., 1968, Electrical Conductivities in Oil-Bearing Shaly Sands, SPE Journal- 8 (2), pp. 107–122, SPE-1863-PA. http://dx.doi.org/10.2118/1863-PA.
- Waxman, M. H. and Thomas, E. C., 1974, Electrical Conductivities in Shaly Sands-I, The Relation Between Hydrocarbon Saturation and Resistivity Index-II. The Temperature Coefficient of Electrical Conductivity, Journal of Petroleum Technology, 26 (2), pp. 213-225. http://dx.doi.org/10.2118/4094-PA.
- Welldrill (UK) Ltd., 1983, Final Well Report, Bakhrabad Wells (BK-1, 2, 3 4 and 5).
- Woodhouse, R. and Warner, H. R., 2005, Sw and Hydrocarbon Pore Volume Estimates in Shaly Sands- Routine Oil-Based-Mud Core Measurements Compared With Several Log Analysis Models, Presented at the SPE Annual Technical Conference and Exhibition, Dallas, Texas, 9-12 October 2005. http://dx.doi.org/10.2118/96618-MS.
- Worthington, P. F., 1985, The Evaluation of Shaly Sand Concepts in Reservoir Evaluation, The Log Analyst-24, No. 1.
- Wyllie, M. R. J, Gregory, A. R., and Gardner, G. H.F, 1956, Elastic Wave Velocity in Heterogeneous and Porous Media, Geophysics-21, January 1956, pp. 41-70.

## Appendix-A1: Lithology and Resistivity logs of BK#9

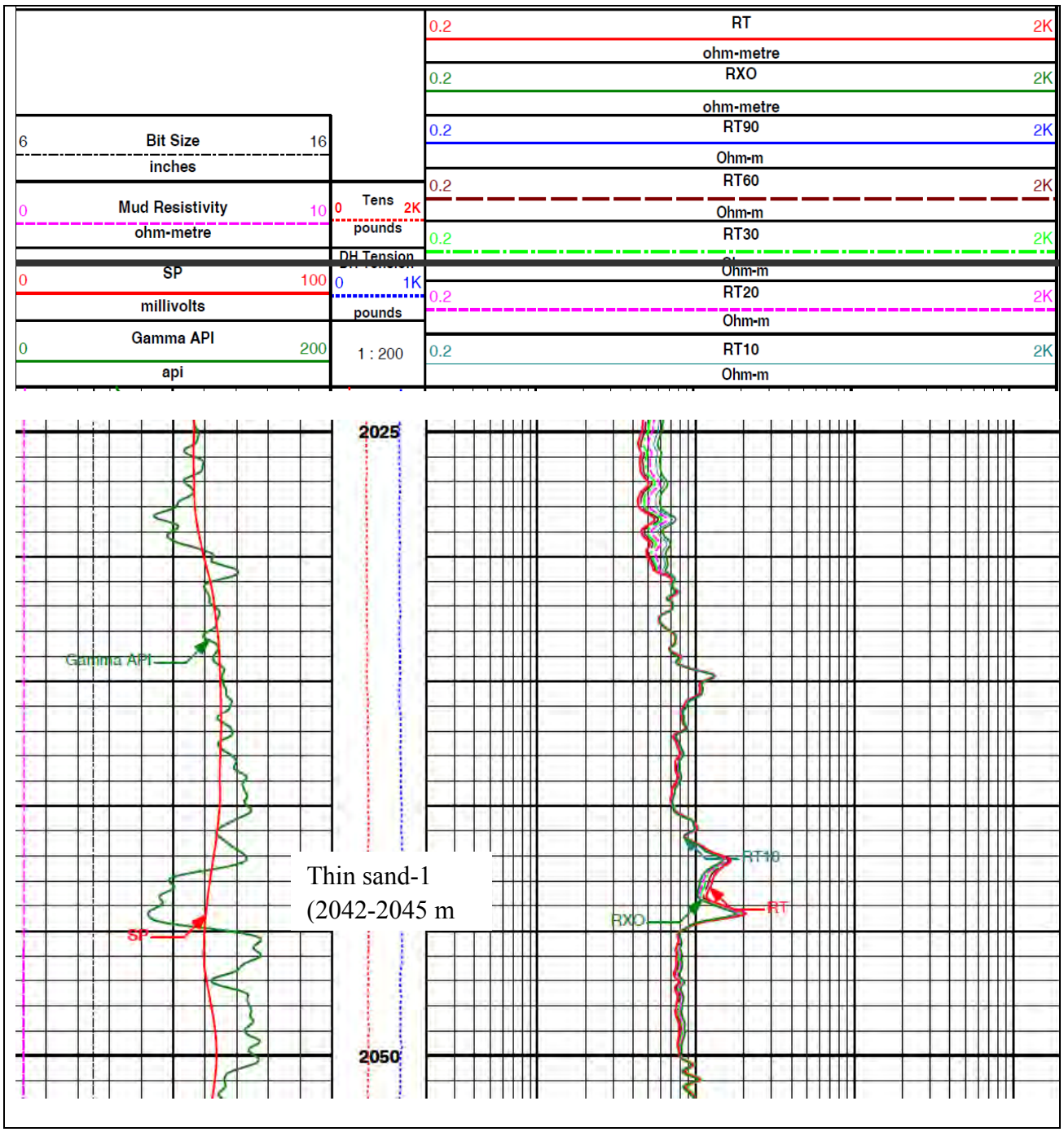

## Appendix-A2: Spectral and natural GR logs of thin sand-1 reservoir

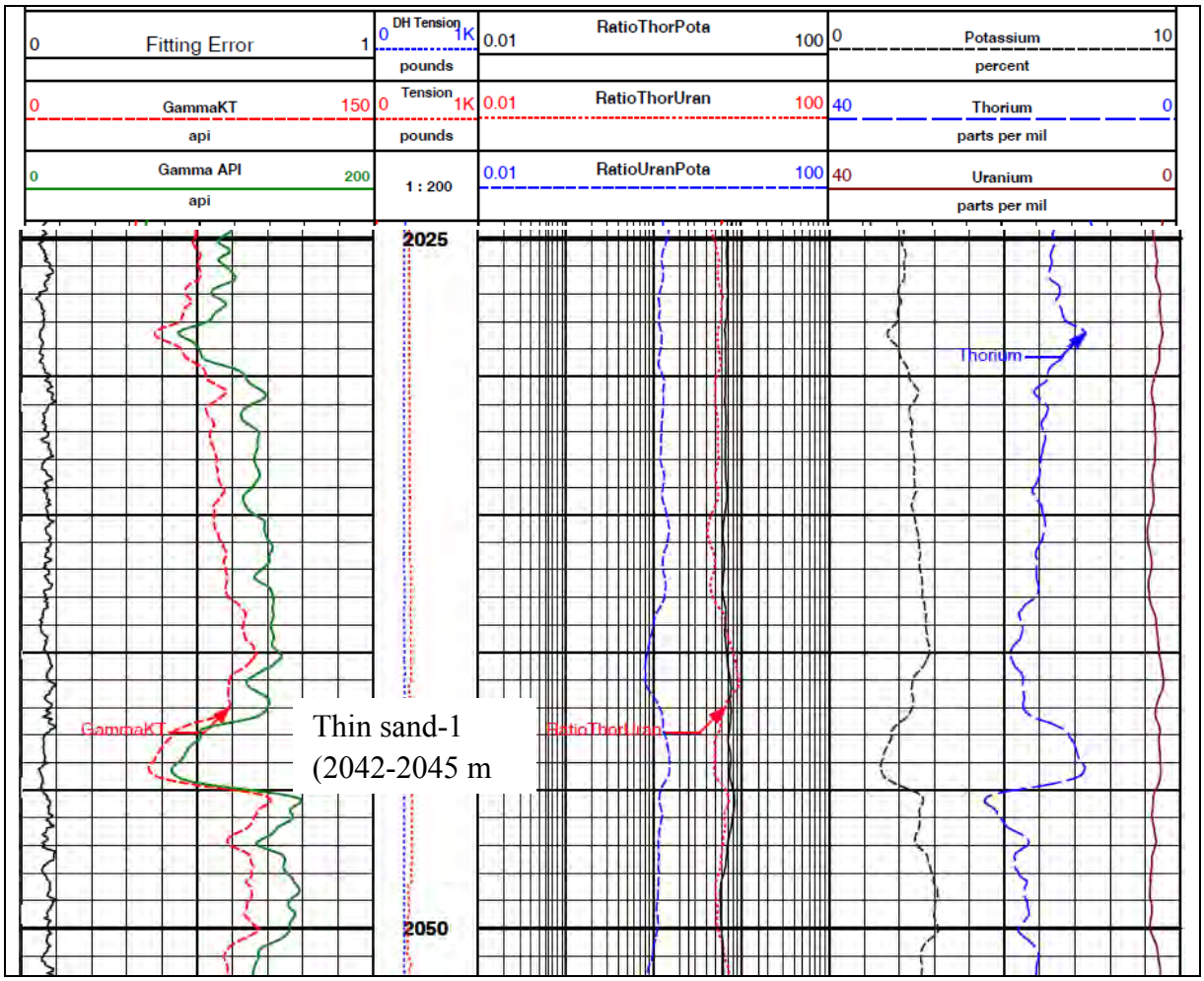

## Appendix-A3: Spectral density, Dual spaced neutron and GR logs

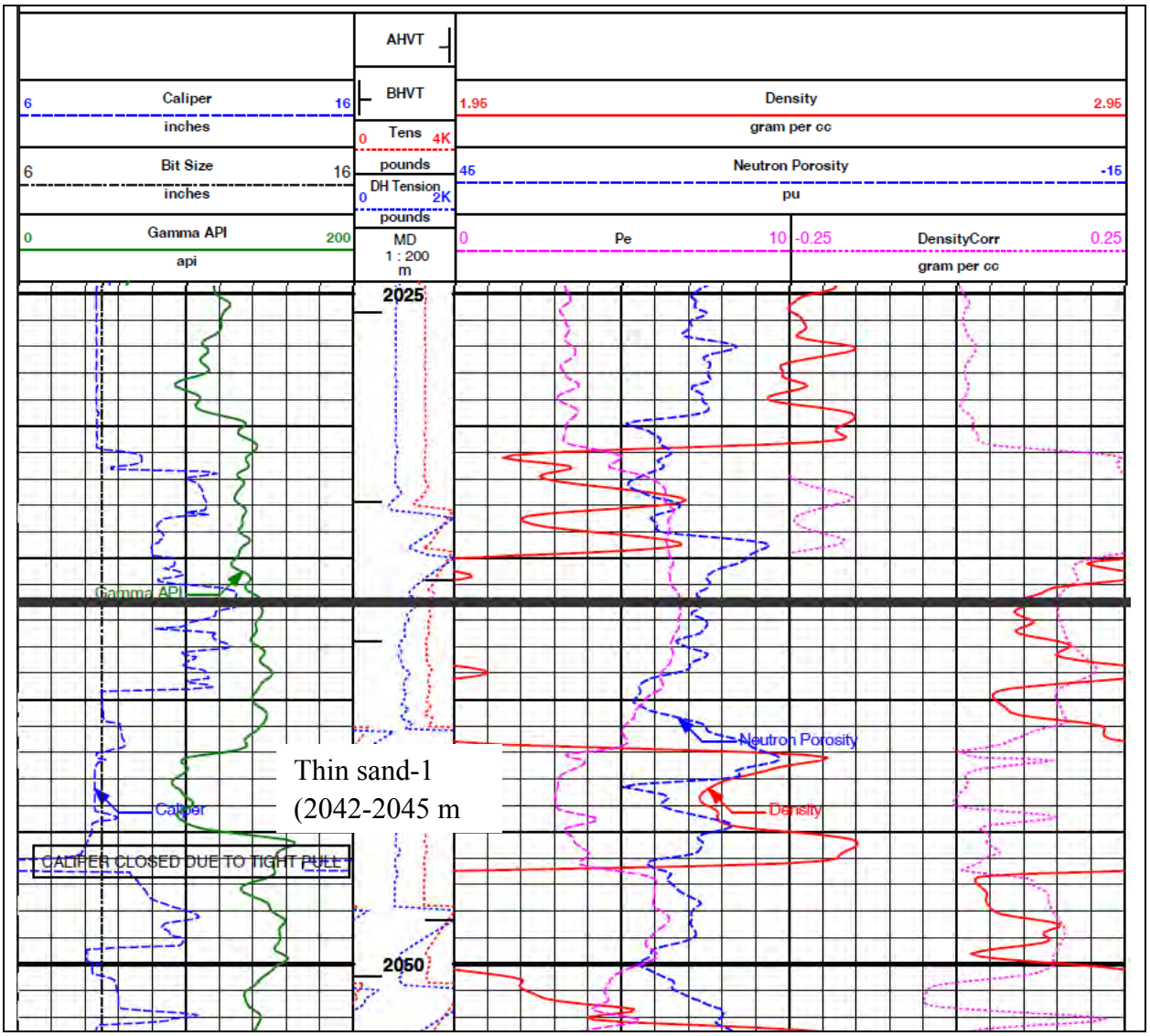

## Appendix-A4: Borehole compensated sonic array log of BK#9

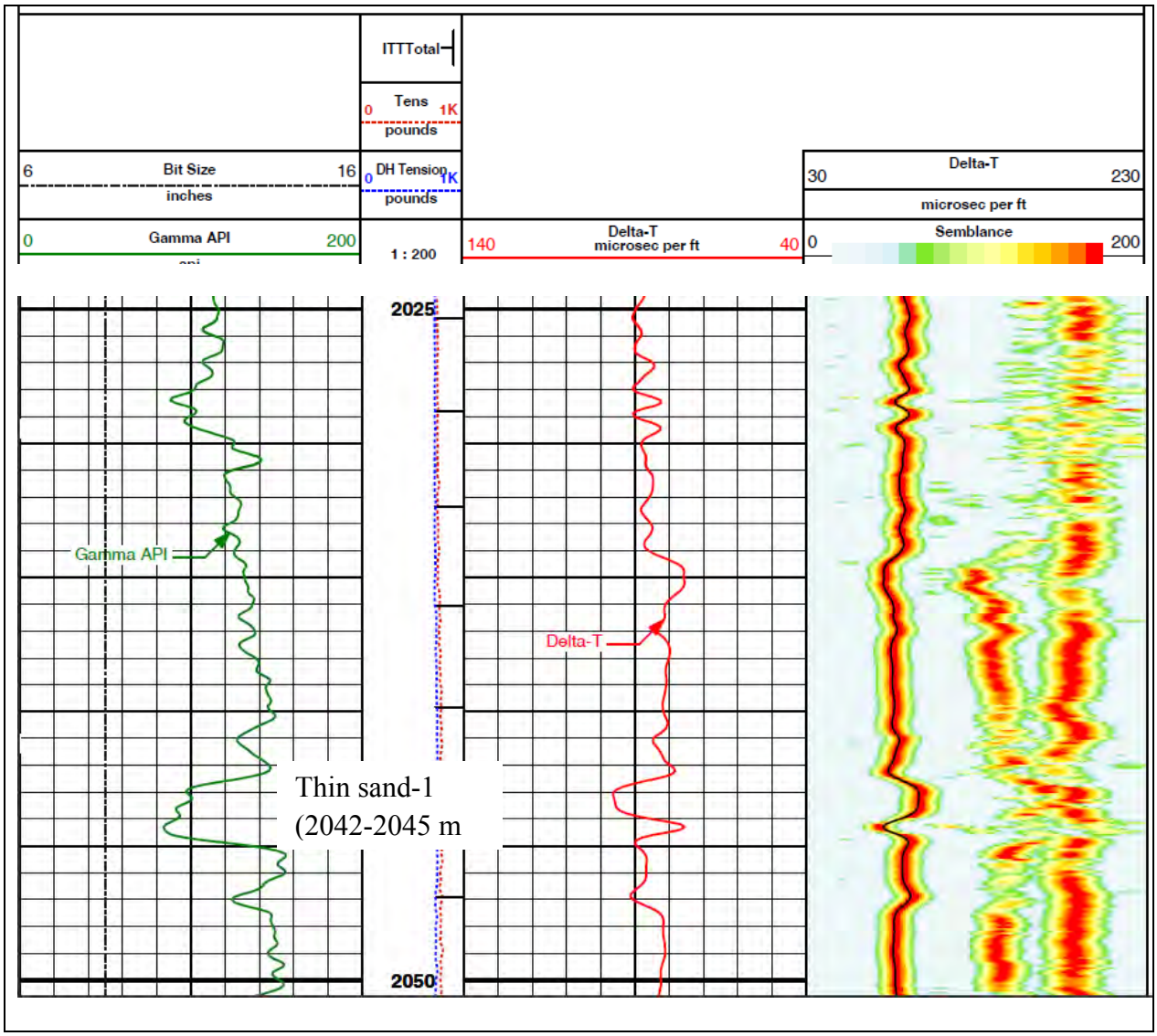

## Appendix-A5: Raw data from different logs for formation evaluation

**Thick sand reservoir (BK#9)**

| Depth interval | | Lithology Logs | | | | Resistivity logs | | Porosity logs | | | | CALI |
|---|---|---|---|---|---|---|---|---|---|---|---|---|
| Top | Bottom | THOR | POTA | URAN | GR | $R_t$ | $R_{xo}$ | $\rho_b$ | NPHI | Pe | DET | Hole, d |
| meter | meter | ppm | % | ppm | API | ohm-meter | | g/cc | % | b/elec. | µs/ft | inc. |
| 2119 | 2120 | 13.444 | 1.672 | 3.193 | 110.0 | 23.0 | 15.0 | 2.38 | 15.68 | 3.26 | 87.55 | 8.35 |
| 2120 | 2121 | 12.444 | 1.542 | 2.806 | 100.0 | 20.0 | 12.0 | 2.39 | 18.02 | 3.29 | 92.80 | 8.33 |
| 2121 | 2122 | 12.887 | 1.689 | 2.688 | 107.0 | 24.0 | 12.5 | 2.33 | 16.67 | 3.07 | 93.28 | 8.31 |
| 2122 | 2123 | 12.490 | 1.716 | 1.682 | 97.0 | 22.5 | 12.0 | 2.33 | 16.66 | 2.91 | 93.38 | 8.32 |
| 2123 | 2124 | 11.698 | 1.680 | 1.425 | 87.0 | 24.5 | 14.0 | 2.40 | 24.56 | 3.13 | 92.58 | 8.32 |
| 2124 | 2125 | 13.030 | 1.968 | 1.891 | 103.0 | 17.0 | 11.0 | 2.39 | 17.85 | 3.11 | 93.68 | 8.33 |
| 2125 | 2126 | 15.038 | 2.066 | 2.536 | 118.0 | 16.5 | 11.0 | 2.41 | 18.99 | 3.26 | 90.85 | 8.34 |
| 2126 | 2127 | 14.476 | 1.783 | 1.250 | 103.0 | 20.5 | 12.5 | 2.38 | 17.04 | 3.10 | 91.73 | 8.33 |
| 2127 | 2128 | 17.429 | 2.092 | 2.827 | 135.0 | 14.0 | 9.5 | 2.46 | 18.87 | 3.67 | 85.84 | 8.34 |
| 2128 | 2129 | 12.746 | 1.601 | 1.747 | 97.0 | 18.5 | 12.0 | 2.36 | 17.31 | 3.18 | 93.86 | 8.33 |
| 2129 | 2130 | 11.252 | 1.552 | 1.849 | 88.0 | 20.5 | 12.0 | 2.88 | 17.25 | 3.34 | 96.80 | 8.32 |
| 2130 | 2131 | 12.821 | 1.736 | 2.182 | 95.0 | 28.0 | 15.0 | 2.38 | 17.37 | 3.51 | 97.15 | 8.31 |
| 2131 | 2132 | 12.057 | 1.709 | 2.246 | 103.0 | 27.5 | 13.5 | 2.35 | 15.96 | 3.13 | 93.70 | 8.31 |
| 2132 | 2133 | 9.602 | 1.485 | 1.942 | 80.0 | 25.0 | 13.5 | 2.34 | 15.65 | 3.11 | 97.14 | 8.32 |
| 2133 | 2134 | 9.208 | 1.618 | 2.105 | 86.0 | 24.5 | 13.5 | 2.33 | 16.17 | 3.21 | 96.05 | 8.32 |
| 2134 | 2135 | 9.760 | 1.620 | 2.399 | 87.0 | 27.5 | 14.0 | 2.36 | 16.19 | 3.15 | 92.83 | 8.32 |
| 2135 | 2136 | 11.016 | 1.608 | 2.522 | 95.0 | 38.0 | 18.0 | 2.32 | 16.06 | 2.90 | 91.63 | 8.33 |
| 2136 | 2137 | 11.966 | 1.670 | 2.868 | 103.0 | 24.0 | 24.5 | 2.34 | 16.15 | 3.06 | 91.46 | 8.33 |
| 2137 | 2138 | 11.105 | 1.530 | 2.546 | 91.0 | 17.0 | 13.0 | 2.35 | 16.74 | 2.90 | 92.85 | 8.34 |
| **Arith. Average** | | **12.340** | **1.702** | **2.248** | **99.2** | **22.8** | **13.6** | **2.39** | **17.33** | **3.17** | **92.90** | **8.33** |

**Thin sand reservoir (meter) TVD**

| Top | Bottom | THOR | POTA | URAN | GR | $R_t$ | $R_{xo}$ | $\rho_b$ | NPHI | Pe | DET | Hole, d |
|---|---|---|---|---|---|---|---|---|---|---|---|---|
| 2042 | 2045 | 11.407 | 1.506 | 2.287 | 96.0 | 14.0 | 11.0 | 2.35 | 24.50 | 3.12 | 96.39 | 8.29 |
| 2100 | 2102 | 12.786 | 1.532 | 2.298 | 102.0 | 17.0 | 13.0 | 2.35 | 19.00 | 3.23 | 86.33 | 8.25 |
| 2150.5 | 2156.5 | 13.843 | 1.855 | 1.990 | 105.1 | 16.0 | 14.0 | 2.42 | 16.47 | 3.34 | 85.26 | 8.35 |
| 2363 | 2368 | 12.833 | 1.657 | 2.459 | 103.0 | 12.9 | 12.9 | 2.33 | 16.50 | 2.92 | 70.05 | 8.33 |
| 2498.5 | 2500.5 | 10.761 | 1.413 | 2.700 | 111.0 | 17.0 | 16.3 | 2.46 | 12.55 | 3.53 | 83.68 | 8.45 |

## Appendix-B1: Shale volume estimation from Gamma Ray and True Resistivity methods

| Thick sand | Vsh from Gamma Ray log | | | $V_{sh}$ from True resistivity method | | | |
|---|---|---|---|---|---|---|---|
| Depth, m | $GR_{log}$ | Calculated | | Log values (ohm-m) | | | Shale Volume |
| | API | $I_{sh}$ | $V_{sh}$ (%) | $R_{tmax}$ | $R_t$ | $R_{clay}$ | $V_{sh}$ (%) |
| 2120 | 110 | 0.430 | 16.73 | 39 | 23 | 6 | 16.10 |
| 2121 | 100 | 0.304 | 9.79 | 39 | 20 | 6 | 20.76 |
| 2122 | 107 | 0.392 | 14.41 | 39 | 24 | 6 | 14.78 |
| 2123 | 97 | 0.266 | 8.11 | 39 | 22.5 | 6 | 16.80 |
| 2124 | 87 | 0.139 | 3.56 | 39 | 24.5 | 6 | 14.15 |
| 2125 | 103 | 0.342 | 11.64 | 39 | 17 | 6 | 26.93 |
| 2126 | 118 | 0.532 | 24.15 | 39 | 16.5 | 6 | 28.17 |
| 2127 | 103 | 0.342 | 11.64 | 39 | 20.5 | 6 | 19.90 |
| 2128 | 135 | 0.747 | 48.05 | 39 | 14 | 6 | 35.62 |
| 2129 | 97 | 0.266 | 8.11 | 39 | 18.5 | 6 | 23.61 |
| 2130 | 88 | 0.152 | 3.95 | 39 | 20.5 | 6 | 19.90 |
| 2131 | 95 | 0.241 | 7.08 | 39 | 28 | 6 | 10.30 |
| 2132 | 103 | 0.342 | 11.64 | 39 | 27.5 | 6 | 10.80 |
| 2133 | 80 | 0.051 | 1.15 | 39 | 25 | 6 | 13.55 |
| 2134 | 86 | 0.127 | 3.18 | 39 | 24.5 | 6 | 14.15 |
| 2135 | 87 | 0.139 | 3.56 | 39 | 27.5 | 6 | 10.80 |
| 2136 | 95 | 0.241 | 7.08 | 39 | 38 | 6 | 1.53 |
| 2137 | 103 | 0.342 | 11.64 | 39 | 24 | 6 | 14.78 |
| 2138 | 91 | 0.190 | 5.21 | 39 | 17 | 6 | 26.93 |
| **Average** | **99.21** | **0.294** | **11.09** | **39** | **22.76** | **6** | **17.87** |

### Thin sands reservoir (BK#9)

| Depth, m | $V_{sh}$ from Gamma Ray log | | | $V_{sh}$ from True resistivity method | | | |
|---|---|---|---|---|---|---|---|
| Top | $GR_{log}$ | Calculated | | Log values (ohm-m) | | | Shale volume |
| | API | $I_{sh}$ | $V_{sh}$ (%) | $R_{tmax}$ | $R_t$ | $R_{clay}$ | $V_{sh}$ (%) |
| 2042 | 96.0 | 0.253 | 7.59 | 39 | 14.0 | 6 | 35.62 |
| 2100 | 102.0 | 0.329 | 11.00 | 39 | 17.0 | 6 | 26.93 |
| 2150.5 | 105.1 | 0.369 | 13.08 | 39 | 16.0 | 6 | 29.59 |
| 2363 | 103.0 | 0.342 | 11.64 | 39 | 12.9 | 6 | 39.78 |
| 2498.5 | 111.0 | 0.443 | 17.55 | 39 | 17.0 | 6 | 26.93 |

**Calculation for 2042m depth (Top):**

$GR_{Ish} = \frac{GR_{log} - GR_{min}}{GR_{max} - GR_{min}} = \frac{90-76}{155-76} = 0.253$; $V_{sh} = 0.083(2^{3.7Ish} - 1) = 0.083(2^{3.7*0.253} - 1) = 7.59$ %

True Resistivity Method, $V_{sh} = [\frac{R_{cl}}{R_t} \times \{\frac{R_{tmax} - R_t}{R_{tmax} - R_{cl}}\}^{\frac{1}{1.5}}] = [\frac{6}{14} \times \{\frac{39-14}{39-6}\}^{\frac{1}{1.5}}] = 35.62\%$

## Appendix-B2: Shale volume estimation from Spectral Gamma Ray method

### Thick sand reservoir (BK#9)

| Depth (Top) m | Log values (%) | | | Calculated | Log value (ppm) | Calculated |
|---|---|---|---|---|---|---|
| | $K_{log}$ | $K_{max}$ | $K_{min}$ | K-$V_{sh}$ (%) | $Th_{log}$ | Th-$V_{sh}$ (%) |
| 2120 | 1.672 | 2.818 | 1.315 | 23.752 | 13.444 | 45.840 |
| 2121 | 1.542 | 2.818 | 1.315 | 15.103 | 12.444 | 36.481 |
| 2122 | 1.689 | 2.818 | 1.315 | 24.884 | 12.887 | 40.627 |
| 2123 | 1.716 | 2.818 | 1.315 | 26.680 | 12.49 | 36.912 |
| 2124 | 1.680 | 2.818 | 1.315 | 24.285 | 11.698 | 29.499 |
| 2125 | 1.968 | 2.818 | 1.315 | 43.446 | 13.03 | 41.965 |
| 2126 | 2.066 | 2.818 | 1.315 | 49.967 | 15.038 | 60.758 |
| 2127 | 1.783 | 2.818 | 1.315 | 31.138 | 14.476 | 55.498 |
| 2128 | 2.092 | 2.818 | 1.315 | 51.697 | 17.429 | 83.135 |
| 2129 | 1.601 | 2.818 | 1.315 | 19.029 | 12.746 | 39.307 |
| 2130 | 1.552 | 2.818 | 1.315 | 15.768 | 11.252 | 25.325 |
| 2131 | 1.736 | 2.818 | 1.315 | 28.011 | 12.821 | 40.009 |
| 2132 | 1.709 | 2.818 | 1.315 | 26.214 | 12.057 | 32.859 |
| 2133 | 1.485 | 2.818 | 1.315 | 11.311 | 9.602 | 9.883 |
| 2134 | 1.618 | 2.818 | 1.315 | 20.160 | 9.208 | 6.196 |
| 2135 | 1.620 | 2.818 | 1.315 | 20.293 | 9.76 | 11.362 |
| 2136 | 1.608 | 2.818 | 1.315 | 19.494 | 11.016 | 23.117 |
| 2137 | 1.670 | 2.818 | 1.315 | 23.619 | 11.966 | 32.007 |
| 2138 | 1.530 | 2.818 | 1.315 | 14.305 | 11.105 | 23.949 |
| **Average** | **1.70** | **2.818** | **1.315** | **25.75** | **12.34** | **35.51** |

### Thin sands reservoir (BK#9)

| Depth, m | Log values (%) | | | Calculated | Log value (ppm) | Calculated |
|---|---|---|---|---|---|---|
| | $K_{log}$ | $K_{max}$ | $K_{min}$ | K-$V_{sh}$ (%) | $Th_{log}$ | Th-$V_{sh}$ (%) |
| 2042 | 1.506 | 2.818 | 1.315 | 12.708 | 11.407 | 26.776 |
| 2100 | 1.532 | 2.818 | 1.315 | 14.438 | 12.786 | 39.682 |
| 2150.5 | 1.855 | 2.818 | 1.315 | 35.947 | 13.843 | 49.576 |
| 2363 | 1.657 | 2.818 | 1.315 | 22.754 | 12.833 | 40.122 |
| 2498.5 | 1.413 | 2.818 | 1.315 | 6.520 | 10.761 | 20.730 |

**Calculation for 2042m (Top):**

$$K\,V_{sh} = \frac{K_{log} - K_{min}}{K_{max} - K_{min}} = \frac{1.506 - 1.315}{2.818 - 1.315} = 0.12708 = 12.708\%$$

$$Th\,V_{sh} = \frac{Th_{log} - Th_{min}}{Th_{max} - Th_{min}} = \frac{11.407 - 8.546}{19.231 - 8.546} = 0.26776 = 26.776\%$$

## Appendix-C1: Porosity assessment from neutron and density logs

### Thick sand reservoir (BK#9)

| Depth, m TVD | Shale Vol. $V_{sh}$ | Neutron Porosity (Percent) | | Bulk Density (gm/cc) | | Porosity (Porosity) | | |
|---|---|---|---|---|---|---|---|---|
| | | $\Phi_N$ | $*\Phi_{Ncorr}$ | $\rho_b$ | $\rho_{b,corr}$ | $\Phi_D$ | $\Phi_{Dcor}$ | $\Phi_{NDe}$ |
| 2120 | 16.73 | 15.7 | 13.04 | 2.383 | 2.43 | 16.18 | 13.55 | 13.30 |
| 2121 | 9.79 | 18.0 | 16.49 | 2.388 | 2.41 | 15.88 | 14.34 | 15.45 |
| 2122 | 14.41 | 16.7 | 14.41 | 2.327 | 2.36 | 19.58 | 17.31 | 15.92 |
| 2123 | 8.11 | 16.7 | 15.40 | 2.326 | 2.35 | 19.64 | 18.36 | 16.94 |
| 2124 | 3.56 | 24.6 | 24.03 | 2.395 | 2.40 | 15.45 | 14.89 | 19.99 |
| 2125 | 11.64 | 17.8 | 16.02 | 2.386 | 2.42 | 16 | 14.17 | 15.12 |
| 2126 | 24.15 | 19.0 | 15.17 | 2.413 | 2.48 | 14.36 | 10.56 | 13.07 |
| 2127 | 11.64 | 17.0 | 15.22 | 2.377 | 2.41 | 16.55 | 14.71 | 14.97 |
| 2128 | 48.05 | 18.9 | 11.22 | 2.456 | 2.58 | 11.76 | 4.186 | 8.47 |
| 2129 | 8.11 | 17.3 | 16.05 | 2.355 | 2.38 | 17.88 | 16.6 | 16.33 |
| 2130 | 3.95 | 17.3 | 16.66 | 2.376 | 2.39 | 16.61 | 15.98 | 16.32 |
| 2131 | 7.08 | 17.4 | 16.28 | 2.381 | 2.40 | 16.3 | 15.19 | 15.74 |
| 2132 | 11.64 | 16.0 | 14.14 | 2.350 | 2.38 | 18.18 | 16.35 | 15.28 |
| 2133 | 1.15 | 15.7 | 15.51 | 2.340 | 2.34 | 18.79 | 18.61 | 17.13 |
| 2134 | 3.18 | 16.2 | 15.70 | 2.334 | 2.34 | 19.15 | 18.65 | 17.24 |
| 2135 | 3.56 | 16.2 | 15.66 | 2.356 | 2.37 | 17.82 | 17.26 | 16.48 |
| 2136 | 7.08 | 16.1 | 14.97 | 2.319 | 2.34 | 20.06 | 18.94 | 17.07 |
| 2137 | 11.64 | 16.2 | 14.33 | 2.338 | 2.37 | 18.91 | 17.07 | 15.76 |
| 2138 | 5.21 | 16.7 | 15.95 | 2.353 | 2.37 | 18.00 | 17.18 | 16.57 |
| **Average** | **11.09** | **17.33** | **15.59** | **2.37** | **2.39** | **17.22** | **15.47** | **15.64** |

### Thin sands reservoir (BK#9)

| Depth, m TVD | Shale Vol. $V_{sh}$ | Neutron Porosity (Percent) | | Bulk Density (gm/cc) | | Porosity (Percent) | | |
|---|---|---|---|---|---|---|---|---|
| | | $\Phi_N$ | $*\Phi_{Ncorr}$ | $\rho_b$ | $\rho_{b,corr}$ | $\Phi_D$ | $\Phi_{Dcor}$ | $\Phi_{NDe}$ |
| 2045 | 7.59 | 24.50 | 23.33 | 2.335 | 2.35 | 19.09 | 17.09 | 20.79 |
| 2103 | 11.00 | 19.00 | 17.28 | 2.35 | 2.38 | 18.18 | 16.45 | 16.87 |
| 2156.5 | 13.08 | 16.47 | 14.42 | 2.417 | 2.45 | 14.10 | 12.04 | 13.28 |
| 2369 | 11.64 | 16.50 | 14.68 | 2.33 | 2.36 | 19.39 | 17.56 | 16.18 |
| 2500.5 | 17.55 | 12.55 | 9.78 | 2.46 | 2.51 | 11.52 | 8.75 | 9.28 |

**Calculation for 2045 m (Base):**

Clay corrected bulk density, $\rho_{b,corr} = \rho_b + V_{sh}(\rho_{ma} - \rho_{cl}) = 2.335 + 0.167(2.65-2.39) = 2.35$ gm/cc

Density porosity, $\Phi_D = \frac{\rho_{ma} - \rho_b}{\rho_{ma} - \rho_f} = \frac{2.65-2.335}{2.65-1.00} = 19.09\%$

Corrected density porosity, $\Phi_{D,corr} = \frac{2.65-2.35}{2.65-1.00}$

$= 17.09\%$

*Corrected neutron porosity, $\Phi_{N,corr} = \Phi_N - V_{sh} \times \Phi_{N,sh}$ + lithology correction

$= (24.50 - 0.076*16) + 0.04$

$= 23.33\%$

Clay corrected Neutron-Density combination formula, $\Phi_e = \sqrt{\frac{\Phi_{N,corr}{}^2 + \Phi_{D,corr}{}^2}{2}} = \sqrt{\frac{23.33^2 + 17.09^2}{2}}$

$= 20.79\%$

## Appendix-C2: Porosity assessment of reservoir from sonic log

### Thick sand reservoir (BK#9)

| Depth, m TVD | Shale Volm. $V_{sh}$ | Sonic Porosity (µs/ft) | | | | |
|---|---|---|---|---|---|---|
| | | Transit time (µs/ft) | | | Calculated (%) | |
| | | ΔTlog | $\Delta T_f$ | $\Delta T_{ma}$ | $\Phi_s$ | $\Phi_{s,corr}$ |
| 2120 | 16.73 | 87.547 | 189 | 55.5 | 24.01 | 16.80 |
| 2121 | 9.79 | 92.801 | 189 | 55.5 | 27.94 | 19.56 |
| 2122 | 14.41 | 93.282 | 189 | 55.5 | 28.30 | 19.81 |
| 2123 | 8.11 | 93.376 | 189 | 55.5 | 28.37 | 19.86 |
| 2124 | 3.56 | 92.575 | 189 | 55.5 | 27.77 | 19.44 |
| 2125 | 11.64 | 93.684 | 189 | 55.5 | 28.60 | 20.02 |
| 2126 | 24.15 | 90.848 | 189 | 55.5 | 26.48 | 18.53 |
| 2127 | 11.64 | 91.726 | 189 | 55.5 | 27.14 | 18.99 |
| 2128 | 48.05 | 85.844 | 189 | 55.5 | 22.73 | 15.91 |
| 2129 | 8.11 | 93.856 | 189 | 55.5 | 28.73 | 20.11 |
| 2130 | 3.95 | 96.798 | 189 | 55.5 | 30.93 | 21.65 |
| 2131 | 7.08 | 97.15 | 189 | 55.5 | 31.20 | 21.84 |
| 2132 | 11.64 | 93.696 | 189 | 55.5 | 28.61 | 20.03 |
| 2133 | 1.15 | 97.142 | 189 | 55.5 | 31.19 | 21.83 |
| 2134 | 3.18 | 96.049 | 189 | 55.5 | 30.37 | 21.26 |
| 2135 | 3.56 | 92.825 | 189 | 55.5 | 27.96 | 19.57 |
| 2136 | 7.08 | 91.63 | 189 | 55.5 | 27.06 | 18.94 |
| 2137 | 11.64 | 91.459 | 189 | 55.5 | 26.94 | 18.85 |
| 2138 | 5.21 | 92.85 | 189 | 55.5 | 27.98 | 19.58 |
| **Average** | **11.09** | **92.90** | | | **28.02** | **19.61** |

### Thin sands reservoir (BK#9)

| Depth m, TVD | $V_{sh}$ | $\Delta T_{log}$ | Sonic log (µs/ft) | | Calculated (%) | |
|---|---|---|---|---|---|---|
| | | | $\Delta T_f$ | $\Delta T_{ma}$ | $\Phi_s$ | $\Phi_{s,corr}$ |
| 2045 | 7.59 | 96.386 | 189 | 55.5 | 30.63 | 21.44 |
| 2103 | 11.00 | 86.327 | 189 | 55.5 | 23.09 | 16.16 |
| 2156.5 | 13.08 | 85.2567 | 189 | 55.5 | 22.29 | 15.60 |
| 2369 | 11.64 | 70.048 | 189 | 55.5 | 10.90 | 7.63 |
| 2500.5 | 17.55 | 83.68 | 189 | 55.5 | 21.11 | 14.78 |

**Calculation for 2045 m (Base):**

Sonic porosity, $\Phi_s = \frac{\Delta T_{ma} - \Delta T_{log}}{\Delta T_{ma} - \Delta T_f} = \frac{55.50 - 96.386}{55.50 - 189} = 30.63\%$

Corrected sonic porosity, $\Phi_e = \Phi_s \times 0.7$ for gas $= 30.63 \times 0.7 = 21.44$

## Appendix-D: Estimation of minimum formation water resistivity (Rw)

### Wet sand interval (BK#9)

| TVD (m) | | Log values | | | | | Porosity (fraction) | | | Resistivity (Ω-m) | |
|---|---|---|---|---|---|---|---|---|---|---|---|
| **Top** | **Base** | **GR** | **$R_t$** | **$R_{xo}$** | **$\Phi_N$** | **$\rho_b$** | **$\Phi_{N,corr}$** | **$\Phi_D$** | **$\Phi_{ND}$** | **$R_{wa}$** | **$R_{mf}$** |
| **1960** | **1969** | **90** | **3.2** | **4.8** | **24** | **2.33** | **0.24** | **0.19** | **0.22** | **0.104** | **0.157** |
| 2165 | 2169 | 85 | 6.2 | 13 | 17 | 2.34 | 0.17 | 0.19 | 0.18 | 0.130 | 0.272 |
| 2176 | 2180 | 84 | 5.5 | 11 | 18.5 | 2.37 | 0.19 | 0.17 | 0.18 | 0.113 | 0.226 |
| 2191 | 2201 | 80 | 6 | 14 | 17 | 2.36 | 0.17 | 0.18 | 0.17 | 0.116 | 0.271 |
| 2249 | 2255 | 92 | 8 | 15 | 16 | 2.38 | 0.16 | 0.16 | 0.16 | 0.133 | 0.250 |
| 2321 | 2327 | 102 | 7.5 | 10 | 17.5 | 2.38 | 0.18 | 0.16 | 0.17 | 0.138 | 0.185 |
| 2485 | 2488 | 95 | 9 | 16 | 18.5 | 2.4 | 0.19 | 0.15 | 0.17 | 0.165 | 0.294 |

**Wet Depth Interval: 1960-1969 m**

Density porosity, $\Phi_D = \frac{\rho_{ma} - \rho_b}{\rho_{ma} - \rho_f} = \frac{2.65 - 2.33}{2.65 - 1.00} = 19.39\%$

Neutron porosity, $\Phi_{N,corr} = \Phi_N$ + lithology correction = 24 + 0.04 = 24.04%

Neutron-Density combination formula, $\Phi_{ND} = \sqrt{\frac{\Phi_N{}^2 + \Phi_D{}^2}{2}}$

$$= \sqrt{\frac{24.04^2 + 19.39^2}{2}}$$

$$= 21.84\%$$

Formation water resistivity, $R_{wa} = [\frac{R_t \times \Phi_{ND}{}^m}{a}]$ for un-invaded zone

$$= [\frac{3.2 \times 0.2184^{2.25}}{1}]$$

= 0.104 Ω-m by Inverse Archie's formula

Formation mud filtrate resistivity, $R_{mf} = [\frac{R_{xo} \times \Phi_{ND}{}^m}{a}]$ for flushed zone.

$$= [\frac{4.8 \times 0.2184^{2.25}}{1}]$$

= 0.104 Ω-m

## Appendix-E1: Estimation of Rw and Rmf at formation temperature

| Top | Base | Average | Log header values | | | Gg | Calculated value | | |
|---|---|---|---|---|---|---|---|---|---|
| TVD, m | | (meter) | TD, m | BHT | $T_s$ | $^0F/100$ | $T_f$ ($^0F$) | $R_w$ (Ω-m) | $R_{mf}$ (Ω-m) |
| **Reference Zone** | | **1964** | **2533** | **180** | **80** | **3.948** | **157.5** | **0.104** | **0.157** |
| 2042 | 2045 | 2043.5 | 2533 | 180 | 80 | 3.948 | 160.68 | 0.102 | 0.154 |
| 2100 | 2103 | 2101.5 | 2533 | 180 | 80 | 3.948 | 162.97 | 0.101 | 0.152 |
| 2120 | 2138 | 2129 | 2533 | 180 | 80 | 3.948 | 164.06 | 0.100 | 0.151 |
| 2151 | 2157 | 2153.5 | 2533 | 180 | 80 | 3.948 | 165.03 | 0.099 | 0.150 |
| 2363 | 2369 | 2366 | 2533 | 180 | 80 | 3.948 | 173.42 | 0.095 | 0.143 |
| 2499 | 2501 | 2499.5 | 2533 | 180 | 80 | 3.948 | 178.69 | 0.092 | 0.139 |

**Calculation for 2042-2045 m interval:**

Geothermal gradient, $Gg = \frac{BHT - T_S}{TD} \times 100 = \frac{180-80}{2533} \times 100 = 3.948\ ^0F$ per 100m

Formation temperature at 2043.5 meter, $T_f = [T_s + (\frac{G_g}{100} \times \text{Formation Depth}]$

$$= 80 + \frac{3.948}{100} \times 2043.5$$

$$= 160.68\ ^0F$$

Formation water resistivity, $R_{w2} = R_{w1} \times \frac{6.66 + T_1}{6.66 + T_2}$

$R_w$ at 2043.5 meter depth $= 0.104 \times \frac{6.66 + 157.50}{6.66 + 160.68}$

$= 0.102$ Ω-m

$R_{mf}$ at 2043.5 meter depth $= 0.157 \times \frac{6.66 + 157.50}{6.66 + 160.68}$

$= 0.154$ Ω-m

# Appendix-E2: Gen-9 Chart for salinity (NaCl) estimation

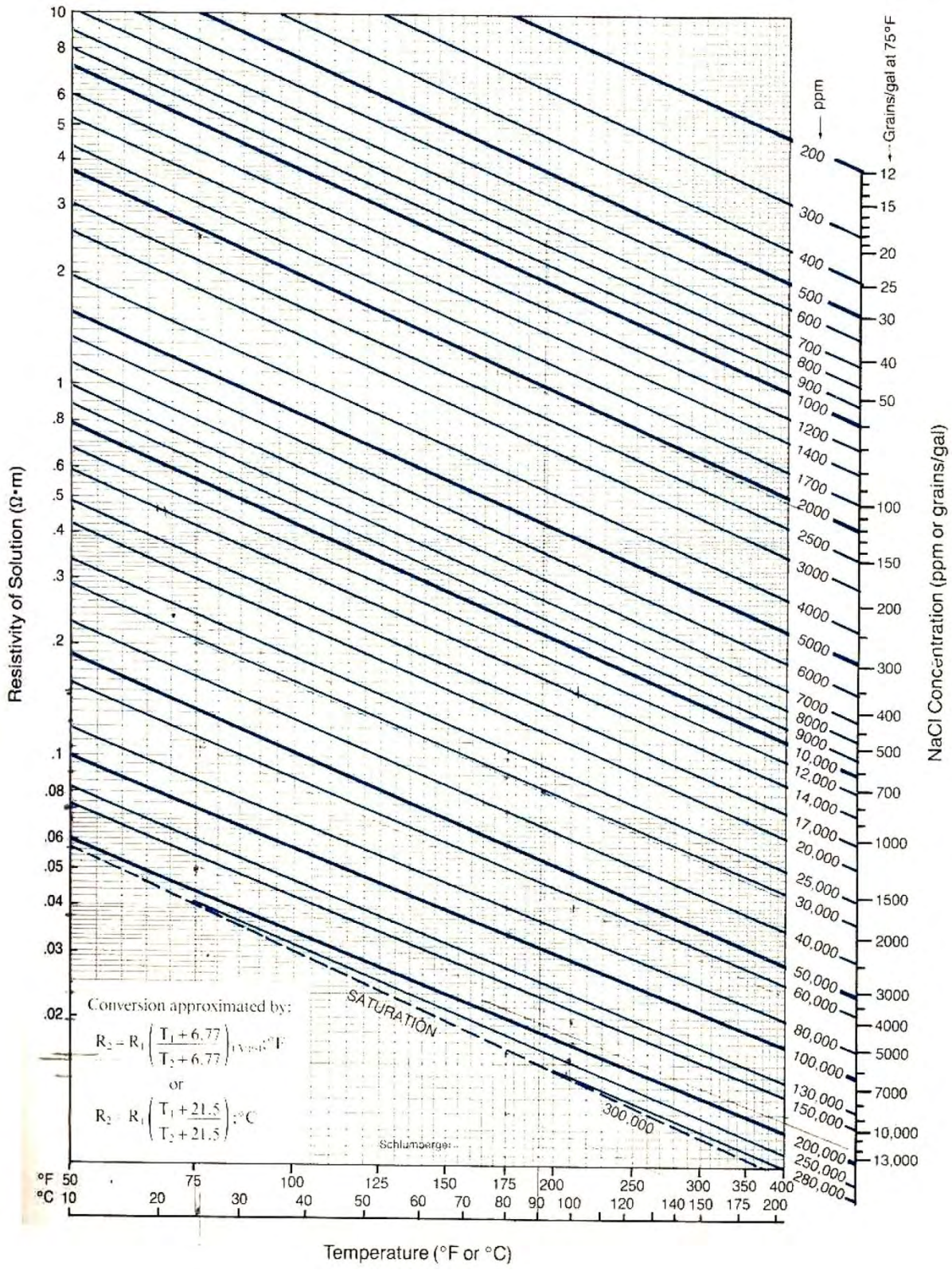

## Appendix-F1: Water saturation estimation from Archie's formula

### Thick sand reservoir (BK#9)

| Depth, m | $R_t$ | $R_{xo}$ | Φ | $R_w$ | $R_{mf}$ | $S_w$ | $S_{xo}$ | BVW | MHI |
|---|---|---|---|---|---|---|---|---|---|
| 2120 | 23.0 | 15.0 | 13.30 | 0.100 | 0.151 | 0.157 | 0.293 | 0.021 | 0.535 |
| 2121 | 20.0 | 12.0 | 15.45 | 0.100 | 0.151 | 0.145 | 0.282 | 0.022 | 0.513 |
| 2122 | 24.0 | 12.5 | 15.92 | 0.100 | 0.151 | 0.128 | 0.268 | 0.020 | 0.478 |
| 2123 | 22.5 | 12.0 | 16.94 | 0.100 | 0.151 | 0.124 | 0.257 | 0.021 | 0.484 |
| 2124 | 24.5 | 14.0 | 19.99 | 0.100 | 0.151 | 0.101 | 0.202 | 0.020 | 0.501 |
| 2125 | 17.0 | 11.0 | 15.12 | 0.100 | 0.151 | 0.160 | 0.301 | 0.024 | 0.533 |
| 2126 | 16.5 | 11.0 | 13.07 | 0.100 | 0.151 | 0.188 | 0.348 | 0.025 | 0.541 |
| 2127 | 20.5 | 12.5 | 14.97 | 0.100 | 0.151 | 0.148 | 0.285 | 0.022 | 0.517 |
| 2128 | 14.0 | 9.5 | 8.47 | 0.100 | 0.151 | 0.316 | 0.578 | 0.027 | 0.546 |
| 2129 | 18.5 | 12.0 | 16.33 | 0.100 | 0.151 | 0.142 | 0.267 | 0.023 | 0.533 |
| 2130 | 20.5 | 12.0 | 16.32 | 0.100 | 0.151 | 0.135 | 0.267 | 0.022 | 0.507 |
| 2131 | 28.0 | 15.0 | 15.74 | 0.100 | 0.151 | 0.120 | 0.248 | 0.019 | 0.485 |
| 2132 | 27.5 | 13.5 | 15.28 | 0.100 | 0.151 | 0.125 | 0.269 | 0.019 | 0.464 |
| 2133 | 25.0 | 13.5 | 17.13 | 0.100 | 0.151 | 0.117 | 0.240 | 0.020 | 0.487 |
| 2134 | 24.5 | 13.5 | 17.24 | 0.100 | 0.151 | 0.117 | 0.238 | 0.020 | 0.492 |
| 2135 | 27.5 | 14.0 | 16.48 | 0.100 | 0.151 | 0.116 | 0.245 | 0.019 | 0.473 |
| 2136 | 38.0 | 18.0 | 17.07 | 0.100 | 0.151 | 0.095 | 0.208 | 0.016 | 0.456 |
| 2137 | 24.0 | 24.5 | 15.76 | 0.100 | 0.151 | 0.130 | 0.194 | 0.020 | 0.669 |
| 2138 | 17.0 | 13.0 | 16.57 | 0.100 | 0.151 | 0.146 | 0.253 | 0.024 | 0.579 |
| Average | 22.76 | 13.6 | 15.64 | 0.100 | 0.151 | 0.143 | 0.276 | 0.021 | 0.515 |

### Thin sands interval (BK#9)

| Top | Base | $R_t$ | $R_{xo}$ | Φ | $R_w$ | $R_{mf}$ | $S_w$ | $S_{xo}$ | BVW | MHI |
|---|---|---|---|---|---|---|---|---|---|---|
| 2042 | 2045 | 14.0 | 11.0 | 20.79 | 0.102 | 0.154 | 0.131 | 0.223 | 0.027 | 0.587 |
| 2100 | 2103 | 17.0 | 13.0 | 16.87 | 0.101 | 0.152 | 0.145 | 0.250 | 0.024 | 0.579 |
| 2151 | 2156.5 | 16.0 | 14.0 | 13.28 | 0.099 | 0.150 | 0.187 | 0.302 | 0.025 | 0.621 |
| 2363 | 2369 | 12.9 | 12.9 | 16.18 | 0.095 | 0.143 | 0.163 | 0.246 | 0.026 | 0.662 |
| 2499 | 2500.5 | 17.0 | 16.3 | 9.28 | 0.092 | 0.139 | 0.241 | 0.371 | 0.022 | 0.649 |

**Calculation for 2042-2045 m interval:**

Water saturation, $S_w = \sqrt[n]{\frac{a \times R_w}{\Phi^m \times R_t}} = \sqrt[2]{\frac{1 \times 0.102}{0.208^2 \times 14}} = 0.13 = 13\%$

$S_{xo} = \sqrt[n]{\frac{a \times R_{mf}}{\Phi^m \times R_{xo}}} = \sqrt[2]{\frac{1 \times 0.154}{0.208^2 \times 11}} = 0.223 = 22.3\%$

BVW = $S_w \times \Phi = 0.131 \times 0.208 = 0.027$, and MHI = $\frac{S_w}{S_{xo}} = \frac{0.131}{0.223} = 0.587$

## Appendix-F2: Water saturation estimation by Indonesia model

### Thick sand reservoir (BK#9)

| Depth Top, m | $V_{cl}$ | Log values, Ω-m | | | Calculated | | | | | | |
|---|---|---|---|---|---|---|---|---|---|---|---|
| | | $R_{cl}$ | $R_{xo}$ | Rt | $\Phi_e$ | $R_w$ | $R_{mf}$ | $S_w$ | $S_{xo}$ | MHI | BVW |
| 2120 | 16.73 | 6 | 15.0 | 23.0 | 13.30 | 0.10 | 0.151 | 0.42 | 0.75 | 0.55 | 0.06 |
| 2121 | 9.79 | 6 | 12.0 | 20.0 | 15.45 | 0.10 | 0.151 | 0.42 | 0.73 | 0.58 | 0.06 |
| 2122 | 14.41 | 6 | 12.5 | 24.0 | 15.92 | 0.10 | 0.151 | 0.36 | 0.69 | 0.52 | 0.06 |
| 2123 | 8.11 | 6 | 12.0 | 22.5 | 16.94 | 0.10 | 0.151 | 0.37 | 0.66 | 0.56 | 0.06 |
| 2124 | 3.56 | 6 | 14.0 | 24.5 | 19.99 | 0.10 | 0.151 | 0.31 | 0.52 | 0.60 | 0.06 |
| 2125 | 11.64 | 6 | 11.0 | 16.0 | 15.12 | 0.10 | 0.151 | 0.47 | 0.77 | 0.61 | 0.07 |
| 2126 | 24.15 | 6 | 11.0 | 16.5 | 13.07 | 0.10 | 0.151 | 0.46 | 0.90 | 0.52 | 0.06 |
| 2127 | 11.64 | 6 | 12.5 | 20.5 | 14.97 | 0.10 | 0.151 | 0.42 | 0.73 | 0.57 | 0.06 |
| 2128 | 48.05 | 6 | 9.5 | 14.0 | 8.47 | 0.10 | 0.151 | 0.53 | 1.49 | 0.36 | 0.05 |
| 2129 | 8.11 | 6 | 12.0 | 18.5 | 16.33 | 0.10 | 0.151 | 0.42 | 0.69 | 0.61 | 0.07 |
| 2130 | 3.95 | 6 | 12.0 | 20.5 | 16.32 | 0.10 | 0.151 | 0.41 | 0.69 | 0.60 | 0.07 |
| 2131 | 7.08 | 6 | 15.0 | 29.0 | 15.74 | 0.10 | 0.151 | 0.35 | 0.64 | 0.55 | 0.06 |
| 2132 | 11.64 | 6 | 13.5 | 27.0 | 15.28 | 0.10 | 0.151 | 0.36 | 0.69 | 0.52 | 0.05 |
| 2133 | 1.15 | 6 | 13.5 | 25.0 | 17.13 | 0.10 | 0.151 | 0.37 | 0.61 | 0.60 | 0.06 |
| 2134 | 3.18 | 6 | 13.5 | 24.5 | 17.24 | 0.10 | 0.151 | 0.36 | 0.61 | 0.59 | 0.06 |
| 2135 | 3.56 | 6 | 14.0 | 27.0 | 16.48 | 0.10 | 0.151 | 0.36 | 0.63 | 0.57 | 0.06 |
| 2136 | 7.08 | 6 | 18.0 | 39.0 | 17.07 | 0.10 | 0.151 | 0.28 | 0.54 | 0.52 | 0.05 |
| 2137 | 11.64 | 6 | 24.5 | 24.0 | 15.76 | 0.10 | 0.151 | 0.37 | 0.50 | 0.74 | 0.06 |
| 2138 | 5.21 | 6 | 13.0 | 17.0 | 16.57 | 0.10 | 0.151 | 0.44 | 0.65 | 0.68 | 0.07 |
| **Average** | **11.09** | **6.0** | **13.6** | **22.8** | **15.64** | **0.10** | **0.15** | **0.39** | **0.71** | **0.57** | **0.06** |

### Thin sands reservoir (BK# 9)

| Depth | $V_{cl}$ | $R_{cl}$ | $R_{xo}$ | Rt | $\Phi_e$ | $R_w$ | $R_{mf}$ | $S_w$ | $S_{xo}$ | MHI | BVW |
|---|---|---|---|---|---|---|---|---|---|---|---|
| 2045 | 7.59 | 6 | 11.0 | 14.0 | 20.79 | 0.102 | 0.154 | 0.39 | 0.57 | 0.69 | 0.08 |
| 2103 | 11.00 | 6 | 13.0 | 17.0 | 16.87 | 0.101 | 0.152 | 0.42 | 0.64 | 0.65 | 0.07 |
| 2156.5 | 13.08 | 6 | 14.0 | 16.0 | 13.28 | 0.099 | 0.150 | 0.52 | 0.78 | 0.67 | 0.07 |
| 2369 | 11.64 | 6 | 12.9 | 12.9 | 16.18 | 0.095 | 0.143 | 0.48 | 0.65 | 0.74 | 0.08 |
| 2500.5 | 17.55 | 6 | 16.3 | 17.0 | 9.279 | 0.092 | 0.139 | 0.62 | 1.00 | 0.63 | 0.06 |

**<u>Calculation for 2045 m (Base):</u>**

$S_w = (\frac{1}{R_t})[\{\frac{V_{cl}{}^{(1-0.5V_{cl})}}{R_{cl}{}^{0.5}}\}+\{\frac{\Phi_e{}^{(0.5m)}}{aR_w{}^{0.5}}\}] = (\frac{1}{14})[\{\frac{0.76^{(1-0.5\times0.76)}}{6^{0.5}}\}+\{\frac{0.208^{(0.5\times2)}}{1\times0.102^{0.5}}\}] = 0.39 = 39\%$

$S_{xo} = (\frac{1}{R_{xo}})[\{\frac{V_{cl}{}^{(1-0.5V_{cl})}}{R_{cl}{}^{0.5}}\}+\{\frac{\Phi_e{}^{(0.5m)}}{aR_{mf}{}^{0.5}}\}] = (\frac{1}{11})[\{\frac{0.76^{(1-0.5\times0.76)}}{6^{0.5}}\}+\{\frac{0.208^{(0.5\times2)}}{1\times0.154^{0.5}}\}] = 0.57 = 57\%$

BVW = $S_w \times \Phi = 0.39\times0.208 = 0.08$, and MHI = $\frac{S_w}{S_{xo}} = \frac{0.39}{0.57} = 0.69$

## Appendix-F3: Water Saturation estimation by Simandoux model

**Thick sand reservoir (BK#9)**

| Sand Zone | TVD | Resistivity, Ω-m | | | Calculated (%) | | | |
|---|---|---|---|---|---|---|---|---|
| | meter | $R_t$ | $R_{sh}$ | $R_w$ | $V_{sh}$ | $\Phi_e$ | $S_w$ | BVW |
| Sub-zone:1 | 2120 | 23.0 | 6.0 | 0.10 | 16.73 | 13.30 | 44.29 | 0.059 |
| Sub-zone:2 | 2121 | 20.0 | 6.0 | 0.10 | 9.79 | 15.45 | 40.90 | 0.063 |
| Sub-zone:3 | 2122 | 24.0 | 6.0 | 0.10 | 14.41 | 15.92 | 36.22 | 0.058 |
| Sub-zone:4 | 2123 | 22.5 | 6.0 | 0.10 | 8.11 | 16.94 | 35.17 | 0.060 |
| Sub-zone:5 | 2124 | 24.5 | 6.0 | 0.10 | 3.56 | 19.99 | 28.58 | 0.057 |
| Sub-zone:6 | 2125 | 17.0 | 6.0 | 0.10 | 11.64 | 15.12 | 45.33 | 0.069 |
| Sub-zone:7 | 2126 | 16.5 | 6.0 | 0.10 | 24.15 | 13.07 | 53.20 | 0.070 |
| Sub-zone:8 | 2127 | 20.5 | 6.0 | 0.10 | 11.64 | 14.97 | 41.71 | 0.062 |
| Sub-zone:9 | 2128 | 14.0 | 6.0 | 0.10 | 48.05 | 8.47 | 88.81 | 0.075 |
| Sub-zone:10 | 2129 | 18.5 | 6.0 | 0.10 | 8.11 | 16.33 | 40.25 | 0.066 |
| Sub-zone:11 | 2130 | 20.5 | 6.0 | 0.10 | 3.95 | 16.32 | 38.26 | 0.062 |
| Sub-zone:12 | 2131 | 28.0 | 6.0 | 0.10 | 7.08 | 15.74 | 33.94 | 0.053 |
| Sub-zone:13 | 2132 | 27.5 | 6.0 | 0.10 | 11.64 | 15.28 | 35.26 | 0.054 |
| Sub-zone:14 | 2133 | 25.0 | 6.0 | 0.10 | 1.15 | 17.13 | 33.03 | 0.057 |
| Sub-zone:15 | 2134 | 24.5 | 6.0 | 0.10 | 3.18 | 17.24 | 33.14 | 0.057 |
| Sub-zone:16 | 2135 | 27.5 | 6.0 | 0.10 | 3.56 | 16.48 | 32.72 | 0.054 |
| Sub-zone:17 | 2136 | 38.0 | 6.0 | 0.10 | 7.08 | 17.07 | 26.86 | 0.046 |
| Sub-zone:18 | 2137 | 24.0 | 6.0 | 0.10 | 11.64 | 15.76 | 36.60 | 0.058 |
| Sub-zone:19 | 2138 | 17.0 | 6.0 | 0.10 | 5.21 | 16.57 | 41.38 | 0.069 |
| **Average** | | | | **0.10** | **11.09** | **15.64** | **40.30** | **0.063** |

**Thin sands reservoir (BK#9)**

| TVD (meter) | | Resistivity, ohm-m | | | Calculated (%) | | | |
|---|---|---|---|---|---|---|---|---|
| Top | Base | $R_t$ | $R_{sh}$ | $R_w$ | $V_{sh}$ | $\Phi_e$ | $S_w$ | BVW |
| 2042 | 2045 | 14.0 | 6.0 | 0.102 | 7.59 | 20.79 | 36.71 | 0.076 |
| 2100 | 2103 | 17.0 | 6.0 | 0.101 | 11.00 | 16.87 | 40.77 | 0.069 |
| 2150.5 | 2156.5 | 16.0 | 6.0 | 0.099 | 13.08 | 13.28 | 53.05 | 0.070 |
| 2363 | 2369 | 12.9 | 6.0 | 0.095 | 11.64 | 16.18 | 47.36 | 0.077 |
| 2498.5 | 2500.5 | 17.0 | 6.0 | 0.092 | 17.55 | 9.28 | 70.78 | 0.066 |

**Calculation for 2042-2045 m interval:**

$$S_w = \left(\frac{0.4R_w}{\Phi_e^{\,2}}\right) \times \left[ \sqrt{\left\{\frac{V_{sh}^{\,2}}{R_{sh}^{\,2}} + \frac{5\Phi_e^{\,2}}{R_w\, R_t}\right\}} - \frac{V_{sh}}{R_{sh}} \right] = \left(\frac{0.4 \times 0.102}{0.208^2}\right) \times \left[ \sqrt{\left\{\frac{0.076^2}{6^2} + \frac{5 \times 0.208^2}{0.102 \times 14}\right\}} - \frac{0.076}{6} \right] = 36.71\%$$

Gas saturation, Sg= 1-0.367=0.633 = 63.3% and BVW = $S_w \times \Phi e$ = 0.3673×0.208 = 0.076

## Appendix-G: Log derived permeability from Wyllie-Rose method

### Thick sand reservoir (BK#9)

| Zone name | Depth, TVD | Porosity (%) | Wylie-Rose Method (mD) |
|---|---|---|---|
| Sub-zone:1 | 2120 | 13.30 | 36.94 |
| Sub-zone:2 | 2121 | 15.45 | 71.55 |
| Sub-zone:3 | 2122 | 15.92 | 81.61 |
| Sub-zone:4 | 2123 | 16.94 | 107.34 |
| Sub-zone:5 | 2124 | 19.99 | 221.99 |
| Sub-zone:6 | 2125 | 15.12 | 65.06 |
| Sub-zone:7 | 2126 | 13.07 | 34.21 |
| Sub-zone:8 | 2127 | 14.97 | 62.16 |
| Sub-zone:9 | 2128 | 8.47 | 5.07 |
| Sub-zone:10 | 2129 | 16.33 | 91.20 |
| Sub-zone:11 | 2130 | 16.32 | 91.07 |
| Sub-zone:12 | 2131 | 15.74 | 77.63 |
| Sub-zone:13 | 2132 | 15.28 | 68.15 |
| Sub-zone:14 | 2133 | 17.13 | 112.50 |
| Sub-zone:15 | 2134 | 17.24 | 115.81 |
| Sub-zone:16 | 2135 | 16.48 | 94.92 |
| Sub-zone:17 | 2136 | 17.07 | 110.94 |
| Sub-zone:18 | 2137 | 15.76 | 78.05 |
| Sub-zone:19 | 2138 | 16.57 | 97.40 |
| **Average** | | | **85.45** |

### Thin sands reservoir (BK#9)

| Thin sand, TVD (m) | | Porosity ($\Phi_e$) | Wylie-Rose Method |
|---|---|---|---|
| Top | Base | | mD |
| 2042 | 2045 | 20.7887 | 263.90 |
| 2100 | 2103 | 16.8687 | 105.23 |
| 2150.5 | 2156.5 | 13.2849 | 36.79 |
| 2363 | 2369 | 16.1828 | 87.67 |
| 2498.5 | 2500.5 | 9.27948 | 7.59 |

**Calculation for 2042-2045 m depth interval:**

Log derived permeability, $K_L = [\frac{(CPERM \times \Phi^{DPERM})}{(S_{wirr}{}^{EPERM})}]^2 = \frac{(8581 \times 0.208^{4.4})}{0.18^2}]^2 = 263.90$ mD

# Presentation on

# "FORMATION EVALUATION USING WIRELINE LOG DATA OF BAKHRABAD GAS FIELD"

**Presented by**

**Mohammad Islam Miah**

**Project Supervisor: Prof. Dr. Mohammad Tamim**

**Date : 29 November, 2014**

# Presentation Outline

Introduction
Objectives
Location of the Study
Methodology
Results and Discussions
Uncertainty
Conclusions
Recommendations

# Introduction

- Formation evaluation is the practice of determining both the physical and chemical properties of rocks and the fluids they contain.

- Wireline log data generally more used for formation evaluation (porosity assessment, water saturation and permeability estimation etc.)

- Reservoir thickness, shale volume, Porosity and Fluid saturation are important parameters for reserve estimation,GIIP and reservoir characterization.

# Objectives

- The main objective of the present study is formation evaluation of BK#9 that is to ascertain the followed parts:

- Lithology identification
- Detection of hydrocarbon bearing zone
- Estimation of shale volume and reservoir thickness
- Assessment of effective porosity
- Determination of water saturation and
- Estimation of log derived permeability

# Previous Study of BK Field

❖This gas field is one of the onshore gas fields in Bangladesh

❖The presence of a potential gas bearing structure at Bakhrabad was first recognized from the results of the gravity survey made by Pakistan Petroleum Company in **1953** (Welldrill, 1989).

❖BK seismic mapping was prepared by (HHS) in **1986**.

❖In **1990**, IKM studied about "Gas Field Appraisal Project- Geological, Geophysical, Petrophysical & Reservoir Engineering report of the BK Gas Field" for BK-1 to BK-8.

# Previous Study of BK Field-Cont'd

- Several reservoir engineering studies on BK field have been done based on IKM findings (Z. Choudhury, **1999** and so on).

- In October **2009**, RPS Energy & Petrobangla studied "Petrophysical Analysis of BK Gas Field" for BK 1 to BK 8.
- After May 2013, BK#9 has been penetrated within this structure.

- The formation evaluation of BK#9 has not been done yet. So this new data can be used for future reservoir analysis.

# Location of Study Area

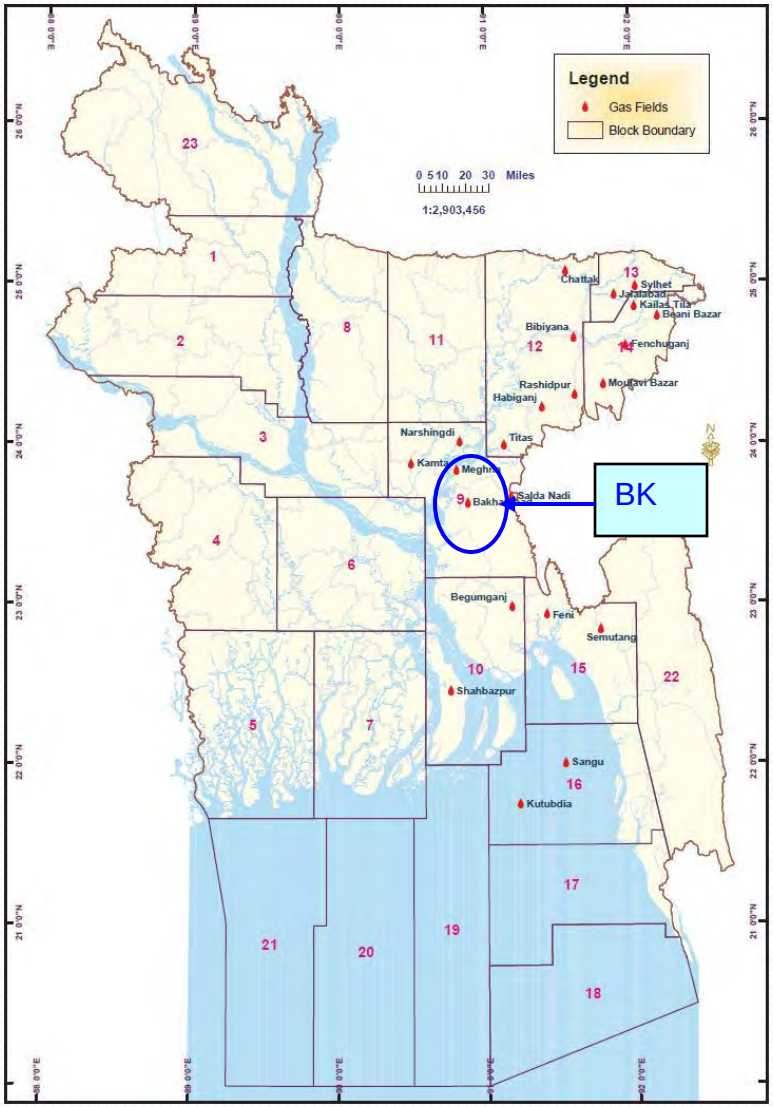


Figure 1: Location of BK Gas Field
(Source: RDMD, Petrobangla)

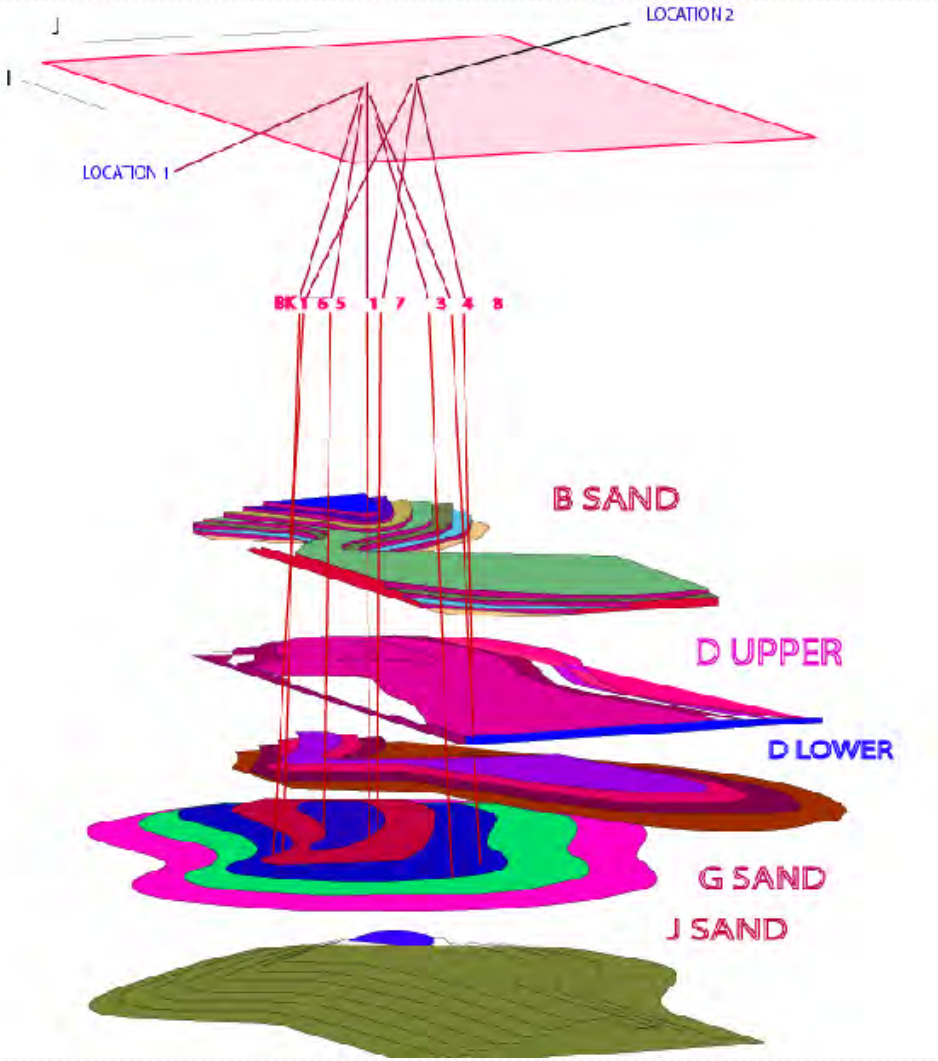


Figure 2: Bakhrabad gas field (drilled) well locations
(Sourse: BGFCL)

# Log Interpretation Methodology

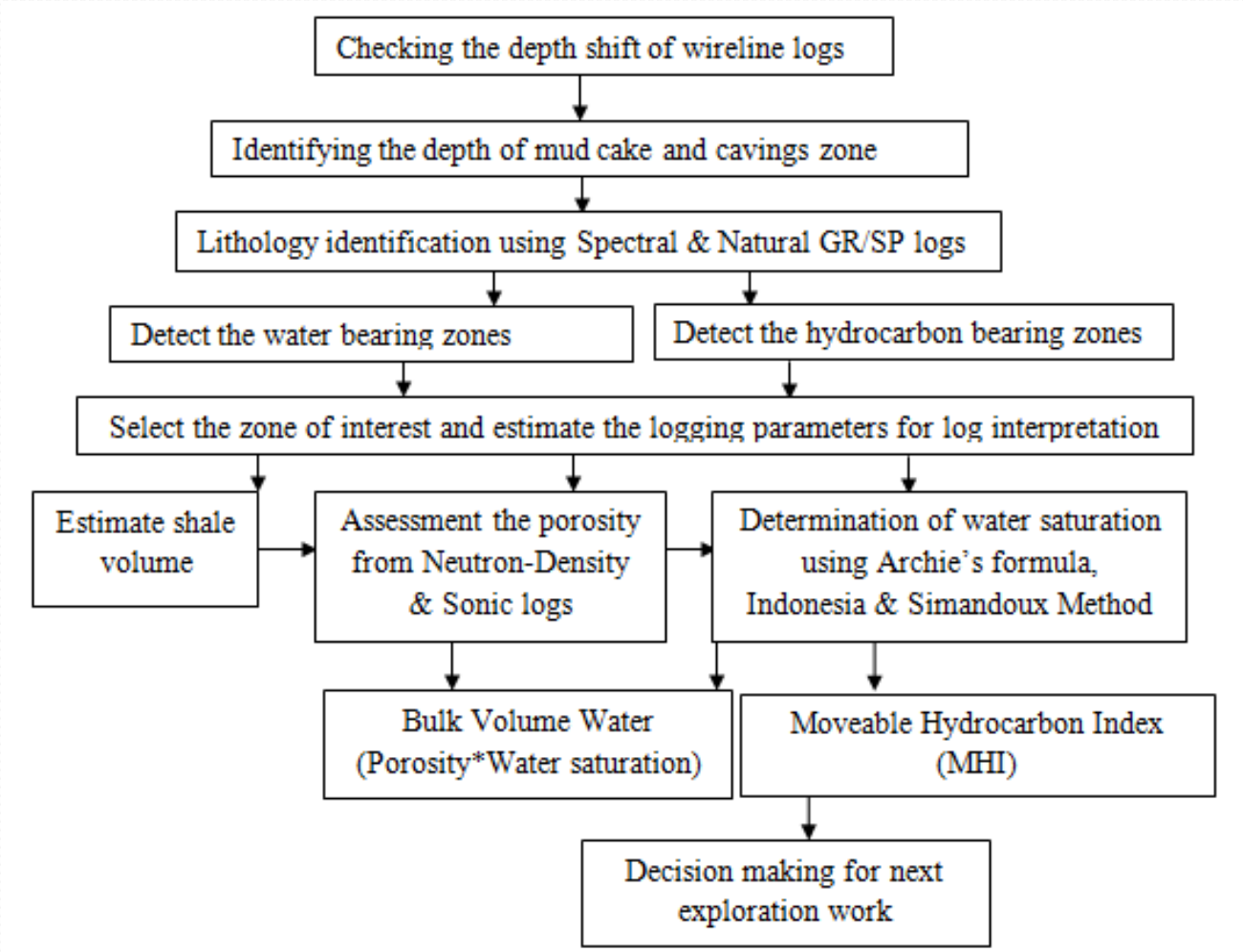


Figure 3 Flow chart for log interpretation and formation evaluation

# Lithology Identification

**Shale or Clay zone:**

- High concentration of radioactive minerals (K40, U & Th)
- High Gamma Ray reading/response

**Sand or Shaly sand zone:**

- Low concentration of radioactive minerals (K, Th, U)
- Generally low GR reading/response

✓

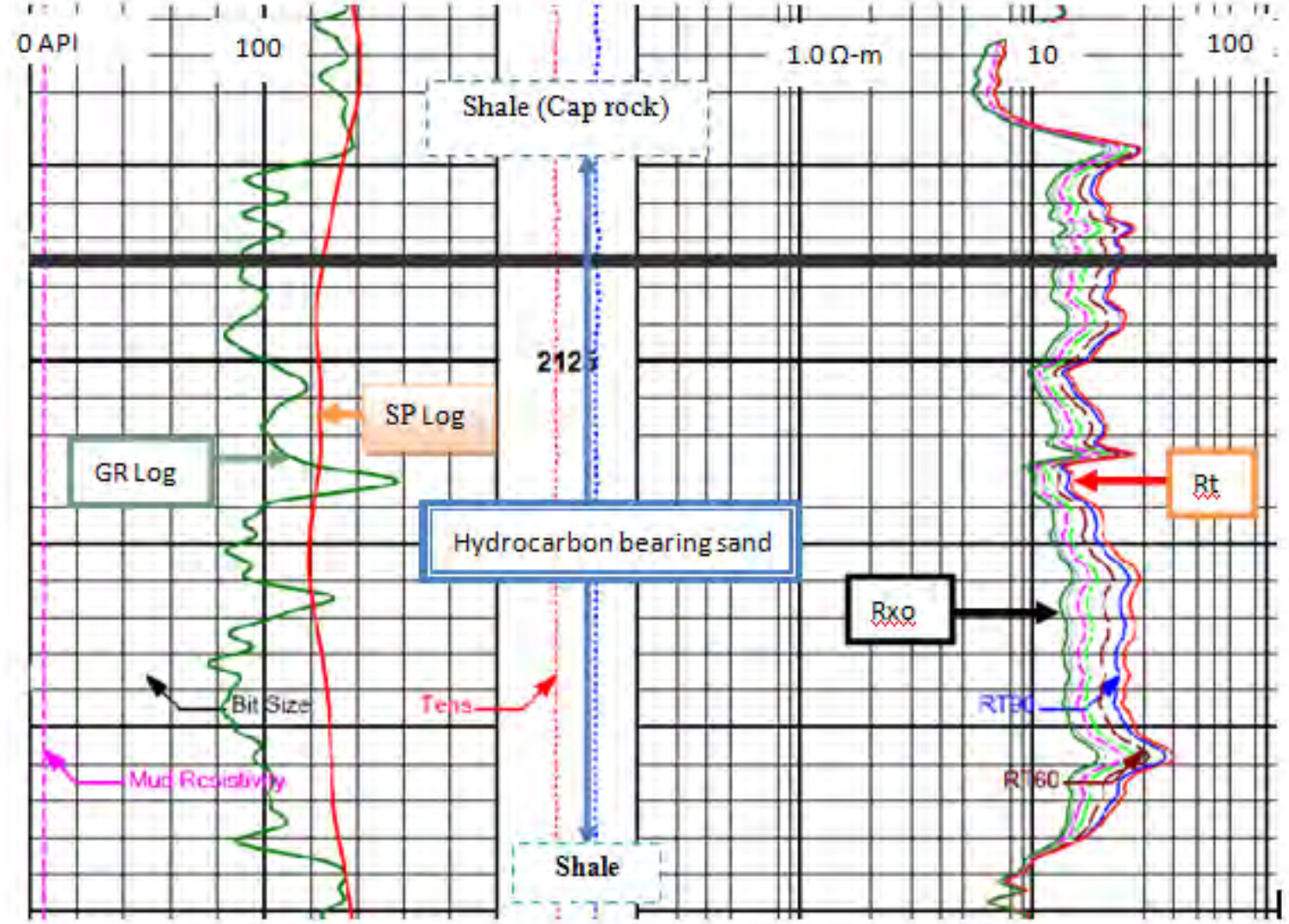


Figure 4: A typical example of resistivity log including lithology logs of hydrocarbon bearing thick sand (BK#9)

# HC Bearing Zone Detection

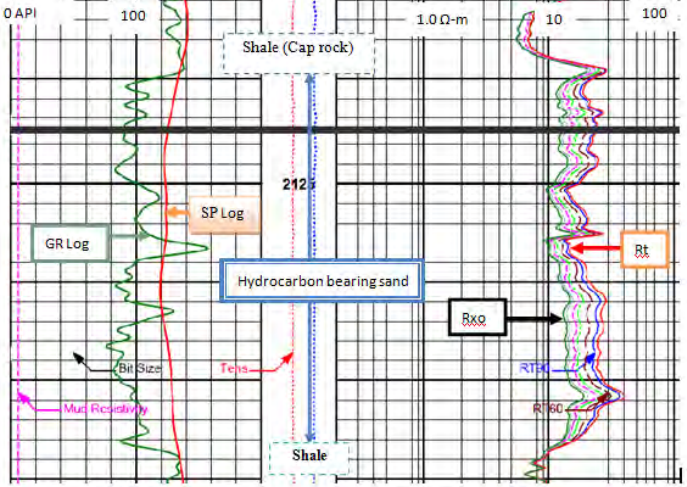


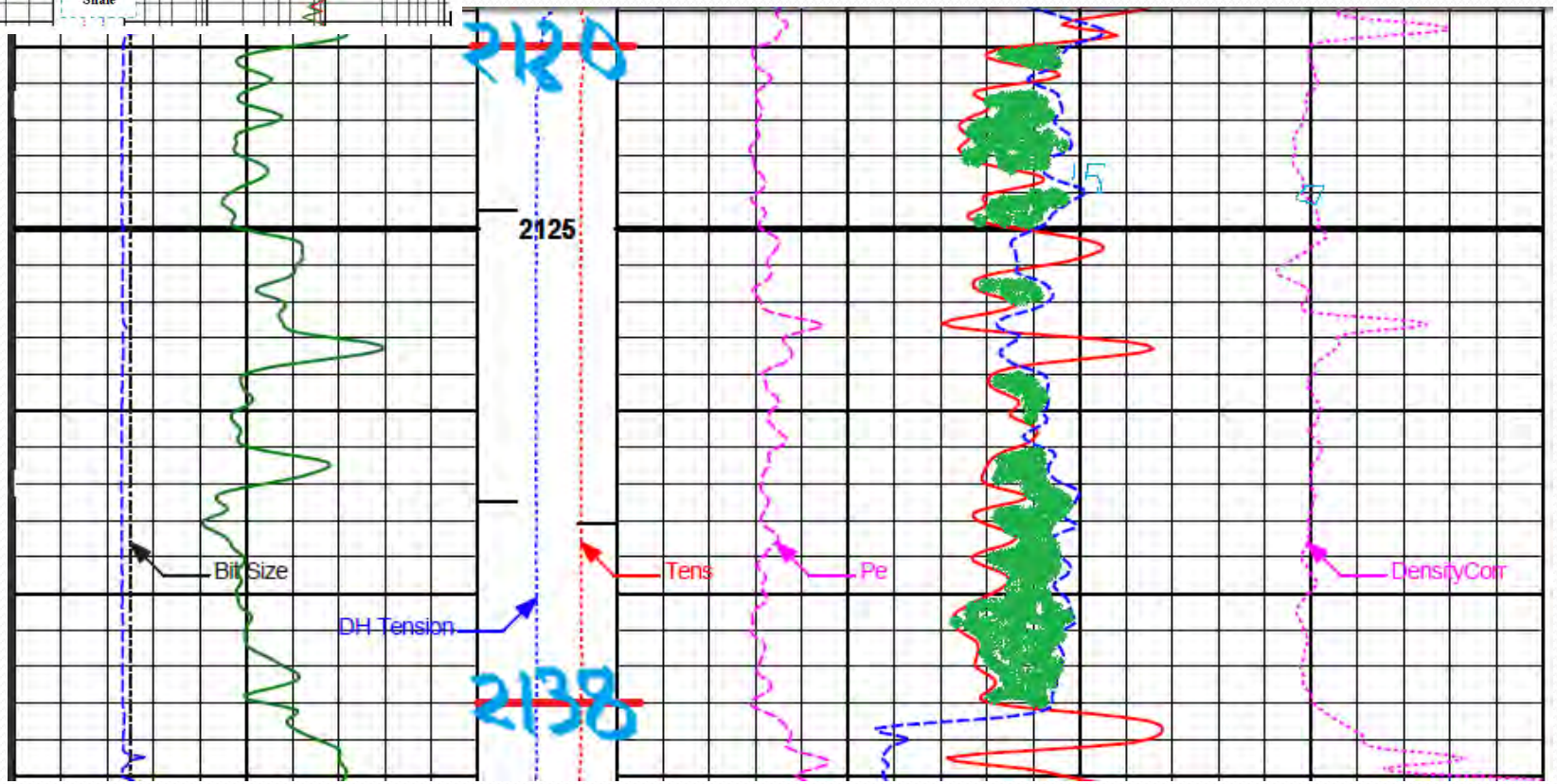


Figure 5: Cross-over of major sand between compensated density and neutron logs

# Shale Content/Volume (Ish/Vsh)

**Vsh** is the ratio of clay fraction to the bulk volume of reservoir rocks

$Y_{Vsh}$= [(Xlog-Xmin)/(Xmax-Xmin)] where Y= GR/K/Th

Xlog= GR/K/Th response in the formation of zone interest,

Xmin= GR/K/Th response in clean shale free formation and

Xmax= GR/K/Th response in clean shale zone over the entire log.

Larionov equation , Shale volume (Vsh) = $0.083(2^{3.7 * Ish} - 1)$ for tertiary rocks

- **True resistivity method:** Vsh=[{(Rcl/Rt)*(Rtmax-Rt)/ (Rtmax-Rcl)}^ (1/1.5)]
  - Rcl = Resistivity of clay, Rtmax =maximum value from deep resistivity over the entire log and

    Rt = from the zone of interest.

# Porosity Assessment

- **Total porosity** is defined as the ratio of pore space to the total volume of reservoir rock
- The effective porosity ($\Phi_e$) is the ratio of interconnected pore space volume to the total bulk volume of the rock.

- Clay corrected Neutron porosity , $\Phi_{N,corr} = \Phi_N - V_{sh} * \Phi_{N,sh}$ + Lithology correction (=0.04%).
- Clay corrected bulk density, $\rho b,corr = \rho b + Vcl(\rho ma - \rho cl)$
- Density porosity, $\Phi_{D,corr} = [(\rho ma - \rho b,corr)/(\rho ma - \rho f)]$
- Neutron-Density combination Formula, $\Phi e = [\{(\Phi_{N,corr})^2 + (\Phi_{D,corr})^2\}/2]^{0.5}$

- Sonic porosity, $\Phi_S = [(\Delta T\ log - \Delta Tma)/(\Delta Tf - \Delta Tma)]$ where

- Hilchie (1978) formula [3] for hydrocarbon effect: $\Phi e = \Phi_S \times 0.7$ for gas

# Geothermal gradient, Gg and Formation Water Resistivity, Rw

$G_g = [\{(BHT-T_s)/TD\}\times 100]$

$T_f = [T_s + (Gg/100)]$

BHT=Bottom Hole Temperature in degree Fahrenheit,
Tf= Formation Temperature
$T_s$ =the surface (ambient) temperature in degree Fahrenheit and
TD is the Total Depth.

**$R_w = [(\Phi_{N\text{-}D}{}^{m} * Rt)/a]$ by Inverse Archie's Formula**

Wyllie and Rose method,
$K_L$ = [CPERM*(Φ^DPERM /$S_{w,irr}$ ^ EPERM]$^2$ in mD for dry gas

# Water Saturation (Sw) Estimation

- Sw is water fraction within the pore space of reservoir rock.

- **Archie's water saturation** formula for clean sands (Archie, 1942):

$S_w = [(FR_w/R_t)]^{(1/n)}$ for un-invaded zone & $S_{xo} = [\{(F*R_{xo})/R_{mf}\}]^{(1/n)}$ for flushed zone where n is the saturation exponent, $F = (a/\Phi^m)$

- **Indoonesia equation** :

- For un-invaded zones, $S_w = (1/Rt)[\{Vcl^{(1-0.5Vcl)}/(Rcl)^{0.5}\} + \{\Phi^{0.5m}/(aR_w)^{0.5}\}]$

**Simandoux method for shaly sand reservoir** :

- $S_w = \{(0.4Rw/\Phi e^2)\}*[\sqrt{\{(Vsh/Rsh)^2 + (5\Phi e^2)/(Rw*Rt)\}} - Vsh/Rsh]$ for sandstones where

- $\Phi_e$ = clay corrected porosity, Rcl or Rsh = Clay resistivity from virgin zone
- $R_t$ = True resistivity, m = Cementation exponent,
- a = Tortousity factor, n = Saturation exponent and Rsh = Shale resistivity.

# Results and Discussions

# Log Availability & Quality

| Log type | Log Name |
|---|---|
| Borehole measurement log | Caliper log with Bit size |
| Lithology logs | Spectral and Natural Gamma Ray log<br>Self-Potential (SP) log |
| Resistivity Logs | Array compensated true resistivity<br>(Shallow and Deep Resistivity logs) |
| Porosity logs | Spectral Density, Dual spaced Neutron log<br>and BHC Sonic Array log |

- The quality of log data of the studied well is good except SP log
- In studied wells:
  - No depth shift has been found in the logs.
  - No borehole caving ( Bite size=Caliper log, shows in sands interval)
  - Mud cake developed (Bite size>Caliper log)
- No environmental corrections were applied to the logs.

# Lithology Identification

- Lithology is mainly sand and shale where sand is the dominant fraction
- GRmax & GRmin: 155API @2405m & 76 API@1912m
- True resistivity: 12.9-22 ohm-m (Rt) for gas bearing sand
- Average sand bulk density: about 2.37 gm/cc (Thick Sand-2120-2138m)
- Average adj. shale density: about 2.39 gm/cc

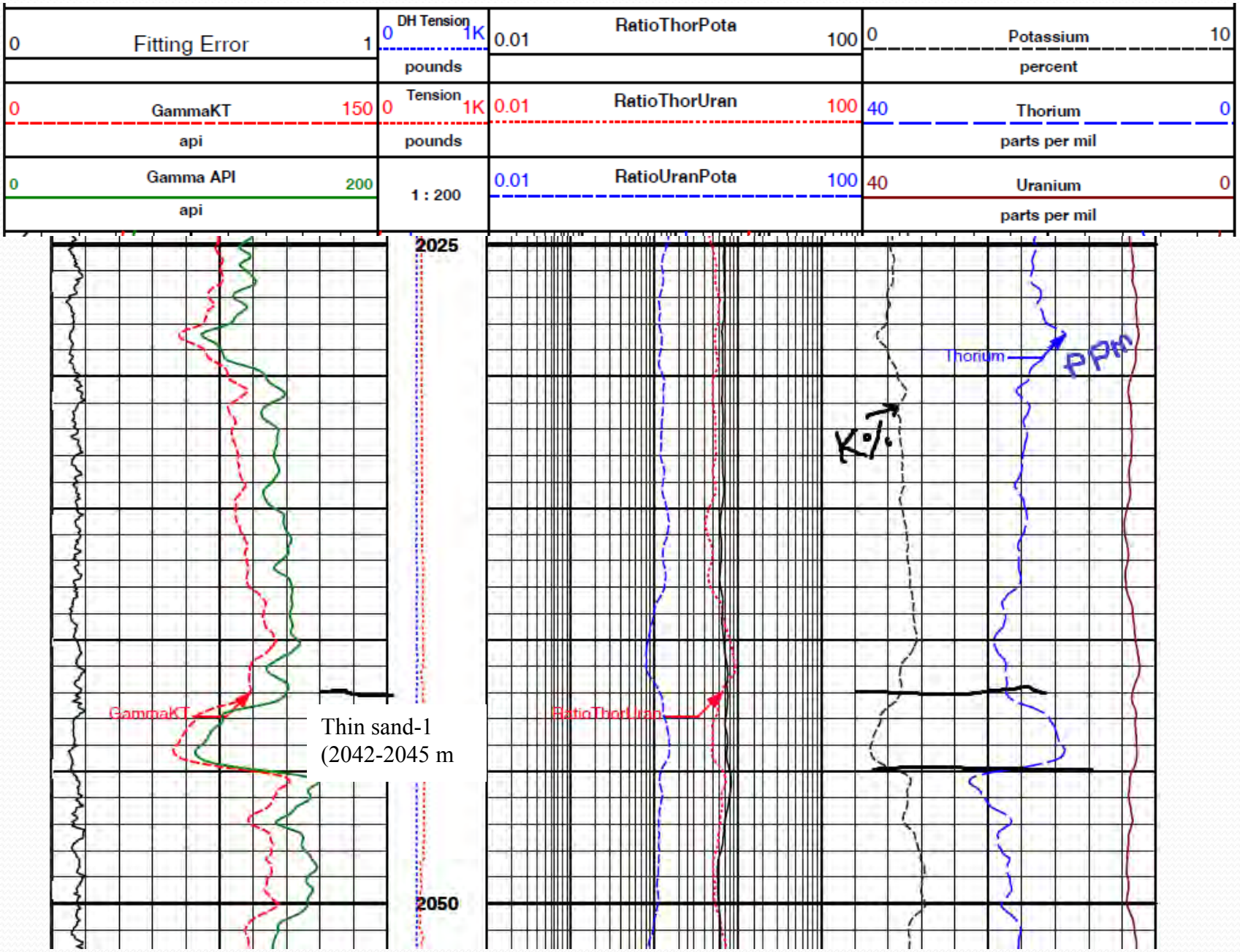


Fig 6. Spectral and natural GR logs of thin sand-1 reservoir

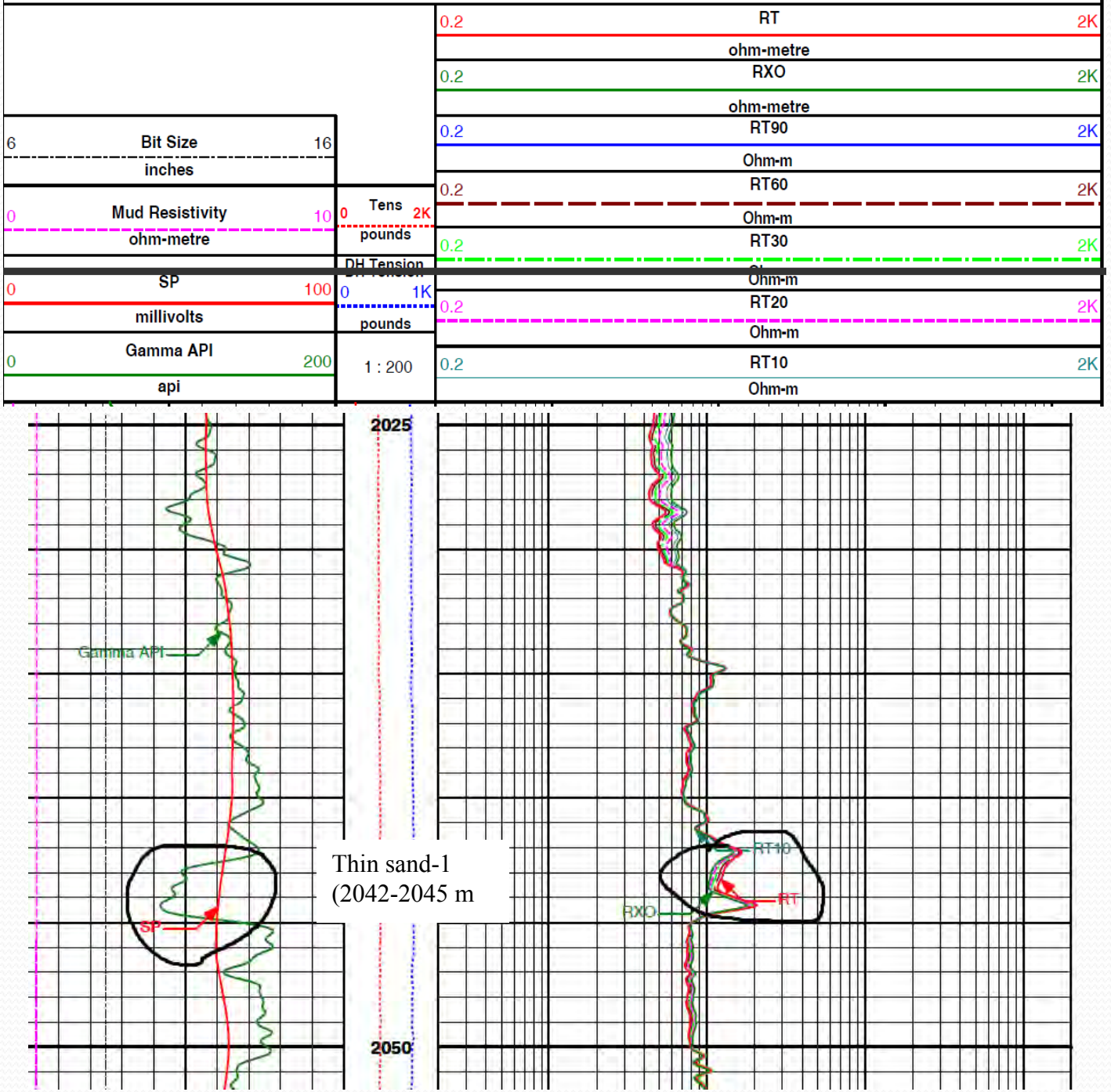


Fig. 7: Lithology and Resistivity logs of BK#9 of thin sand-1 reservoir

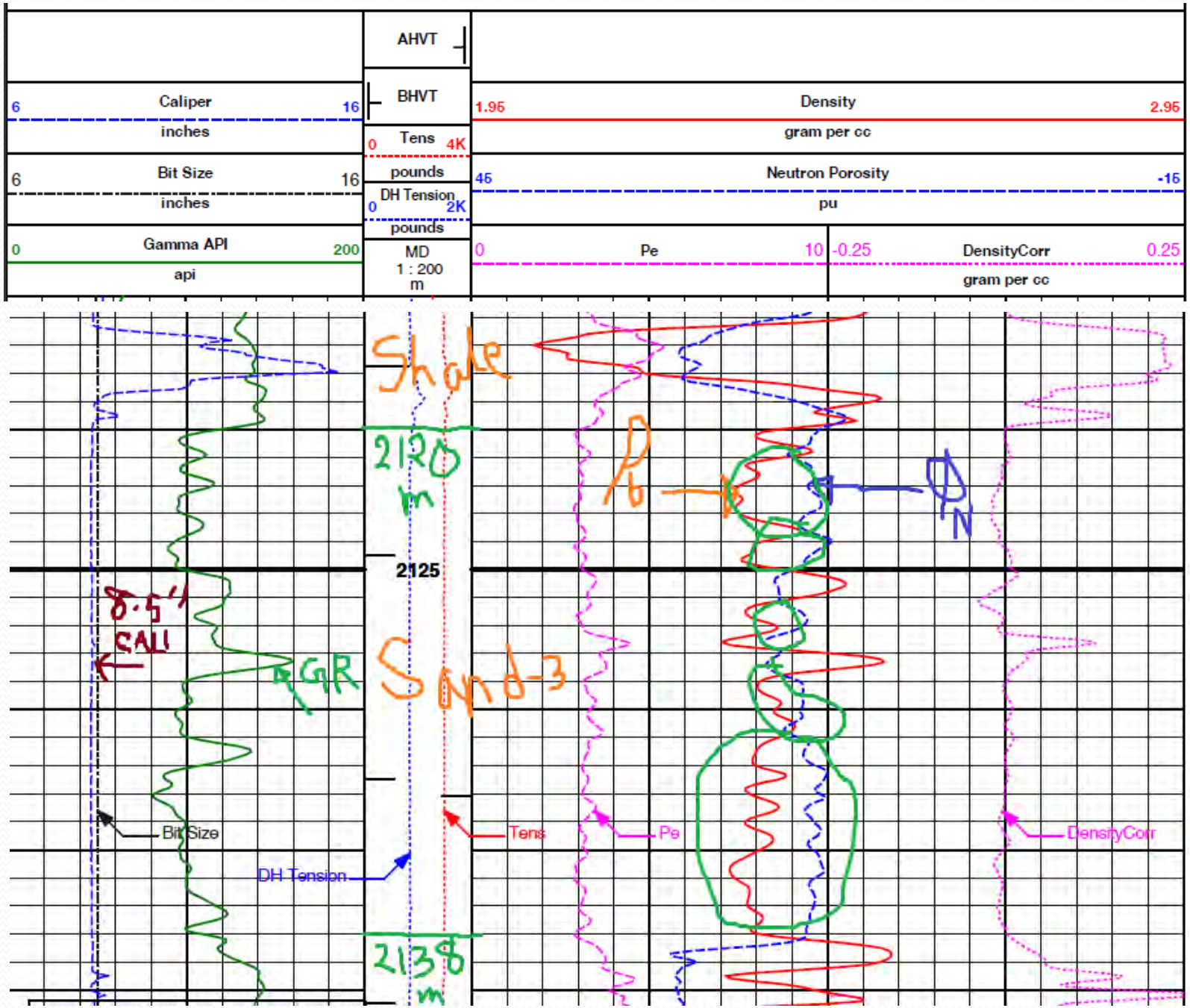


Figure 8: Spectral density & Dual spaced neutron with GR logs

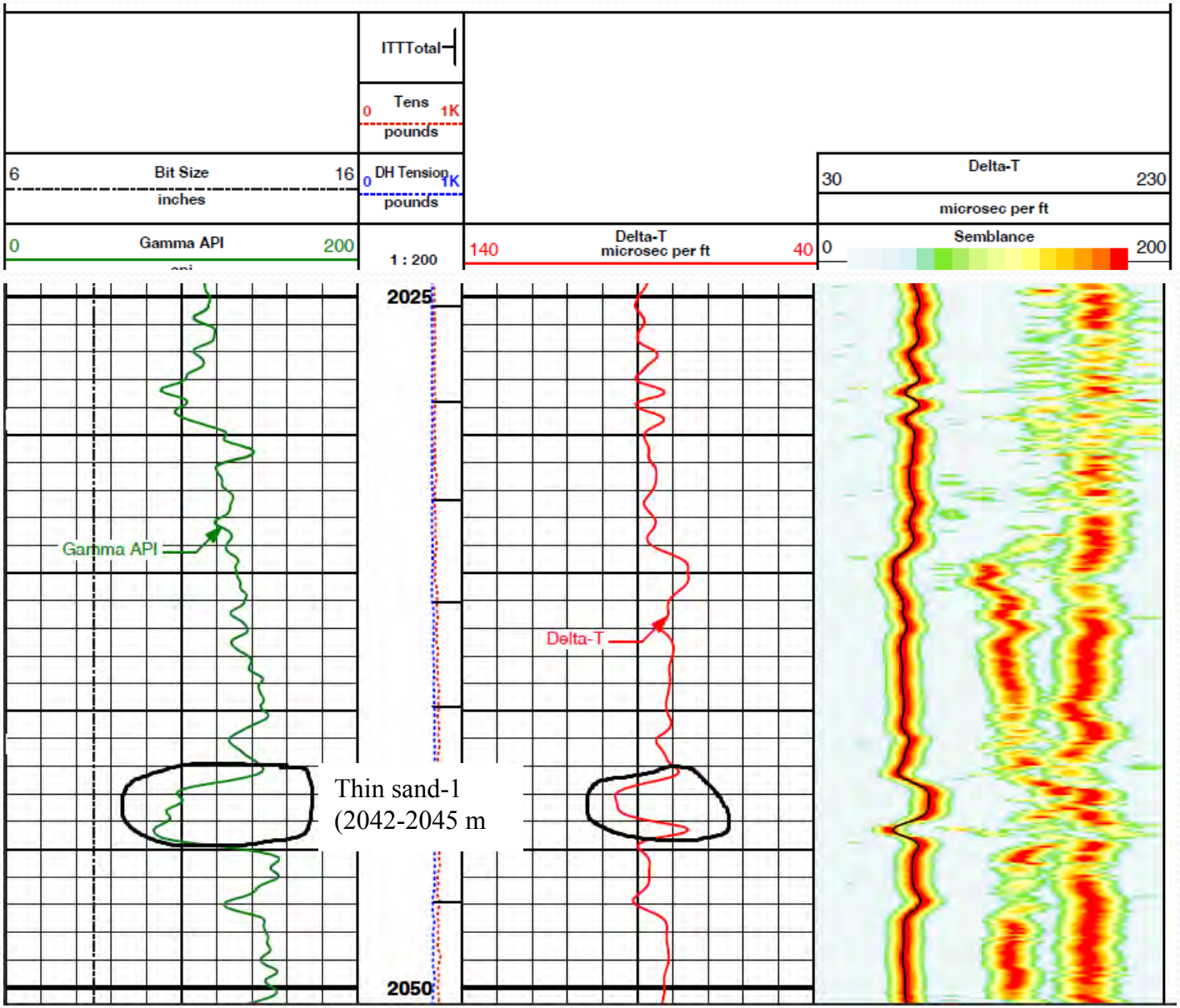


Figure 9: Borehole compensated sonic array log of BK#9

# Hydrocarbon Bearing Zone Detection & Reservoir Thickness

- Hydrocarbon bearing sand zone:

**6 zones**

(2042 m to 2500.5 m TVD)

Table 3 Values of formation radioactive minerals, bulk density, resistivity and others

| Parameters | Sand-1 | Sand-2 | **Sand-3 (Thick)** | Sand-4 | Sand-5 | Sand-6 |
|---|---|---|---|---|---|---|
| Top-Base (TVD), meter | 2042-2045 | 2100-2102 | **2120-2138** | 2150.5-2156.5 | 2363-2368 | 2498.5-2500.5 |
| Gross thickness | 3.00 | 2.00 | **18.00** | 6.00 | 5.00 | 2.00 |
| Normal GR (API) | 96.00 | 102.00 | **99.00** | 105.00 | 103.00 | 111.00 |
| Th (ppm) | 11.407 | 12.786 | **12.340** | 13.843 | 12.833 | 10.761 |
| U (ppm) | 2.287 | 2.298 | **2.248** | 1.990 | 2.459 | 2.700 |
| K (%) | 1.506 | 1.532 | **1.702** | 1.855 | 1.657 | 1.413 |
| Rt (ohm-m) | 14.00 | 17.00 | **16.00** | 22.80 | 12.90 | 17.00 |
| RHOb (g/cc) | 2.35 | 2.35 | **2.39** | 2.42 | 2.33 | 2.46 |
| NPHI (%) | 24.50 | 19.00 | **17.33** | 16.47 | 16.50 | 12.55 |
| Pe (barns/electron) | 3.12 | 3.23 | **3.17** | 3.34 | 2.92 | 3.53 |
| DELT (µs/ft) | 96.39 | 86.33 | **92.90** | 85.26 | 70.05 | 83.68 |

# Shale Volume (Vsh)

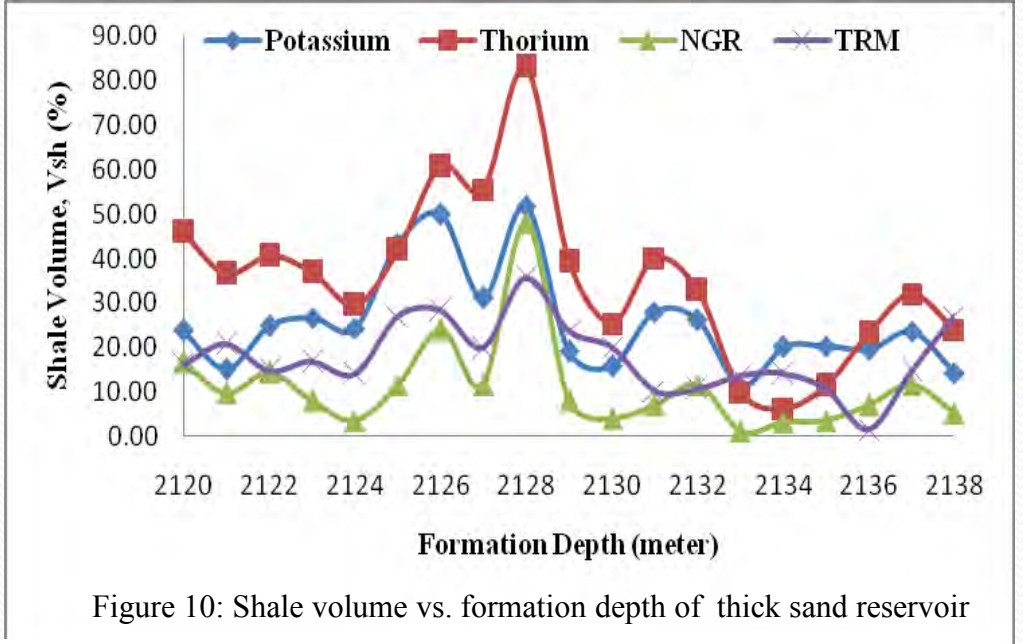


Figure 10: Shale volume vs. formation depth of thick sand reservoir

Table 4 Estimated shale volume (Vsh) using spectral, normal GR and TR Methods

| Sand Type (Thickness, m) | Spectral GRM (%) | | Natural GRM (%) | TRM (%) |
|---|---|---|---|---|
| | K-Vsh | Th-Vsh | GR-Vsh | TR-Vsh |
| Sand-1 (3m) | 12.71 | 26.78 | 7.59 | 35.62 |
| Sand-2 (2m) | 14.44 | 39.68 | 11.00 | 26.93 |
| Thick Sand-1 (18m) | 25.75 | 35.51 | 11.09 | 17.87 |
| Sand-4 (6m) | 35.95 | 49.58 | 13.08 | 29.59 |
| Sand-5 (5m) | 22.75 | 40.12 | 11.64 | 39.78 |
| Sand-5 (2m) | 6.52 | 20.73 | 17.55 | 26.53 |

# Porosity Assessment

Rock matrix density($\rho_{ma}$)= 2.65
& Fluid density= 1.0 gram/cc
(fresh water based mud)

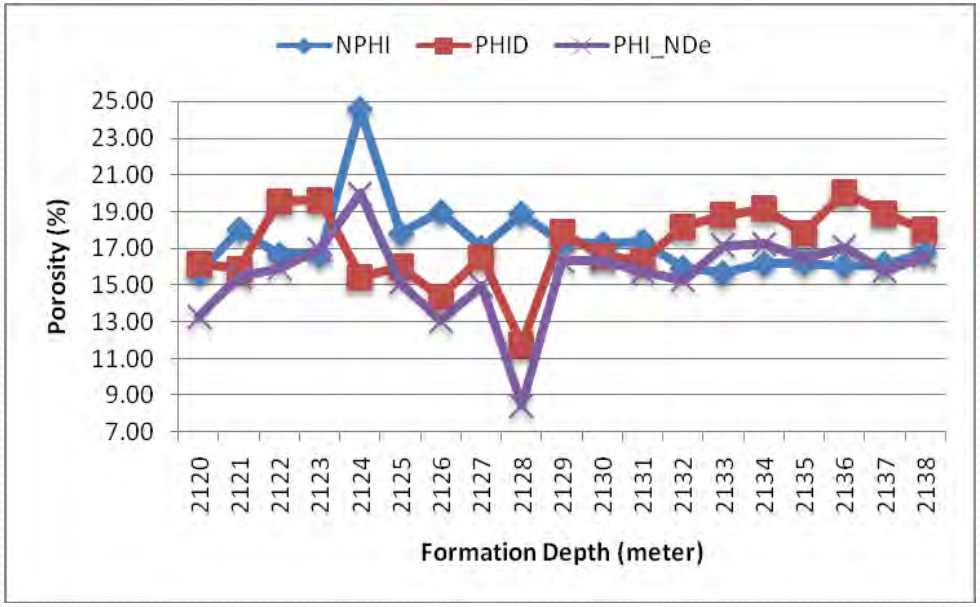


Figure 11: Depth versus average porosity of thick sand reservoir

Table 5 Estimated porosity from neutron, density and sonic logs

| Sand Name | Sand-1 | Sand-2 | Sand-3 | Sand-4 | Sand-5 | Sand-6 |
|---|---|---|---|---|---|---|
| $\Phi_N$ (%) | 24.50 | 19.00 | 17.33 | 16.47 | 16.50 | 12.55 |
| $\Phi_D$ (%) | 19.09 | 18.18 | 17.22 | 14.10 | 19.39 | 11.52 |
| $\Phi_{N\text{-}D}$ (%) | 21.96 | 18.60 | 17.36 | 15.33 | 11.52 | 12.04 |
| $\Phi_{N\text{-}D\ corr}$ (%) | 20.79 | 16.87 | 15.64 | 13.28 | 16.18 | 9.28 |
| $\Phi_{sonic,\ gas}$ (%) | 21.44 | 16.16 | 19.61 | 15.60 | 7.63 | 14.78 |

# Geothermal Gradient, Gg and Formation Temperature, Tf

- Gg: 3.948 $^{0}$F/100 meter with of BKB#9
- Tf of thick (major) sand depth interval: 163.71 to 164.42 $^{0}$F.
- It is found that this (2120-2138m TVD) well shows lower Gg comparing with 5.91 $^{0}$F/100m of G sand (IKM, 1991).
- The Gg and Tf are varied with respect to depth of the formation.

# Formation Water Resistivity, Rw

**Table Estimated Rw by Inverse Archie's Formula**

| Sand type | TVD, m | Tf (deg F) | Rw (ohm-m) | Rmf (ohm-m) |
|---|---|---|---|---|
| **Reference (Wet sand)** | 1964.5 | - | **0.104** | 0.157 |
| **Thin-1** | 2043.5 | 160.68 | **0.102** | 0.154 |
| **Thin-2** | 2101.5 | 162.97 | **0.102** | 0.154 |
| **(Thick -1)** | 2129 | 164.06 | **0.100** | 0.151 |
| **Thin-4** | 2153.5 | 165.03 | **0.099** | 0.150 |
| **Thin-5** | 2366 | 173.42 | **0.095** | 0.143 |
| **Thin-6** | 2499.5 | 178.69 | **0.092** | 0.139 |

Rw=0.2 @ 175 deg. F & Rws= 0.38@ 76 deg. F (IKM,1991)

# Estimation of Sw

The tortousity (a), saturation (n) and cementation exponent (m) value of 1, 2 and 2.25 have been used for saturation estimation.

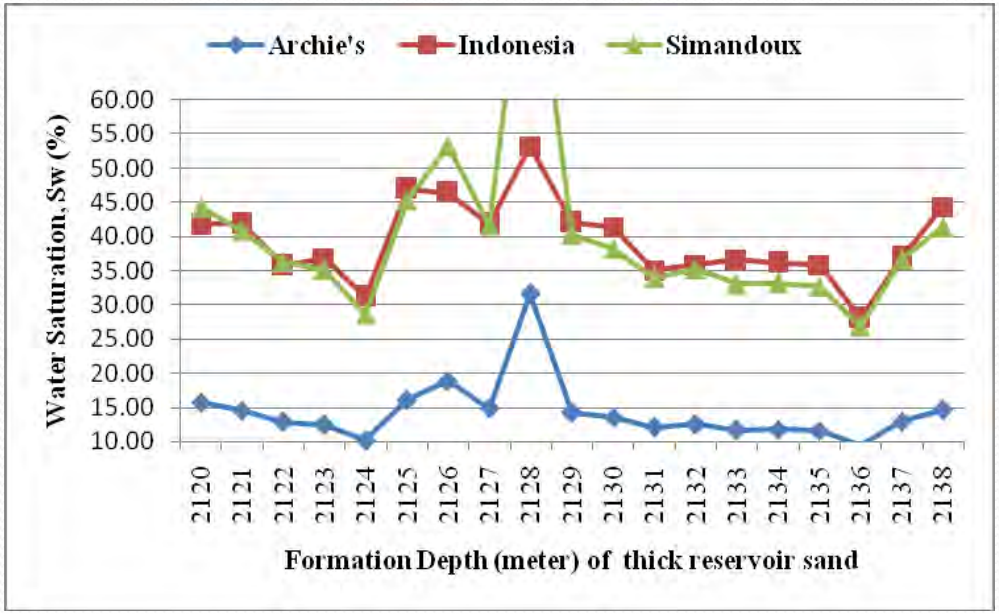


**Figure 12: Average water saturation of reservoir (thick sand-1)**

**Table 6 Estimated water saturation from different methods**

| Sand type | Thickness (meter) | Archie's formula (average, %) | | Indonesia formula (average, %) | | Simandoux method (average, %) |
|---|---|---|---|---|---|---|
| | | Swa | Sxo | Sw | Sxo | Sw |
| Thin sand-1 | 3 | 13.12 | 22.34 | 39.02 | 56.92 | 36.71 |
| Thin sand-2 | 2 | 14.47 | 25.98 | 41.64 | 64.09 | 40.77 |
| Thick sand-1 | 18 | 14.26 | 27.60 | 39.18 | 70.96 | 40.30 |
| Thin sand-3 | 6 | 18.74 | 30.15 | 51.84 | 77.83 | 53.05 |
| Thin sand-4 | 5 | 16.31 | 24.63 | 48.05 | 65.09 | 47.36 |
| Thin sand-5 | 2 | 24.08 | 37.12 | 62.31 | 99.54 | 71.21 |

# Log Derived Permeability, $K_L$

| sand, TVD (m) | | PHIe | Swirr | Coefficent values | | | Permeability (mD) |
|---|---|---|---|---|---|---|---|
| Top | Base | | | CPERM | DPERM | EPERM | Wylie-Rose Method |
| 2042 | 2045 | 20.79 | 0.18 | 8581 | 4.40 | 2 | 263.90 |
| 2100 | 2103 | 16.87 | 0.18 | 8581 | 4.40 | 2 | 105.23 |
| **2120** | **2138** | **15.64** | **0.18** | **8581** | **4.40** | **2** | **85.45** |
| 2150.5 | 2156.5 | 13.28 | 0.18 | 8581 | 4.40 | 2 | 36.79 |
| 2363 | 2369 | 16.18 | 0.18 | 8581 | 4.40 | 2 | 87.67 |
| 2498.5 | 2500.5 | 9.28 | 0.18 | 8581 | 4.40 | 2 | 7.59 |

$S_{wirr}$ of 18%, and CPERM= 8581 (RPS Energy, 2010)

Irreducible saturation exponent (EPERM) of 2.0, and porosity constant (DPERM) of 4.4 (IKM, 1991)

# Discussions

- Sand interval, sand and shaly sand appeared as alternating units

- Vsh is 7.6 – 17.6 % from Gamma Ray log for 18m thick sand-1
- From Gama Ray method, estimated shale volume is optimistic (than TRM and others) and more reliable for calculating effective porosity for shaly sand gas reservoir

- Neutron-density combination formula gives better results of porosity for shaly sand (thick) gas reservoir of this field as 15.64%

- For Sw estimation, Indonesian/Simdoux formula is more reliable for this well

- Log derived permeability KL (7.59 to 263.90 mD) of this reservoirs

# Comparison of Petrophysical Properties

| Parameters / Properties | IKM, 1991 | | | | | | | | RPS Energy, 2009 (P50 to P90) | Current Study |
|---|---|---|---|---|---|---|---|---|---|---|
| Well No. | BK# 1 | BK# 2 | BK# 3 | BK# 4 | BK# 5 | BK# 6 | BK# 7 | BK# 8 | BK# 1-8 | BK#9 |
| G sand Interval, ft (TVD) | 6850 - 7030 | 6920 - 7000 | 6840 - 7020 | 6920 - 7000 | 6960 - 7103 | 6920 - 7100 | 6820 - 7000 | 6912 - 7028 | 7813 – 8826 (MD) | 6953 - 7013 |
| Net Pay, ft | 49.5 | 74.5 | 81.5 | 58.0 | 100 | 59.5 | 89.0 | 61.5 | 32.5- 144 | 63 |
| Vsh (%) | 18.0 | 23.0 | 11.0 | 17.0 | - | 19 | 20.0 | 18.0 | 8.5-32.0 | 11.0 |
| PHI (%) | 19.8 | 16.8 | 21.6 | 20.0 | - | 15.7 | 16.7 | 19.0 | 13.6 -21.2 | 15.6 |
| Sw (%) | 26.8 | 26.2 | 37.5 | 27.9 | - | 35.5 | 31.0 | 25.9 | 18.4- 37.8 | 39.1 |
| Rt (Ω-m) | 30-70 | | | | | | | | N/A | 17-38 |
| Permeability (mD) | 109.4 (BK#2) and 98.8 mD (BK#3) from Production Test Data | | | | | | | | 61.3- 219.3 | 34.2- 222.0 |
| MHI | N/A | | | | | | | | N/A | 0.57 |
| BVW | N/A | | | | | | | | N/A | 0.06 |

# Uncertainty

- Manual interpreted log readings may be slightly change
- Matrix density and transit time can be changed for the heterogeneity of the studied gas reservoir
- Clean wet sand zones are uncommon in the studied well. As a result, the estimation of corrected $R_w$ may be wrong due to changing of cementation exponent (m) and actual sub-surface formation temperature.
- Exponents (a=1, m=2 and n=2) are critical in calculating porosity, formation water resistivity and water saturation of flushed zones as well as un-invaded zones.
- Reservoir porosity and fluid saturation in sandstone may be changed causes for grain size distribution and grain shapes, packing arrangement, cementation and clay volume changes.

# Conclusions

Based on the log interpretation and analyzed results:

- The shales are laminated & gross reservoir thickness: 18m for thick sand
- Estimated average Vsh is 7.59-17.55 % (GR Method)
- porosity quality is good
- Reservoir is productive (Sw=39.18-40.30 % (Thick sand)
- Gas is also moveable within major and thin sands reservoir of this reservoirs or formation.
- KL from Wylie-Rose method has been estimated as 34-222 mD which is a good permeability for sand reservoirs.
- So the gas pools of this formation are potential for producing gas.

# Recommendations

- To estimate the water saturation for a reservoir, the special or routine core analysis is required.
- The estimated reservoir thickness, porosity and hydrocarbon saturation can be used for future reserve estimation and reservoir properties analysis of this formation.
- To assess the quality of the gas reservoirs accurately, special logging tools such as NMR and BHI logs can be run with conventional wire line logs.
- To date, no wells has been drilled in the flank of the structure that could tell the extension and quality of the reservoir as well as its gas saturation, presence of fluid contact (GWC) and minimizes the uncertainty of estimation of hydrocarbon reserve.

# Acknowledgement


❖ I would like to express my deepest gratitude to:

- **Professor Dr. Mohammad Tamim** (Research Supervisor, PMRE depth, BUET)
- Md. Abdus Sultan (GM-In charge, RDMD, Petrobangla)
- Mr. Mijanur Rahman (GM-In charge, Geological Division, BAPEX)
- Mr. Sheik Muktadir and Engr. Ashraf, BGFCL.
- All Teachers, PMRE Dept., BUET.

**THANKS TO ALL**